Herbicide Dynamics and Bioavailability in the Soil

Gavin Styles

BSc (Hons) Monash University

A thesis submitted to the Faculty of Science, Monash University
in fulfilment of the requirements for the degree of
DOCTOR OF PHILOSOPHY

School of Chemistry
Monash University
Australia
March 2020

Table of Contents

Abstract

Herbicides are used globally in agricultural systems in order to reduce competition of desired crops with unwanted weed and other plant life, in order to increase yields. As the world population grows and there is a need to increase agricultural production in order to feed this growing population, reliance on these chemicals is likely to increase. However, there are concern around both the environmental and health impacts of herbicide usage, along with the possibility of persistence leading to herbicide injury in later rotations, and thus economic impact for agronomic land holders.

One of the major processes controlling herbicide mobility and bioavailabilty, and thus leaching and persistence, is soil adsorption. As such, a greater understanding of the processes driving adsorption would allow for improvements in management strategies for herbicide usage. Similarly, adsorption can vary greatly between soils, leading to a need for more spatially explicit management strategies than the climatic regions used currently in herbicide labelling. However, determining adsorption behaviour in a given soil requires expensive and time consuming HPLC or ^{14}C labelling experiments. As such, a predictive model of adsorption based on more routine or rapid agronomic tests would allow for a wider adoption of this spatially explicit management.

Glyphosate is the most widely used herbicide in both Australia and globally. While it has traditionally been considered of low ecological impact due to its rapid breakdown rate and high adsorption capacity in soil, recent studies have shown that the frequency and dosage rate of glyphosate usage can outweigh the breakdown rate, leading to longer persistence. This makes it an ideal candidate for adsorption mechanism exploration, and predictive modelling.

The first four experimental chapters of this thesis (Chapters 2-5) explore the development of predictive models for glyphosate adsorption in soil, and the mechanisms driving this process. A predictive model based on routinely measured soil physico-chemical properties was developed

using a database of 90 soils with widely varying properties and verified using an additional set of 7 external soil samples, not used for the intial model development (Chapter 2). This led to a model using only pH and phosphorus buffering index to predict adsorption behaviour (in the form of Freundlich constants), with an R^2 of 0.967 (for K_f), and an average prediction error of 26% across Freundlich constants (both K_f and n_f) of the validation set. A second model was built using a data base of the same size (n = 90), but with MIR spectra as the criteria for prediction, and model validation done by venetian blinds methodology, rather than an external validation set (Chapter 3). This led to a final model with a cross-validated R^2 of 0.839 and a cross-validated real mean squared error (RMSECV) of 17.338 for K_f predictions.

In order to explore the adsorption/desorption mechanisms of glyphosate from individual components of soil, 6 soil minerals were chosen, and a series of adsorption experiments conducted (Chapter 4). This led to a comparison of the Langmuir and Frumkin-Fowler-Guggenheim isotherms and the physical information that can be drawn from them. High levels of lateral interactions between the glyphosate adsorbate molecules were seen with increasing pH, along with a decreased attraction to the adsorbate surface, particularly for variable charge metal oxides. Following this, the desorption of glyphosate from these surfaces under variety of conditions, and in particular, the competition of glyphosate and phosphate ions, was tested (Chapter 5). This showed that glyphosate likely binds to the surface of these minerals at 2 distinct energy levels, the lower level of which may be disrupted by columbic screening due to salt solutions. This suggests a bilayer adsorption system, or significant edge effects due to surface topology. Along with this, phosphate and glyphosate ions adsorb via the same binding sites, leading to significant competition. However, phosphate ions will preferentially bind to empty sites prior to removing pre-adsorbed glyphosate. This has significant implications for the release of glyphosate in soil following phosphorus fertilisation, and thus the possibility of herbicide injury.

The final section experimental chapter of this thesis deals with the development of a test for "plant-available" herbicide in soil using diffusive gradient thin film (DGT) technology (Chapter 6). Most current forms of herbicide content testing is based on total extraction of the soil, and does not given information on the amount of herbicide available for plant uptake. The benefits of DGT sampling include the passive nature, which mimics plant root uptake, and the sheltered adsorbent which prevents degradation of the analyte post-sampling. Imazamox was chosen as the test herbicide for the development of this method, due its long halflife in soil (106-295 days under laboratory conditions). The uptake of imazamox from four agricultural soils by DGT samplers was compared to uptake by two varieties of rapeseed (one sensitive and one resistant to imazamox). This showed DGT uptake to be a better predictor of plant uptake than any individual soil property, lending credence to DGT as a measure of plant-available herbicide in soil.

General Declaration

In accordance with Monash University Doctorate Regulation 17.2 Doctor of Philosophy and Research Master's regulations the following declarations are made:

I hereby declare that this thesis contains no material which has been accepted for the award of any other degree or diploma at any university or equivalent institution and that, to the best of my knowledge and belief, this thesis contains no material previously published or written by another person, except where due reference is made in the text of the thesis.

This thesis includes one original paper published in peer reviewed journals and four unpublished papers currently under review. The core theme of the thesis is the development of new predictive tools and measurement protocols for herbicides in soil, in order to improve management strategies. The ideas, development and writing up of all the papers in the thesis were the principal responsibility of myself, Gavin Styles, working within the School of Chemistry under the supervision of Professor Antonio Patti, Professor Bart Follink, Dr Michael Rose (NSW-DPI) and Associate Professor Lukas Van Zwieten (NSW-DPI).

The inclusion of co-authors reflects the fact that the work came from active collaboration between researchers and acknowledges input into team-based research.

In the case of Chapters 2-6, my input is summarised in the table on the following page

Thesis Chapter	Publication Title	Status	Nature and % of student contribution	Co-author name(s) Nature and % of Co-author's contribution*	Co-author(s), Monash student Y/N*
2	A New Predictive Model of Glyphosate Adsorption in soil Based on pH and Phosphorus Buffering Index	Submitted	75% (Development of concept, all lab work, significant portion of modelling and writing)	1) Gavin McGrath (10%, modelling and editing) 2) Mick Rose (5% concept development and editing) 3) Lukas Van Zwieten (5% concept development and editing) 4) Tony Patti (5%, PI, concept development and editing)	N
3	Development of a Predictive Model for Glyphosate Adsorption in Soils Using MIR Spectra	Submitted	55% (Development of concept, all lab work, small portion of modelling and significant portion of writing)	1) Miguela Martin (25%, modelling and editing) 2) Mick Rose (5% concept development and editing) 3) Lukas Van Zwieten (5% concept development and editing) 4) Baden Wood (5% editing) 5) Tony Patti (5%, PI, concept development and editing)	Y (Miguela Martin)
4	Adsorption of Glyphosate to Model Soil Minerals	Submitted	80% (Development of concept, all lab work, writing)	1) Tony Patti (5% concept development and editing) 2) Mick Rose (5% concept development and editing) 3) Lukas Van Zwieten (5% concept development and editing) 4) Bart Follink (5%, PI, concept development and editing)	N
6	Uptake of Imazamox by Diffusive Gradient Thin Films and a Model Plant System	Submitted	85% (Development of concept, all lab work, writing)	1) Mick Rose (5% concept development and editing) 2) Lukas Van Zwieten (5% concept development and editing) 1) Tony Patti (5%, PI, concept development and editing) 3)	N

I have renumbered sections of submitted or published papers in order to generate a consistent presentation within this thesis.

Student name: Gavin Styles

Student signature: **Date:**

I hereby certify that the above declaration correctly reflects the nature and extent of the student's and co-authors' contributions to this work. In instances where I am not the responsible author I have consulted with the responsible author to agree on the respective contributions of the authors.

Main Supervisor name: Antonio Patti

Main Supervisor signature: **Date:**

Acknowledgements

I am extremely grateful for the support and guidance I have received throughout the three years of my PhD from my supervisors Tony Patti, Bart Follink, Mick Rose and Lukas Van Zwieten. Thank you for having me on board, and for all the work you have put into me over the course of this project. I feel extremely privileged to have been able to work with and learn from you all.

An enormous thankyou to my Colleagues in the Patti Group, in particular Karen Little, Cuyler Borrowman and Temma Carruthers-Taylor. You have all been an amazing source of support, knowledge and especially friendship and guidance. I am exceedingly lucky to have been a part of such a wonderful group and community. I would also like to thank Kei Saito for his constant mentorship and guidance, despite the fact I no longer worked directly with him.

I would also like to thank Monash University for my scholarship, the New South Wales Department of Primary Industries, Yitpi Foundation, German Academic Exchange Service and Fraunhofer Institute of Molecular Ecology for the funding that made all of this research possible, along with Agriculture Victoria and the Monash Centre for Electron Microscopy for their in-kind support.

Abbreviations

AIC = Akaike information criterion

AMPA = Aminomethylphosphonic acid

CEC = Cation exchange capacity

DGT = Diffusive gradient thin-films

EC = Electrical conductivity

EPSPS = 5-enolpyruvylshikimate-3-phosphate synthase enzyme

FFG = Frumkin-Fowler-Guggenheim

GAM = General additive model

GCV = Generalised cross validation

HPLC = High performance liquid chromatography

IR = Infrared

LM = Linear regression model

MIR = Mid-infrared

MLR = Multiple linear regression

PC = Principle component

PCA = Principle component analysis

PCR = Principle component regression

PLS-R = Partial least squares regression

OC = Organic carbon

PBI = Phosphorus Buffering Index

RMSECV = Real mean squared error (cross validated)

SVM = Support vector machine

UV = Ultraviolet

1. Introduction

1.1 Herbicide Usage and Impacts

Pesticides are used frequently in modern agriculture, with a specific pesticide chosen to leave the desired crop unaffected, while improving productivity by preventing crop damage by insects, competition from weeds, and diseases caused by various bacteria and fungi[1-2]. Herbicides are a class of pesticide used to kill or prevent the growth of one or several classes of plants. The Weed Science Society of America currently recognises 29 classes of herbicides[3], whereas Croplife Australia recognises 19[4]. Both divide these classes by their chemistry and mode of action[5] (eg. synthetic auxins, mitosis inhibitors). Recently, the use of herbicide resistant crops paired with non-selective herbicides (such as glyphosate) has been more frequently employed, particularly where weed resistance to herbicides has become prevalent.

Because of the increase in herbicide use worldwide, the potential impacts of herbicides on the surrounding environment has been of increasing concern, with studies on impacts of leaching into ground water[6], runoff from highways[7], toxicity to wildlife[8], soil health effects[9-10] and even appearance/transport of herbicides in the atmosphere[11]. Human health has also been a high priority, with significant investment of resources being put into the study of herbicide residues in foods and any impacts these may have on consumers[12], as well as impacts on the health of farmers caused by exposure during the application of herbicides[13-14].

The need to assess and mitigate potential impacts has led to the development of quick tests for herbicides to rapidly assess any contamination of food or animal feedstock, as well as soil contamination prior to the planting of crops. Further to these tests, research into the behaviour of herbicides in soil, particularly sorption[15] and degradation[16], have been undertaken to develop better herbicide fate models and management methods to mitigate any damage the herbicides may cause to the environment or future agricultural pursuits.

Of major interest in this thesis are the herbicides glyphosate and imazamox, the structures of which can be seen in Figure 1. The reason for the focus on these two chemicals is due to their common usage, and potential for persistence and leaching after application.

Glyphosate (N-(phosphonomethyl)glycine), sold most commonly under the tradename RoundUp™, is the most widely used herbicide both in Australia and globally, with 125,384 tonnes sold in the US alone in 2014[17]. Glyphosate is a systemic 5-enolpyruvylshikimate-3-phosphate synthase enzyme (EPSPS) inhibitor contact herbicide, that is applied post emergence for control of broad leaf flora. Its popularity is primarily derived from its low cost and broad spectrum (non-selective) nature, and the high availability of glyphosate resistant crop varieties[17].

While glyphosate has previously been considered to be have a relatively low ecological risk profile[18], owing to its high levels of adsorption leading to low mobility[19], rapid breakdown rate, and low toxicity to non-target organisms[10]. However, recent studies have shown glyphosate to be "pseudo-persistent" due to the rate of application outweighing the rate of breakdown, leading to accumulation in the soil[20]. This is particularly of concern due to recent work showing the possibility of release of previously adsorbed residues of glyphosate upon phosphorus fertilisation[21]. This is a concern both for increased risk of herbicide injury in later crop rotations[22], but also for movement of glyphosate off-site[23] or non-target effects. Glyphosate has been detected in several environmental compartments including waterways[6], soil[24], dust[25], sediment[26] and rainwater[27]. Glyphosate resistant crops are widely adopted due to glyphosate's broad spectrum nature, and the general lack of drawbacks of glyphosate resistant crops when compared to non-resistant varieties in terms of similar nutrient uptake and disease resistance[28]. However, recent works have shown that aminomethylphosphonic acid (AMPA), the main degradation product of glyphosate, has phytotoxic properties[29], and may even lead to herbicide injury in glyphosate resistant crops[30].

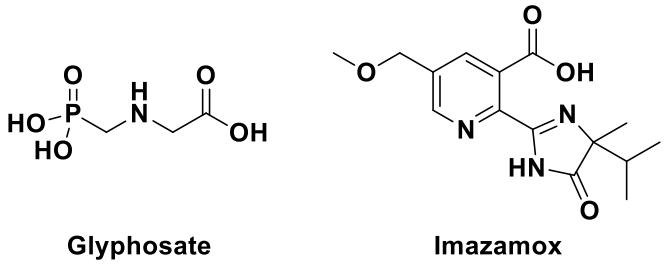

Figure 1: Structure of glyphosate (left) and imazamox (right)

While the bulk of the work presented in this thesis focuses on the glyphosate, there was an additional focus on the herbicide imazamox (2-[(RS)-4-isopropyl-4-methyl-5-oxo-2-imidazolin2-yl]-5-methoxymethylnicotinic acid). Commonly sold under the tradename Raptor®, imazamox is a systemic group 2 (Acetolactate Synthase inhibitor) herbicide that may be applied either pre- or post- emergence for the control of broad leaf weeds in several cropping systems[31-32]. It may exist as a zwitterion in the soil, and has pKa's of 2.3, 3.3 and 10.8[33]. It has been shown to have a relatively long persistence, producing herbicide injury in crops planted one year post application in some sites[34], and is metabolised slower under acidic conditions[35]. Imazamox may also form complexes with metal ions such as Fe^{3+} [36], resulting in increased adsorption and thus persistence. It was developed by BASF and is part of the "Clearfield" system, which partners imidazole herbicides with crops which have been bred specifically to have resistance to these herbicides. Imazamox is degraded aerobically in the soil, with no known herbicidal metabolites produced[37]. It may also undergo photo degradation, through cleavage of the C-O, C-N and C=N bonds[38].

1.2 Adsorption

1.2.1 Adsorption Isotherms. Use and Differences

Adsorption is the phenomena by which a molecule (adsorbate) binds to the surface of a secondary material (adsorbent). The mechanism of this adsorption and level to which it occurs has impacts on solubility of compound, and thus its concentration. In soil science in particular, this translates to soil pore water concentration, and thus availability of herbicide for plant uptake and microbial metabolism. Isotherms are a common way of describing adsorption in a

given bulk system. While they do not necessarily describe the mechanism of this binding itself, depending on the isotherm, they can give information on the process at an individual molecular scale. To develop an isotherm, the target adsorbate is plotted as a function of equilibrium solution concentration. Data is then fitted against a known isotherm equation, such as the Freundlich isotherm[39]. Isotherm equations are chosen based on the assumptions involved, and theoretical knowledge of the system. Some isotherms are empirical (Freundlich), whereas others are based on a solid theoretical footing (e.g. Volmer[40], Langmuir[41]). For example, based on the thermodynamic premises in its derivation, a Langmuir isotherm assumes a smooth homogeneous surface, for a rough surface, a Freundlich may provide a better fit, despite providing no physical information.

The three adsorption isotherm equations explored in this thesis are the Freundlich, Langmuir and Frumkin-Fowler-Guggenheim (FFG)[42-43] isotherms. A Freundlich isotherm takes the form of Equation (1), where q is the concentration of adsorbate adsorbed to the surface (µg g^{-1}), C is the concentration of adsorbate in solution (µg ml^{-1}) K_f and n_f are arbitrary fitting variables, determined based on the data. While interlinked, the main role of K_f is to describe how readily the adsorbate will bind to the surface, an empirical measure of the affinity of the adsorbate for the interface and n_f describes the saturation point of the system (though due to the nature of the equation, a true "saturation" point does not exist). Due to the arbitrary nature of K_f and n_f, no physical information about the system can be extrapolated from this fitting, although it is a useful way of describing and comparing adsorption data under variable conditions. The empirical nature of the Freundlich equation makes it useful to describe adsorption on poorly defined rough and heterogeneous surfaces, making it popular in soil science.

$$q = K_f C^{\frac{1}{n_f}} \tag{1}$$

$$\frac{\theta}{1-\theta} = K_L C \tag{2}$$

$$\frac{\theta}{1-\theta}\, e^{b\theta} = K_{Fr}C \tag{3}$$

$$\theta = \frac{q}{q_{max}} \tag{4}$$

$$K_{ads} = e^{\frac{\Delta G}{RT}} \tag{5}$$

Langmuir isotherms are given by Equation (2), where Θ is described by Equation (4), q_{max} is the maximum adsorbed adsorbate concentration possible (µg g^{-1}), or saturation point, and K_L is the Langmuir constant, which is defined by the Gibbs energy of adsorption (as given in Equation (5), where *T* is temperature and *R* is the ideal gas constant) and describes how stronglyy the adsorbate binds to the surface. Fitting of a Langmuir isotherm gives far more information about the chemistry of the system, including the saturation concentration of the surface. K_L may also be used to calculate the Gibbs Free Energy of adsorption in the system. However, it is not without its drawbacks, as it assumes a smooth, homogeneous surface, and a constant energy of adsorption, irrespective of the fractional occupancy of the surface. It also assumes q_{max} to be entirely spatially defined, which suggest that as the environment in which the adsorption occurs changes, only the energy of adsorption should change, and that the final saturation level should remain constant.

To overcome some of these drawbacks, the Frumkin –Fowler-Guggenheim isotherm equation was developed[42-43], and is described by Equation (3). The addition of the exponential term allows for the lateral interaction of adsorbate molecules, and charge – charge interactions between the adsorbate and adsorbent surface (these interactions are described by the *b* term). This allows for a changing energy of adsorption as the surface is filled. This means that while q_{max} is still spatially defined, and will remain constant regardless of the environment in which the adsorption occurs, the "effective" maximum adsorption can change, as the energy of adsorption can increase to the point where adsorption becomes thermodynamically unfavourable unless the chemical potential (approximately equivalent to concentration of adsorbate in the system)

reaches extreme levels. This allows for much more physicochemical information about the system to be extracted from the fitting of results than can be determined from the other two isotherms explored here. It should be noted that all of the isotherms here assume single layer adsorption, and do not account for possible double layer effects.

Isotherms are generally fitted to experimental data through the linearization of the appropriate isotherm equation (with the same transformations being performed to the experimental data), followed by a linear regression to determine the fitting constants. For example, Equation (1) can be linearised to Equation (6) by taking the natural logarithm of each side. Thus the natural logarithm of experimental adsorbed and solution concentration can be taken, and a linear regression performed (with adsorbed concentration as the independent variable and solution concentration as the dependent variable). The slope of this regression gives the value for one on n_f, and the exponent of the intercept-on-slope gives K_f

$$\log q = \log K_f + \frac{1}{n_f} \log C \tag{6}$$

1.2.2 Glyphosate Adsorption Behaviour

Biological exposure to glyphosate is regulated by its persistence, mobility and bioavailability. These factors are, in turn, largely regulated by its adsorption to soil. Sorption can moderate the efficacy of glyphosate by reducing its uptake by plants[44], as well as influencing pathways for mobilization through the soil[45-46], including its movement to waterways during a flooding event[47]. Sorption is also known to significantly affect the persistence of glyphosate in soil[48], altering how readily it is available for microbial metabolism or co-metabolism.

Glyphosate exists as a zwitterion in soil, with a negatively charged phosphonic acid and carboxylic acid group and a positively charged amine group, depending on the pH of the soil[49]. It primarily binds to amorphous soil minerals such as iron and aluminium oxides and hydroxides[50]. Soil pH and mineralogy therefore have a significant effect on binding, with

adsorption decreasing as pH increases[51]. This is mainly due to the change in surface charge on soil minerals, rather than the change in ionic form of glyphosate (pK_a = 2, 2.6, 5.8 and 10.8, occurring due to protonation and deprotonation of the phosphate, amine and carboxylic acid groups, respectively), as glyphosate is negatively charged at pH above 2.6[49]. Most metal oxides found in soil are positively charged at environmentally relevant pH, however, as pH increases, negatively charged sites may develop[52], this would suggest an attraction of glyphosate to these surfaces at low pH (acidic soils), reducing as pH increases[53]. The binding of glyphosate to metal oxide surfaces has been shown to occur predominantly through the phosphonic acid functional group of the molecule[54]. Based on this binding through the phosphate head group, it might be expected that glyphosate shows a high affinity for metal oxides, similar to phosphate[55-56].

Due to the nature of glyphosate adsorption, it seems likely that competition may occur between glyphosate and inorganic phosphate[57-58], including the remobilisation of glyphosate from biochar (carbonized organic matter)[59]. In other studies the rate of desorption of glyphosate from goethite was found to be independent of the competing entering ligand[60], disputing the competitive mechanism. Regardless, multiple studies have shown a risk of soil borne residues of glyphosate being re-released by the addition of P fertiliser, increasing the risk of herbicide injury in rotational crops in some soil types[21-22, 61].

Due to the general paucity of information on the mechanisms in which glyphosate adsorbs to the various soil minerals, the work in this thesis study aims to develop an understanding of the sorption behaviour and mechanism as it relates to individual components in the soil, such as metal oxides and fixed charge clay minerals. Mechanistic understanding of adsorption would allow for the improvement of regulatory procedures, and an understanding of the impact that soil management, such as liming (to increase pH of acidic soils) and “claying” (clay applied to sandy soils to improve a range of structural and chemical properties), may have on herbicide behaviour in the soil. This information would also be essential as inputs for highly successful

predictive physicochemical models of the behaviour and fate of organic “contaminants” like glyphosate in soils, such as sophisticated models developed by the Dutch soil science school, including ORCHESTRA[62].

1.3 Predictive Modelling of Glyphosate Adsorption Behaviour

1.3.1 Pedotransfer Rules Using Physico-chemical Properties

Despite the factors influencing glyphosate sorption being relatively well-known[63], there have been few attempts to formalise rapid, inexpensive, and easy to use models for estimating glyphosate sorption based on soil properties as an alternative to constructing soil-specific isotherms via batch or column sorption studies (Table 1). Paradelo et al. (2015) proposed a multiple linear regression model based on soil characteristics as predictors providing the best fit for linear adsorption of glyphosate (K_d). Glyphosate sorption was shown to increase with increasing clay and iron content, but to decrease with increasing pH, electrical conductivity (EC) and P levels. Although pH and clay content are often the best predictors of glyphosate sorption, there is often variation from study to study, due in part to the limited number of soils examined (Table 1).

Table 1: Overview of previous adsorption predictive modelling

Reference	# Soil Samples	Parameters Predicted	Type of Model	R^2	Predictors included in best model [c]
Dollinger et al. (2015)[64]	19-51[a]	K_d, K_f, n_f	MLR	K_d: 0.48 K_f: 0.52 n_f: 0.62	K_d: CEC, Clay K_f: CEC, Clay, OC n_f: Clay, pH
Paradelo et al. (2015)[65]	114 (2 fields)	K_d	MLR	0.70 (4 variables)	pH, EC, Clay, Sand (both fields)
Sidoli et al. (2016)[66]	17	K_f [b]	MLR, exponential	0.94 (4 variables)	pH, Olsen P[67], Al_{ox}, Fe_{ox}
De Geronimo et al. (2018)[68]	12	K_f	MLR	0.994 (7 variables)	Clay, pH, Bray P[69], Al_{in}, OC, Sand, Fe_{ox}

[a] Depending on predicted parameter and available predictors

[b] calculated using average n_f value of all soils

[c] Fe_{ox} and Al_{ox} = oxalate extractable iron and aluminium

[d]CEC = cation exchange capacity, EC = electrical conductivity, P = phosphorus, OC = organic carbon, MLR = Multiple linear Regression

K_d is the slope of a linear fit of adsorption data, K_f and n_f are fitting variables of adsorption derived from the Freundlich equation

Furthermore, as acknowledged by Paradelo et al. (2015), non-linear relationships between predictor variables and sorption may better describe interactions (e.g. the change in surface charge on clay minerals at high pH). More recently, Sidoli et al. (2016) built on the previous work from Paradelo et al. (2015) by increasing the sample size from 2 to 17 contrasting sites, fitting a variety of linear and nonlinear regressions to a Freundlich isotherm derived sorption value (K_f) and evaluating the relevance of different measures of pH (i.e. in water, KCl and $CaCl_2$). However, despite the increased number of different soil types, the use of a single sample from each site resulted in a total of only 17 data points. Sidoli et al. (2016) also restricted their modelling framework to linear and exponential relationships between the dependent and independent

variables, which may not adequately account for certain interactions involved in glyphosate binding. De Geronimo et al. (2018) conducted similar modelling using 12 Argentinian soils, finding seven variables to be important for predicting glyphosate adsorption (Table 1). While these soils had greater variation than those in the previous two studies, the relatively small number of data points and lack of alkaline soils limits the broader applicability of the model. Furthermore, despite the clear link between P and glyphosate binding[51, 70-71], no previous work has examined whether a correlation exists between glyphosate sorption and routinely collected measures of the binding affinity for P, such as the P buffering index (PBI).

1.3.2 MIR Modelling

Mid-infrared reflectance (MIR) spectroscopy is a cheap, rapid, holistic technique that can bypass the need for time consuming, sometimes expensive wet chemical techniques, provided adequate calibration is conducted. MIR spectroscopy is based on the adsorbance of infrared light by molecular bonds, in the form of vibrational and rotational energies. As such, the spectra are impacted not only by the atomic makeup and connectivity of the substrate, but also by the molecular arrangement and physical properties, such as surface topology, which may impact intramolecular bonding and thus vibrational/rotational energy of the bonds. This allows MIR to provide significant information about the substrate through the use of multivariate modelling[72]. Common techniques for calibrating a MIR model from a sample data set include linear techniques such as principle component regression (PCR)[73] and partial least squares regression (PLS-R)[74], and non-linear techniques such as support vector machines (SVM)[75].

Infrared spectra may provide information on a wide range of soil properties, and can accurately predict soil texture[76], mineralogy[77], speciation of organic matter[78] and pH[79]. Previous studies have also used MIR to produce robust predictive models for the adsorption to soil of other herbicides such as diuron[74, 80], atrazine[81], lindane and linuron[82]. Although Paradelo et al (2016) also used this technique to predict glyphosate adsorption in soils with a relatively high level of

success[83], the calibration set only contained samples from two adjacent fields, covering a limited amount of soil variation.

To address this current paucity of data on the use of MIR to predict glyphosate adsorption , work in this thesis looks at the development of various predictive models of glyphosate adsorption in soil, using both physicochemical properties and MIR spectra as predictors. This bypasses the need for lengthy, difficult and expensive ^{14}C-labelling or HPLC based adsorption studies, thus making adsorption data for individual soils more accessible and producing more spatially explicit recommendations for glyphosate management.

1.4 Current and Emerging Methods for Herbicide Monitoring

Due to the possible impacts of herbicides on the surrounding environment and later crop rotations, routine testing for herbicides in soil is important. Current soil analysis methods are relatively expensive, and are generally based on an exhaustive extraction of the soil[84], giving a value of "total" herbicide present, rather than herbicide available for uptake by plants (the "bioavailable" fraction), which is more useful for risk assessment[85]. Herbicide bioavailability is impacted by a wide range of factors in the soil, in particular adsorption of the herbicide to the soil[86-87]. The development of a method which measures only the bioavailable fraction (thus excluding herbicide unavailable for uptake due to adsorption or other processes) would provide significant advantages in assessing the possibility of crop damage and leaching at sites where pesticide persistence is likely.

Diffusive Gradient Thin Film (DGT) sampling has been used extensively in water sampling to produce an average "over-time" measurement of contamination (both organic and inorganic), as opposed to the "snapshot' produced by grab sampling. The first instance of the use of DGTs, for assessing heavy metal contamination in waterways, was reported in 1994 by Davison and Zhang[88], and has since seen significant research interest[89-90]. Due to the nature of capture through adsorption in a relatively sheltered environment, these passive samplers limit the

amount of degradation of contaminant that may occur during collection and transport[91], leading to a more accurate result.

DGT samplers consist of a binding layer, diffusive layer, and in some cases a porous membrane filter to protect the other layers from particulate matter. The diffusive and binding layers are hydrogels, with the binding layer including an adsorbent dispersed throughout the gel. The adsorbent in the binding layer is chosen specific to the analyte of interest, to increase potential adsorption, and thus reduce the likelihood of saturation. The construction of a standard DGT with protective membrane filter is shown in Figure 2. The analyte moves through the diffusive layer and binds to the adsorbent in binding layer removing it from solution, this leads to a constant concentration gradient throughout the diffusive layer, and thus a steady rate of diffusion and uptake[92]. Because of this, uptake of a given analyte by the DGT is dependent on the size of the exposure window, thickness of the diffusive gel layer, exposure time, and concentration of the analyte in the sampling media[88]. It is commonly assumed that lateral diffusion, and the thickness of the diffusive boundary layer created at the interface of solution and sampler due to water viscosity are negligible. This situation can be described using Fick's Laws of diffusion[93], resulting in Equation 6, where C is the concentration of the analyte in solution, D is the diffusion coefficient of the analyte, t is exposure time, A is the area of the exposure window, Δg is the thickness of the diffusive gel, and m is the mass of analyte contained in the binding layer.

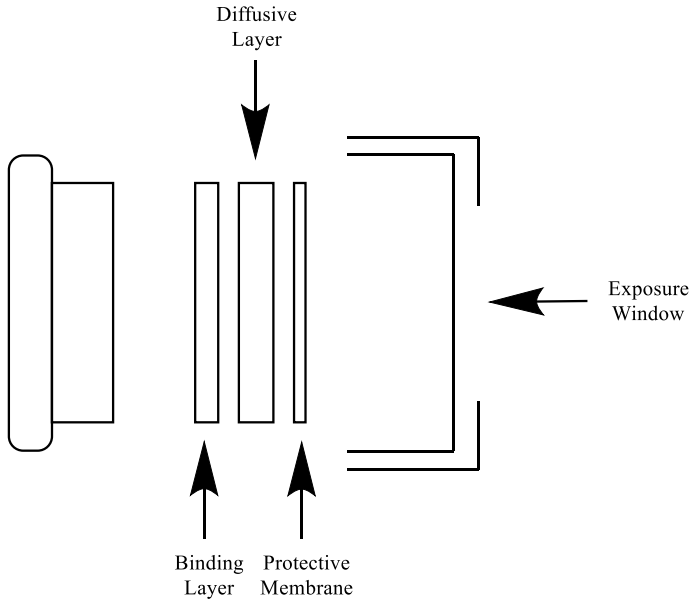

Figure 2: DGT Construction

$$C = \frac{m \times \Delta g}{t \times D \times A} \tag{6}$$

However, in reality, the diffusive boundary layer will not be two dimensional, and lateral diffusion can occur around the edges of the exposure window. In order to account for this, Equation (7) can be used, where k_{id} is the lateral diffusion flux increase coefficient, D_w is the diffusion coefficient of the analyte in water, and δ is the thickness of the diffusive boundary layer.

$$C = \frac{m}{k_{id}At}\left(\frac{\Delta g}{D} + \frac{\delta}{D_w}\right) \tag{7}$$

More recently, the technology has been applied in assessing heavy metal contamination in soils[94-95], mineral and nutrient plant availability[96-97], and some organic contaminants in waterways[98] and soil[99]. The application of DGTs to organic contaminants in soil has been undertaken for a wide variety of pesticides in recent a study[100]. Due to the passive nature of uptake of contaminants by DGT, it has been suggested they mimic the uptake by plant roots and give a measurement of bioavailable herbicide[101-102]. However, to date, very few studies[99] have compared the uptake of DGT samplers directly to uptake by a plant species in order to

determine its ability to mimic a root system. This comparison would add further credence to the use of DGTs in risk assessment scenarios, and allow a higher level of confidence in their use under field conditions. This would be extremely beneficial, as DGTs would allow a more rapid testing, due to the 24-48 hour exposure, compared to the several weeks growth time required for plant testing. DGT testing is also likely to be more consistent, due to both the reduction in breakdown of herbicide post uptake (plant roots may metabolise or compartmentalise herbicides removed from soil) and removing the biological variability inherent in plant trials (ie. damaged roots or individual variations in plant growth leading to different uptake levels).

1.5 Study Context

With increasing concern around the environmental, ecological, economic and health concerns surrounding herbicide usage, combined with a growing world population and thus reliance on agrochemicals for a stable food supply, a greater understanding of herbicide behaviour in soil, and new methods for assessing herbicide persistence and risk is needed.

The mobility and degradation of widely used glyphosate and imazamox, chosen for this study are heavily dependent on their adsorption behaviour and bioavailability. This is generally not accounted for by herbicide labels, which focus instead on climatic conditions of a given region influencing their degradation rate. Thus the results of this study have the potential to greatly improve on-farm herbicide management strategies, by providing site (soil)-specific information of herbicide behaviour in soil.

1.6 Study Aims

With a heightened awareness of the environmental and economic impacts of herbicide usage due to leaching and persistence, along with a growing population and thus increased reliance on these chemicals, this study aimed to increase the understanding of herbicide behaviour in soil, and to develop new tools (methods) that are more applicable to the assessment of risk from the herbicides. In brief, this can be outlined in the following research objectives

- Develop new predictive models of glyphosate adsorption to soil based on physicochemical properties or MIR spectra of soil
- Elucidate the adsorption/desorption behaviour of glyphosate to model soil minerals, and the impacts of pH and competitive binding of phosphate
- Assess the ability of DGT techniques to predict the level of herbicide in soil available for plant uptake, by way of a comparison with the uptake of imazamox by two varieties of rapeseed

From these research objectives, the following hypotheses can be derived:

- Glyphosate adsorption in contrasting soils can be predicted more efficiently by routinely measured soil physicochemical properties and MIR spectroscopy than previous attempts (Chapter 2 and 3)
- Glyphosate adsorption to soil minerals is dependent on surface area and ionic charge considerations that are better described by FFG than other historically preferred sorption isotherms (Chapter 4)
- Glyphosate and phosphate compete for soil binding sites, hence glyphosate desorption will occur upon addition of a phosphate source to mineral systems to which glyphosate is adsorbed (Chapter 5)
- DGT samplers will be able to accurately replicate and predict levels of plant-available imazamox in contrasting agricultural soils (Chapter 6)

1.7 Thesis Outline

This thesis outlines the development of new predictive models for glyphosate adsorption in the soil. Based on the results from this, further exploration of the mechanisms involved in glyphosate adsorption to and desorption from model soil minerals was undertaken, in particular assessing the role of pH and phosphorus competition, to understand the impacts of agronomic practices on glyphosate efficacy and release. Finally, a comparative study was performed, comparing a new herbicide monitoring technique (DGT) to plant uptake of imazamox, in order to provide further evidence of DGT as a measure of 'available' herbicide in the soil.

A predictive model for glyphosate adsorption to soil based on physicochemical characteristics of the soil is presented in Chapter 2. A database of 90 soils is developed, with various measures such as pH, Colwell P, phosphorus buffering index (PBI) and soil texture. Glyphosate adsorption experiments were conducted, and a statistical model (GAMS) used to produce predictions of glyphosate adsorption affinity based on these characteristics. A further set of 7 soils outside of the initial model building database is used to validate the predictive capabilities of the model.

A second predictive model of glyphosate adsorption, based on MIR spectroscopy, is presented in Chapter 3. This again used a modified database of 90 soils, with the same adsorption experiments conducted, but instead MIR spectra is used to predict this adsorption behaviour, and some physicochemical properties of the soils. This model is then cross validated by a venetian blinds methodology (discussed in detail in Chapter 3), and the loadings compared to MIR spectra of pure soil minerals to develop an understanding of the components of soil most important for glyphosate adsorption.

Based on the results of the previous two chapters, a study of glyphosate adsorption to model soil minerals was conducted to elucidate the mechanisms by which this occurs. This study compares the binding affinity of glyphosate to various metal oxides and clays under different pH conditions. From this, details about the role of charge, lateral interactions between

adsorbate molecules and attraction of the adsorbate molecule to the adsorbent surface are elucidated. The results of this study are presented in Chapter 4.

Chapter 5 is a logical extension of the adsorption study described in Chapter 4 and presents a study of the desorption of glyphosate from model soil minerals, and the competition that occurs between glyphosate and inorganic phosphate for binding sites. This study is practically relevant, as it highlights the impacts phosphorus fertilisation may have both on the efficacy of applied glyphosate, but also on the release of bound glyphosate residues in the soil.

Adsorption is one of the many mechanisms that impact the level of herbicide available for plant uptake and hence the efficacy of herbicides. Diffusive gradient thin films have been presented as an alternative methodology for the measurement of herbicide in soils, providing a measure of available rather than total herbicide. In order to test the practical significance of Diffusive Gradient Thin Film devices, Chapter 6 of this thesis presents a comparative study of the uptake of imazamox from soils by DGT and by two varieties of rapeseed. Finally, Chapter 7 collates the key findings of the research presented in this thesis, and recommends avenues that should be pursued in future work.

1.8 References

1. Cooper, J.; Dobson, H., The benefits of pesticides to mankind and the environment. *Crop Protection* **2007,** *26* (9), 1337-1348.
2. Wasim, A.; Dwaipayan, S.; Ashim, C., Impact of pesticides use in agriculture: their benefits and hazards. *Interdisciplinary Toxicology* **2009,** *2* (1), 1-12.
3. WSSA, Summary of Herbicide Mechanism of Action According to the Weed Science Society of America (WSSA). Weed Science Society of America: **2016**.
4. Croplife Australia., Herbicide Mode of Action Groups. Croplife Australia: **2017**.
5. Moreland, D. E., Mechanisms of action of herbicides. *Annual Review of Plant Physiology* **1980,** *31*, 597-638.
6. Borggaard, O. K.; Gimsing, A. L., Fate of glyphosate in soil and the possibility of leaching to ground and surface waters: a review. *Pest Management Science* **2008,** *64* (4), 441-456.
7. Huang, X.; Fong, S.; Deanovic, L.; Young, T. M., Toxicity of herbicides in highway runoff. *Environmental Toxicology and Chemistry* **2005,** *24* (9), 2336-2340.
8. Druart, C.; Millet, M.; Scheifler, R.; Delhomme, O.; de Vaufleury, A., Glyphosate and glufosinate-based herbicides: fate in soil, transfer to, and effects on land snails. *Journal of Soils and Sediments* **2011,** *11* (8), 1373-1384.

9. Nguyen, D. B.; Rose, M. T.; Rose, T. J.; Morris, S. G.; van Zwieten, L., Impact of glyphosate on soil microbial biomass and respiration: A meta-analysis. *Soil Biology and Biochemistry* **2016,** *92*, 50-57.
10. Rose, M. T.; Cavagnaro, T. R.; Scanlan, C. A.; Rose, T. J.; Vancov, T.; Kimber, S.; Kennedy, I. R.; Kookana, R. S.; Van Zwieten, L., Impact of Herbicides on Soil Biology and Function., *Advances in Agronomy*, Donald, L. S., Ed. Academic Press: **2016**; Vol. 136, pp 133-220.
11. Chang, F.; Simcik, M. F.; Capel, P. D., Occurrence and fate of the herbicide glyphosate and its degradate aminomethylphosphonic acid in the atmosphere. *Environmental Toxicology and Chemistry* **2011,** *30* (3), 548-555.
12. Picó, Y.; Blasco, C.; Font, G., Environmental and food applications of LC–tandem mass spectrometry in pesticide-residue analysis: An overview. *Mass Spectrometry Reviews* **2004,** *23* (1), 45-85.
13. Alavanja, M. C. R.; Samanic, C.; Dosemeci, M.; Lubin, J.; Tarone, R.; Lynch, C. F.; Knott, C.; Thomas, K.; Hoppin, J. A.; Barker, J.; Coble, J.; Sandler, D. P.; Blair, A., Use of agricultural pesticides and prostate cancer risk in the agricultural health study cohort. *American Journal of Epidemiology* **2003,** *157* (9), 800-814.
14. Hoppin, J. A.; Umbach, D. M.; London, S. J.; Alavanja, M. C. R.; Sandler, D. P., Chemical predictors of wheeze among farmer pesticide applicators in the agricultural health study. *American Journal of Respiratory and Critical Care Medicine* **2002,** *165* (5), 683-689.
15. Palma, G.; Demanet, R.; Jorquera, M.; Mora, M. L.; Briceño, G.; Violante, A., Effect of pH on sorption kinetic process of acidic herbicides in a volcanic soil. *Journal of soil science and plant nutrition* **2015,** *15*, 549-560.
16. Cheah, U.B.; Kirkwood, R. C.; Lum, K.Y., Degradation of four commonly used pesticides in malaysian agricultural soils. *Journal of Agricultural and Food Chemistry* **1998,** *46* (3), 1217-1223.
17. Benbrook, C. M., Trends in glyphosate herbicide use in the United States and globally. *Environmental Sciences Europe* **2016,** *28* (1), 3.
18. Giesy, J. P.; Dobson, S.; Solomon, K. R., Ecotoxicological Risk Assessment for Roundup® Herbicide., *Reviews of Environmental Contamination and Toxicology: Continuation of Residue Reviews*, Ware, G. W., Ed. Springer New York: New York, NY, **2000**; pp 35-120.
19. Roy, D. N.; Konar, S. K.; Banerjee, S.; Charles, D. A.; Thompson, D. G.; Prasad, R., Persistence, movement, and degradation of glyphosate in selected Canadian boreal forest soils. *Journal of Agricultural and Food Chemistry* **1989,** *37* (2), 437-440.
20. Primost, J. E.; Marino, D. J. G.; Aparicio, V. C.; Costa, J. L.; Carriquiriborde, P., Glyphosate and AMPA, "pseudo-persistent" pollutants under real-world agricultural management practices in the Mesopotamic Pampas agroecosystem, Argentina. *Environmental Pollution* **2017,** *229*, 771-779.
21. Bott, S.; Tesfamariam, T.; Kania, A.; Eman, B.; Aslan, N.; Römheld, V.; Neumann, G., Phytotoxicity of glyphosate soil residues re-mobilised by phosphate fertilisation. *Plant and Soil* **2011,** *342* (1), 249-263.
22. Rose, T.; Van Zwieten, L.; Claassens, A.; Scanlan, C.; Rose, M., Phytotoxicity of soilborne glyphosate residues is influenced by the method of phosphorus fertiliser application. *Plant Soil* **2017**; *422*, 455-465.
23. Norgaard, T.; Moldrup, P.; Ferré, T. P. A.; Olsen, P.; Rosenbom, A. E.; de Jonge, L. W., Leaching of glyphosate and aminomethylphosphonic acid from an agricultural field over a twelve-year period. *Vadose Zone Journal* **2014,** *13* (10).
24. Silva, V.; Montanarella, L.; Jones, A.; Fernández-Ugalde, O.; Mol, H. G. J.; Ritsema, C. J.; Geissen, V., Distribution of glyphosate and aminomethylphosphonic acid (AMPA) in agricultural topsoils of the European Union. *Science of The Total Environment* **2018,** *621*, 1352-1359.

25. Mendez, M. J.; Aimar, S. B.; Aparicio, V. C.; Ramirez Haberkon, N. B.; Buschiazzo, D. E.; De Gerónimo, E.; Costa, J. L., Glyphosate and aminomethylphosphonic acid (AMPA) contents in the respirable dust emitted by an agricultural soil of the central semiarid region of Argentina. *Aeolian Research* **2017,** *29*, 23-29.
26. Xu, D.; Meyer, S.; Gaultier, J.; Farenhorst, A.; Pennock, D., Land use and riparian effects on prairie wetland sediment properties and herbicide sorption coefficients. *Journal of Environmental Quality* **2009,** *38* (4), 1757-65.
27. Battaglin, W. A.; Meyer, M. T.; Kuivila, K. M.; Dietze, J. E., Glyphosate and its degradation product AMPA occur frequently and widely in U.S. soils, surface water, groundwater, and precipitation. *Journal of the American Water Resources Association* **2014,** *50* (2), 275-290.
28. Duke, S. O.; Lydon, J.; Koskinen, W. C.; Moorman, T. B.; Chaney, R. L.; Hammerschmidt, R., Glyphosate effects on plant mineral nutrition, crop rhizosphere microbiota, and plant disease in glyphosate-resistant crops. *Journal of Agricultural and Food Chemistry* **2012,** *60* (42), 10375-10397.
29. Blackshaw, R. E.; Harker, K. N., Wheat, field pea, and canola response to glyphosate and AMPA soil residues. *Weed Technology* **2017,** *30* (4), 985-991.
30. Ding, W.; Reddy, K. N.; Zablotowicz, R. M.; Bellaloui, N.; Arnold Bruns, H., Physiological responses of glyphosate-resistant and glyphosate-sensitive soybean to aminomethyl-phosphonic acid, a metabolite of glyphosate. *Chemosphere* **2011,** *83* (4), 593-598.
31. Walker, G. W.; Kookana, R. S.; Smith, N. E.; Kah, M.; Doolette, C. L.; Reeves, P. T.; Lovell, W.; Anderson, D. J.; Turney, T. W.; Navarro, D. A., Ecological risk assessment of nano-enabled pesticides: A perspective on problem formulation. *Journal of Agricultural and Food Chemistry* **2018,** *66* (26), 6480-6486.
32. Eizenberg, H.; Hershenhorn, J.; Ephrath, J. E., Factors affecting the efficacy of Orobanche cumana chemical control in sunflower. *Weed Research* **2009,** *49* (3), 308-315.
33. Hatzios, K., *Herbicide Handbook of the Weed Science Society of America. 7th ed.* Weed Sci Soc Amer: Champagen, IL, **1998**.
34. Ball, D. A.; Yenish, J. P.; Alby, T., Effect of imazamox soil persistence on dryland rotational crops. *Weed Technology* **2017,** *17* (1), 161-165.
35. Aichele, T. M.; Penner, D., Adsorption, desorption, and degradation of imidazolinones in soil. *Weed Technology* **2017,** *19* (1), 154-159.
36. Cabrera, A.; Celis, R.; Hermosín, M. C., Imazamox–clay complexes with chitosan- and iron(III)-modified smectites and their use in nanoformulations. *Pest Management Science* **2016,** *72* (7), 1285-1294.
37. U. S. EPA, Imazamox (Raptor Herbicide) Pesticide Fact Sheet. Office of Prevention, Pesticide and Toxic Substances, **1997**.
38. Harir, M.; Frommberger, M.; Gaspar, A.; Martens, D.; Kettrup, A.; El Azzouzi, M.; Schmitt-Kopplin, P., Characterization of imazamox degradation by-products by using liquid chromatography mass spectrometry and high-resolution Fourier transform ion cyclotron resonance mass spectrometry. *Analytical and Bioanalytical Chemistry* **2007,** *389* (5), 1459-1467.
39. Freundlich, H., Über die adsorption in lösungen. *Zeitschrift für Physikalische Chemie* **1907,** *57* (4), 385-470.
40. Volmer, M. A.; Manhert, P., Solution of solid substances in liquid surfaces and the characteristics of layers thus produced. *Zeitschrift für Physikalische Chemie* **1925,** *115*, 253.
41. Langmuir, I., The adsorption of gases on plane surface of glass, mica and platinum. *The Research Laboratory of the General Electric Company* **1918,** *40* (9), 1361-1402.
42. Fowler, R. H.; Guggenheim, E. A., *Statistical Thermodynamics*. Cambridge University Press: **1939**.

43. Lyklema, J., Appendix 1 - Survey of adsorption isotherms and two-dimensional equations of state for homogeneous, nonporous surfaces. Monolayer regime. In *Fundamentals of Interface and Colloid Science*, Ed. Academic Press: **1995**; Vol. 2, pp A1-1-A1-2.
44. Simonsen, L.; Fomsgaard, I. S.; Svensmark, B.; Spliid, N. H., Fate and availability of glyphosate and AMPA in agricultural soil. *Journal of Environmental Science and Health, Part B* **2008,** *43* (5), 365-375.
45. McGrath, G. S.; Hinz, C.; Sivapalan, M., A preferential flow leaching index. *Water Resources Research* **2009,** *45* (11), W114505.
46. McGrath, G. S.; Hinz, C.; Sivapalan, M., Modelling the impact of within-storm variability of rainfall on the loading of solutes to preferential flow pathways. *European Journal of Soil Science* **2008,** *59* (1), 24-33.
47. Dollinger, J.; Dagès, C.; Negro, S.; Bailly, J.-S.; Voltz, M., Variability of glyphosate and diuron sorption capacities of ditch beds determined using new indicator-based methods. *Science of The Total Environment* **2016,** *573*, 716-726.
48. Al-Rajab, A. J.; Schiavon, M., Degradation of ^{14}C-glyphosate and aminomethylphosphonic acid (AMPA) in three agricultural soils. *Journal of Environmental Sciences* **2010,** *22* (9), 1374-1380.
49. Sprankle, P.; Meggitt, W. F.; Penner, D., Adsorption, mobility, and microbial degradation of glyphosate in the soil. *Weed Science* **1975,** *23* (3), 229-234.
50. Morillo, E.; Undabeytia, T.; Maqueda, C.; Ramos, A., Glyphosate adsorption on soils of different characteristics.: Influence of copper addition. *Chemosphere* **2000,** *40* (1), 103-107.
51. Zhao, B.; Zhang, J.; Gong, J.; Zhang, H.; Zhang, C., Glyphosate mobility in soils by phosphate application: Laboratory column experiments. *Geoderma* **2009,** *149* (3), 290-297.
52. de Jonge, H.; Wollesen de Jonge, L., Influence of pH and solution composition on the sorption of glyphosate and prochloraz to a sandy loam soil. *Chemosphere* **1999,** *39* (5), 753-763.
53. Pereira, R. C.; Anizelli, P. R.; Di Mauro, E.; Valezi, D. F.; da Costa, A. C. S.; Zaia, C. T. B. V.; Zaia, D. A. M., The effect of pH and ionic strength on the adsorption of glyphosate onto ferrihydrite. *Geochemical Transactions* **2019,** *20* (1), 3.
54. Sheals, J.; Sjöberg, S.; Persson, P., Adsorption of glyphosate on goethite: Molecular characterization of surface complexes. *Environmental Science & Technology* **2002,** *36* (14), 3090-3095.
55. Geelhoed, J. S.; Hiemstra, T.; Van Riemsdijk, W. H., Phosphate and sulfate adsorption on goethite: Single anion and competitive adsorption. *Geochimica et Cosmochimica Acta* **1997,** *61* (12), 2389-2396.
56. Lookman, R.; Freese, D.; Merckx, R.; Vlassak, K.; van Riemsdijk, W. H., Long-Term kinetics of phosphate release from soil. *Environmental Science & Technology* **1995,** *29* (6), 1569-1575.
57. Laitinen, P.; Siimes, K.; Rämö, S.; Jauhiainen, L.; Eronen, L.; Oinonen, S.; Hartikainen, H., Effects of soil phosphorus status on environmental risk assessment of glyphosate and glufosinate-ammonium. *Journal of Environmental Quality* **2008,** *37* (3), 830-838.
58. Padilla, J. T.; Selim, H. M., Interactions among Glyphosate and Phosphate in Soils: Laboratory Retention and Transport Studies. *Journal of Environmental Quality* **2019,** *48* (1), 156-163.
59. Hall, K. E.; Spokas, K. A.; Gamiz, B.; Cox, L.; Papiernik, S. K.; Koskinen, W. C., Glyphosate sorption/desorption on biochars – interactions of physical and chemical processes. *Pest Management Science* **2018,** *74* (5), 1206-1212.
60. Arroyave, J. M.; Waiman, C. C.; Zanini, G. P.; Tan, W.; Avena, M. J., Desorption rate of glyphosate from goethite as affected by different entering ligands: hints on the desorption mechanism. *Environmental Chemistry* **2017,** *14* (5), 288-294.

61. Rosenbom, A.; Haarder, B.; Badawi, N.; Gudmundsson, L.; Von Platten-Hallermund, F.; H Hansen, C.; B Nielsen, C.; Plauborg, F.; Olsen, P., *The Danish Pesticide Leaching Assessment Programme. Monitoring results May 1999–June 2016*. **2017**.
62. Janot, N.; Pinheiro, J. P.; Botero, W. G.; Meeussen, J. C. L.; Groenenberg, J. E., PEST-ORCHESTRA, a tool for optimising advanced ion-binding model parameters: derivation of NICA-Donnan model parameters for humic substances reactivity. *Environmental Chemistry* **2017,** *14* (1), 31-38.
63. Vereecken, H., Mobility and leaching of glyphosate: a review. *Pest Management Science* **2005,** *61* (12), 1139-1151.
64. Dollinger, J.; Dagès, C.; Voltz, M., Glyphosate sorption to soils and sediments predicted by pedotransfer functions. *Environmental Chemistry Letters* **2015,** *13* (3), 293-307.
65. Paradelo, M.; Norgaard, T.; Moldrup, P.; Ferré, T. P. A.; Kumari, K. G. I. D.; Arthur, E.; de Jonge, L. W., Prediction of the glyphosate sorption coefficient across two loamy agricultural fields. *Geoderma* **2015,** *259–260*, 224-232.
66. Sidoli, P.; Baran, N.; Angulo-Jaramillo, R., Glyphosate and AMPA adsorption in soils: laboratory experiments and pedotransfer rules. *Environmental Science and Pollution Research* **2016,** *23* (6), 5733-5742.
67. Olsen, S.; Cole, C.; Watanabe, F.; Dean, L., Estimation Of Available Phosphorus In Soils By Extraction With Sodium Bicarbonate., *USDA Circular Nr 939*, US Gov. Print Office: Washington, D.C., **1954**.
68. De Gerónimo, E.; Aparicio, V. C.; Costa, J. L., Glyphosate sorption to soils of Argentina. Estimation of affinity coefficient by pedotransfer function. *Geoderma* **2018,** *322*, 140-148.
69. Bray, R.; Kurtz, L., Determination of total, organic, and available forms of phosphorus in soils. *Soil Science* **1945,** *59*, 39-45.
70. Gimsing, A. L.; Borggaard, O. K., Effect of phosphate on the adsorption of glyphosate on soils, clay minerals and oxides. *International Journal of Environmental Analytical Chemistry* **2002,** *82* (8-9), 545-552.
71. Wang, Y. J.; Zhou, D. M.; Sun, R. J., Effects of phosphate on the adsorption of glyphosate on three different types of Chinese soils. *Journal of Environmental Science* **2005,** *17* (5), 711-5.
72. Forina, M.; Lanteri, S.; Casale, M., Multivariate calibration. *Journal of Chromatography A* **2007,** *1158* (1), 61-93.
73. Næs, T.; Martens, H., Principal component regression in NIR analysis: Viewpoints, background details and selection of components. *Journal of Chemometrics* **1988,** *2* (2), 155-167.
74. Forouzangohar, M.; Kookana, R. S.; Forrester, S. T.; Smernik, R. J.; Chittleborough, D. J., Midinfrared spectroscopy and chemometrics to predict diuron sorption coefficients in soils. *Environmental Science & Technology* **2008,** *42* (9), 3283-3288.
75. Siqueira, L. F. S.; Morais, C. L. M.; Araújo Júnior, R. F.; de Araújo, A. A.; Lima, K. M. G., SVM for FT-MIR prostate cancer classification: An alternative to the traditional methods. *Journal of Chemometrics* **2018,** *32* (12), e3075.
76. Hobley, E. U.; Prater, I., Estimating soil texture from vis–NIR spectra. *European Journal of Soil Science* **2019,** *70* (1), 83-95.
77. Robinson, N. J.; Kitching, M., The 3D distribution of phyllosilicate clay minerals in western Victoria. *Geoderma* **2016,** *284*, 152-177.
78. Baldock, J. A.; Hawke, B.; Sanderman, J.; Macdonald, L. M., Predicting contents of carbon and its component fractions in Australian soils from diffuse reflectance mid-infrared spectra. *Soil Research* **2013,** *51* (8), 577-595.
79. Pirie, A.; Singh, B.; Islam, K., Ultra-violet, visible, near-infrared, and mid-infrared diffuse reflectance spectroscopic techniques to predict several soil properties. *Soil Research* **2005,** *43* (6), 713-721.

80. Forouzangohar, M.; Cozzolino, D.; Kookana, R. S.; Smernik, R. J.; Forrester, S. T.; Chittleborough, D. J., Direct comparison between visible near- and mid-infrared spectroscopy for describing diuron sorption in soils. *Environmental Science & Technology* **2009,** *43* (11), 4049-4055.
81. Kookana, R. S.; Janik, L. J.; Forouzangohar, M.; Forrester, S. T., Prediction of atrazine sorption coefficients in soils using mid-infrared spectroscopy and partial least-squares analysis. *Journal of Agricultural and Food Chemistry* **2008,** *56* (9), 3208-3213.
82. Bengtsson, S.; Berglöf, T.; Sjöqvist, T., Predicting the leachability of pesticides from soils using near-infrared reflectance. *Journal of Agricultural and Food Chemistry* **1996,** *44* (8), 2260-2265.
83. Paradelo, M.; Hermansen, C.; Knadel, M.; Moldrup, P.; Greve, M. H.; de Jonge, L. W., field-Scale predictions of soil contaminant sorption using visible–near infrared spectroscopy. *Journal of Near Infrared Spectroscopy* **2016,** *24* (3), 281-291.
84. Gan, J.; Papiernik, S. K.; Koskinen, W. C.; Yates, S. R., Evaluation of accelerated solvent extraction (ASE) for analysis of pesticide residues in soil. *Environmental Science & Technology* **1999,** *33* (18), 3249-3253.
85. Ortega-Calvo, J.-J.; Harmsen, J.; Parsons, J. R.; Semple, K. T.; Aitken, M. D.; Ajao, C.; Eadsforth, C.; Galay-Burgos, M.; Naidu, R.; Oliver, R.; Peijnenburg, W. J. G. M.; Römbke, J.; Streck, G.; Versonnen, B., From bioavailability science to regulation of organic chemicals. *Environmental Science & Technology* **2015,** *49* (17), 10255-10264.
86. Kookana, R. S., The role of biochar in modifying the environmental fate, bioavailability, and efficacy of pesticides in soils: a review. *Soil Research* **2010,** *48* (7), 627-637.
87. Daly, K.; Styles, D.; Lalor, S.; Wall, D. P., Phosphorus sorption, supply potential and availability in soils with contrasting parent material and soil chemical properties. *European Journal of Soil Science* **2015,** *66* (4), 792-801.
88. Davison, W.; Zhang, H., In situ speciation measurements of trace components in natural waters using thin-film gels. *Nature* **1994,** *367* (6463), 546-548.
89. Menegário, A. A.; Yabuki, L. N. M.; Luko, K. S.; Williams, P. N.; Blackburn, D. M., Use of diffusive gradient in thin films for in situ measurements: A review on the progress in chemical fractionation, speciation and bioavailability of metals in waters. *Analytica Chimica Acta* **2017,** *983*, 54-66.
90. Davison, W.; Zhang, H., Progress in understanding the use of diffusive gradients in thin films (DGT) – back to basics. *Environmental Chemistry* **2012,** *9* (1), 1-13.
91. Morin, N.; Miège, C.; Coquery, M.; Randon, J., Chemical calibration, performance, validation and applications of the polar organic chemical integrative sampler (POCIS) in aquatic environments. *TrAC Trends in Analytical Chemistry* **2012,** *36*, 144-175.
92. Li, C.; Ding, S.; Yang, L.; Wang, Y.; Ren, M.; Chen, M.; Fan, X.; Lichtfouse, E., Diffusive gradients in thin films: devices, materials and applications. *Environmental Chemistry Letters* **2019,** *17* (2), 801-831.
93. Guibal, R.; Buzier, R.; Lissalde, S.; Guibaud, G., Adaptation of diffusive gradients in thin films technique to sample organic pollutants in the environment: An overview of o-DGT passive samplers. *Science of The Total Environment* **2019,** *693*, 133537.
94. Dai, Y.; Nasir, M.; Zhang, Y.; Wu, H.; Guo, H.; Lv, J., Comparison of DGT with traditional methods for assessing cadmium bioavailability to *Brassica chinensis* in different soils. *Scientific Reports* **2017,** *7* (1), 14206.
95. Bade, R.; Oh, S.; Shin, W. S., Diffusive gradients in thin films (DGT) for the prediction of bioavailability of heavy metals in contaminated soils to earthworm (*Eisenia foetida*) and oral bioavailable concentrations. *Science of The Total Environment* **2012,** *416*, 127-136.
96. Degryse, F.; Smolders, E.; Zhang, H.; Davison, W., Predicting availability of mineral elements to plants with the DGT technique: a review of experimental data and interpretation by modelling. *Environmental Chemistry* **2009,** *6* (3), 198-218.

97. Tandy, S.; Mundus, S.; Yngvesson, J.; de Bang, T. C.; Lombi, E.; Schjoerring, J. K.; Husted, S., The use of DGT for prediction of plant available copper, zinc and phosphorus in agricultural soils. *Plant and Soil* **2011,** *346* (1), 167-180.
98. Challis, J. K.; Hanson, M. L.; Wong, C. S., Development and calibration of an organic-diffusive gradients in thin films aquatic passive sampler for a diverse suite of polar organic Contaminants. *Analytical Chemistry* **2016,** *88* (21), 10583-10591.
99. Weng, Z.; Rose, M. T.; Tavakkoli, E.; Van Zwieten, L.; Styles, G.; Bennett, W.; Lombi, E., Assessing plant-available glyphosate in contrasting soils by diffusive gradient in thin-films technique (DGT). *Science of The Total Environment* **2019,** *646*, 735-744.
100. Li, Y.; Chen, C.-E. L.; Chen, W.; Chen, J.; Cai, X.; Jones, K. C.; Zhang, H., Development of a passive sampling technique for measuring pesticides in waters and soils. *Journal of Agricultural and Food Chemistry* **2019,** *67* (22), 6397-6406.
101. Cattani, I.; Capri, E.; Boccelli, R.; Del Re, A. A. M., Assessment of arsenic availability to roots in contaminated Tuscany soils by a diffusion gradient in thin films (DGT) method and uptake by Pteris vittata and Agrostis capillaris. *European Journal of Soil Science* **2009,** *60* (4), 539-548.
102. Pérez, A. L.; Anderson, K. A., DGT estimates cadmium accumulation in wheat and potato from phosphate fertilizer applications. *Science of The Total Environment* **2009,** *407* (18), 5096-5103.
103. Sudianto, E.; Beng-Kah, S.; Ting-Xiang, N.; Saldain, N. E.; Scott, R. C.; Burgos, N. R., Clearfield® rice: Its development, success, and key challenges on a global perspective. *Crop Protection* **2013,** *49*, 40-51.

2. A New Predictive Model for Glyphosate Adsorption in Soil Based on pH and Phosphorus Buffering Index

Gavin Styles[a], Gavan S. McGrath[b], Michael T. Rose[c], Lukas Van Zwieten[a, c] and Antonio F. Patti[a]

[a] *School of Chemistry, Monash University, Wellington Rd., Clayton, 3800, Victoria, Australia*

[b] *Ishka Solutions, Western Australia, Australia*

[c] *New South Wales Department of Primary Industries, 1243 Bruxner Highway, Wollongbar, 2477, New South Wales, Australia*

Declarations of interest: none

2.1 Abstract

Sorption is considered one of the most significant processes affecting the mobility and rate of degradation of glyphosate in soil. The ability to accurately predict glyphosate sorption using routinely-measured soil physico-chemical characteristics would provide an inexpensive alternative to lengthy and expensive adsorption experiments. Adsorption isotherms were developed for 90 agricultural soils (45 sites, surface and subsurface layers) from around Australia using radiolabelled glyphosate. Multiple Linear Regressions (MLRs) and General Additive Models (GAMs) were developed to predict Freundlich sorption coefficients (K_f) for glyphosate, based on soil physiochemical properties. Of the properties measured, soil pH and phosphorus buffering index (PBI) were the two most important for predicting K_f, which ranged from 4.6 to 186 mg kg^{-1} (L mg^{-1})$^{-1/nf}$. The predictive capability of the best model (R^2 = 0.967) was confirmed by the characterisation of an additional seven soils with contrasting chemical properties, with the predicted K_f of each soil from the verification set being within 15-40% of the experimentally determined K_f. The development of such a tool will facilitate improved glyphosate risk assessment and management strategies.

2.2 Introduction

Glyphosate (N-(phosphonomethyl)glycine), the most widely used herbicide worldwide, is a systemic 5-enolpyruvylshikimate-3-phosphate synthase enzyme (EPSPS) inhibitor. Glyphosate is considered to have a low-risk ecological profile compared with other commonly used herbicides, in part because of a low inherent toxicity to non-target organisms, a relatively rapid breakdown rate and high soil adsorption capacity[1-3]. However, glyphosate and its main breakdown product aminomethylphosphonic acid (AMPA) have recently been shown to be 'pseudo-persistent' in some soils due to frequency of use outweighing the rate of breakdown, potentially leading to periodic accumulation in soil[4]. Additionally, mobilisation of glyphosate and AMPA residues has been observed following fertilisation[5-6]. This is thought to be the result of superior competition for sorption sites by phosphate[7-8]. The recent evidence highlighting the persistence of glyphosate and mechanisms for mobilisation raise new concerns about in-field agronomic risks[5], off-site movement and ecological risk[9]. Recent surveys have frequently detected glyphosate in a wide variety of environments, including sediment[10], water[11], soil[12], rainwater[13] and groundwater[14] many months after application.

Biological exposure to glyphosate is regulated by its persistence, mobility and bioavailability. These factors are, in turn, largely determined by its sorption characteristics to soil. Sorption can moderate the efficacy of glyphosate by reducing its uptake by plants[15], as well as influencing pathways for mobilization through the soil[16-17], including its movement to waterways[18]. Sorption is also known to significantly affect the persistence of glyphosate in the soil[19]. Glyphosate exists as a zwitterion in soil, with a negatively charged phosphonic acid and carboxylic acid group and a positively charged amine group, depending on the pH of the soil[20]. It primarily binds to amorphous soil minerals such as iron and aluminium oxides and hydroxides[21]. Soil pH and mineralogy therefore have a significant effect on binding, with adsorption decreasing as pH increases[22]. This is mainly due to the change in surface charge on soil minerals, rather than the change in ionic form of glyphosate (pKa = 2, 2.6, 5.8 and 10.8, occurring due to protonation and

deprotonation of the phosphate, amine and carboxylic acid groups), as glyphosate is negatively charged at pH above 2.6[20]. Most of these minerals are positively charged at environmentally relevant pH, however, as pH increases, negatively charged sites may appear[23]. Because the binding to metal oxides occurs predominantly through the phosphonic acid functional group of the glyphosate molecule[24], competition has been shown to occur between glyphosate and inorganic phosphate (PO_4^{3-}/HPO_4^{2-}/$H_2PO_4^-$)[25-26]. Glyphosate may be desorbed by the addition of P fertiliser, increasing the risk of herbicide injury in rotational crops in some soil types[5, 14, 27]. Glyphosate has also been shown to bind to soil organic matter including soil humic substances[28-29].

Despite the factors influencing glyphosate sorption being relatively well-known[30], there have been few attempts to formalise rapid, inexpensive, easy to use models for estimating glyphosate sorption based on soil properties as an alternative to constructing soil-specific isotherms via laboratory studies (Table 2). Paradelo et al. (2015) proposed a multiple linear regression model based on soil characteristics as linear predictors providing the best fit for linear adsorption of glyphosate (K_d). Glyphosate sorption was shown to increase with increasing clay and iron content, but decrease with increasing pH, EC and P levels. Although pH and clay content are often the best predictors of glyphosate sorption, there is often variation from study to study, due in part to the often limited number of soils examined (Table 2).

Table 2: Overview of previous adsorption predictive modelling

Reference	# Soil Samples	Parameters Predicted	Type of Model	R^2	Predictors included in best model [c]
Dollinger et al. (2015)	19-51[a]	K_d, K_f, n_f	MLR	K_d: 0.48 K_f: 0.52 n_f: 0.62	K_d: CEC, Clay K_f: CEC, Clay, OC n_f: Clay, pH
Paradelo et al. (2015)	114 (2 fields)	K_d	MLR	0.70 (4 variables)	pH, EC, Clay, Sand (both fields)
Sidoli et al. (2016)	17	K_f [b]	MLR, exponential	0.94 (4 variables)	pH, Olsen P, Al_{ox}, Fe_{ox}
De Geronimo et al. (2018)	12	K_f	MLR	0.994 (7 variables)	Clay, pH, Bray P, Al_{in}, OC, Sand, Fe_{ox}

[a] Depending on predicted parameter and available predictors

[b] calculated using average n_f value of all soils

[c] Fe_{ox} and Al_{ox} = oxalate extractable iron and aluminium

[d]CEC = cation exchange capacity, EC = electrical conductivity, P = phosphorus, OC = organic carbon, MLR = Multiple linear Regression

K_d is the slope of a linear fit of adsorption data, K_f and n_f are fitting variables of adsorption derived from the Freundlich equation

Furthermore, as acknowledged by Paradelo et al. (2015), non-linear relationships between predictor variables and sorption may better describe interactions (e.g. the change in surface charge on clay minerals at high pH). More recently, Sidoli et al. (2016) built on the previous work from Paradelo et al. (2015) by increasing the sample size from 2 to 17 contrasting sites, fitting a variety of linear and nonlinear regressions to a Freundlich isotherm derived sorption value (K_f) and evaluating the relevance of different measures of pH (i.e. in water, KCl and $CaCl_2$). However, despite the increased number of different soil types, the use of a single sample from each site resulted in only a total of 17 data points. Sidoli et al. (2016) also restricted their modelling framework to linear and exponential relationships between the dependent and independent variables, which may not adequately account for certain interactions involved in glyphosate

binding. De Geronimo et al. (2018) conducted similar modelling using 12 Argentine soils, finding seven variables to be important for predicting glyphosate adsorption (Table 2). While these soils had greater variation than those in the previous two studies, the relatively small number of data points and lack of alkaline soils limits the broader applicability of the model. Furthermore, despite the clear link between P and glyphosate binding, no previous work has examined whether a correlation exists between glyphosate sorption and routinely collected measures of the binding affinity of P, such as the P buffering index (PBI).

The aim of this work was therefore to develop a statistical model capable of predicting glyphosate sorption based on an expanded dataset of more than 40 contrasting farm soils from across Australia, divided into 2 depth profiles. The soil properties used to train the model were deliberately selected from those that are included in routine agronomic soil tests, to enable practical application of derived models. Different modelling strategies (beyond linear regression) were tested for their ability to increase model accuracy. The development of such a tool will facilitate improved glyphosate risk assessment and management decisions.

2.3 Material and Methods

2.3.1 Soil Samples and Characterisation

Soils were sampled from agricultural paddocks in April-May 2015 from various locations (45 sites) in Australia (Appendix Table 1), with sites represented by grain cropping systems (predominantly wheat, barley and pulses) pasture and sugarcane systems. Samples were taken with a 25 mm diameter stainless steel open-faced push corer to a depth of 30 cm, and were divided into 0-10 cm and 10-30 cm layers. At each location, 12 subsamples were randomly taken from a 50 m by 50 m grid in each paddock, and these were composited as a single sample. Samples were air-dried, crushed and sieved to < 2 mm. Samples were stored air-dried until analysis. An additional 7 soils were collected for use as a validation set, these soils were all surface soils (0-20 cm depth) and were otherwise collected analysed using the same

methodology. Soil pH (1:5 soil:water), EC, bicarbonate-extractable P (Colwell P) and total OC content were determined using methods described in Rayment and Lyons (2010)[31]. Phosphorus buffering index (PBI_{+ColP}) was determined according to Rayment and Lyons method 9I2B (2010). Briefly this involves dosing soil with 100 mg P L^{-1} solution at a soil:solution ratio of 1:10 and determining the amount of P sorbed after 17 h of mixing. PBI_{+ColP} is then calculated as the freshly sorbed P (mg P kg^{-1}) plus the Colwell-P (mg kg^{-1}), divided by the final solution P concentration (mg P L^{-1}). Soil particle size distribution (clay, silt, and sand) was estimated by mid-infrared (MIR) analysis of pulverised soil (<200 nm) using the method and model of Robinson and Kitching (2016)[32]. MIR spectra were acquired using a PerkinElmer Spectrum One Fourier Transform MIR spectrometer equipped with a diffuse reflectance accessory. Background levels of glyphosate and AMPA in sampled soils were quantified using the method of Zhang et al. (2019). Briefly, this involved extraction of soil in a 1:4 (soil:solution) mixture with 0.6 M NaOH, followed by solid phase extraction on mixed mode exchange resin (Bond Elut Plexa Pax, 60 mg, Agilent, CA). Eluates (1:1 of 2.5% formic acid:methanol) were separated and analysed by liquid chromatography triple quadrupole mass spectrometry (Waters Quattro MicroTM Micromass, Milford, MA) using optimised multiple reaction monitoring conditions.

2.3.2 Glyphosate Sorption

^{14}C labelled glyphosate (1.85 GBq mol^{-1}) was purchased from American Radiolabelled Chemicals (Saint Louis, USA) and mixed with analytical grade glyphosate (Accustandard, New Haven, USA) to produce five one litre solutions of varying concentration (0.3, 1, 3, 9 and 27 mg L^{-1}, standard radioactivity of ~10 nCi per sample).

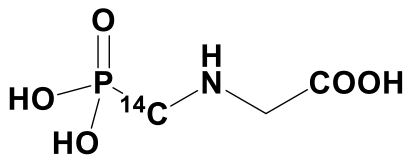

Figure 3: ^{14}C Labelled Glyphosate

Soils were irradiated under 254 nm UV light (1 hour, <1 mm thick layer, mixed and respread every 20 minutes) prior to adsorption testing in order to minimise microbial degradation of the glyphosate. Respiration tests (headspace CO_2 concentration) indicated a reduction in soil respiration by up to 60% due to UV exposure. Sorption trials were conducted with a 1:5 soil-to-liquid ratio at five concentrations of glyphosate (0.3, 1, 3, 9 and 27 mg L^{-1}) using 1 g aliquots of air dried soil. Soil-glyphosate mixtures were rotated on an end-over-end shaker (33 rpm) at 22 ^{o}C for 24 hours to allow equilibration, before being centrifuged at 2600 g for 20 min (Thermo Scientific Megafuge 8). The supernatant was then removed and filtered through a 0.2 µm polyethylene (Merck) membrane to remove any remaining clay particles. Supernatant (2 mL) was then mixed with scintillation cocktail (18 mL, Optifluor, PerkinElmer) and glyphosate concentration determined by scintillation counting (Tricarb 2810, Packard). The amount of adsorbed glyphosate was then determined indirectly by subtracting equilibrium glyphosate concentration from initial glyphosate concentration. Controls conducted in the same manner without soil material showed negligible adsorption of glyphosate to the centrifuge tubes or filters. A microbial degradation control was conducted using a 0.5 M NaOH trap for CO_2, these trials showed <1% mineralisation of glyphosate to CO_2 over 24 hours.

Sorption coefficients were calculated, where *C* is concentration of glyphosate in solution (µg ml^{-1}) and *x* is the concentration of glyphosate adsorbed to the soil (µg g^{-1}). The parameters K_f and *n* of the Freundlich isotherm:

$$x = K_f C^{\frac{1}{n}} \tag{1}$$

were calculated using the full concentration range and regression of the log-transformed concentrations.

2.3.3 Statistical Analysis

Exploratory modelling was conducted using multiple linear regression analysis within Python[33-36], comparing the K_f values for each soil to various physiochemical properties individually, and the pairwise products of each these variables (e.g. pH * PBI) to begin to account for interactions between the variables.

$$K_f = \sum_{x=1}^{n} a_x S_x + e \tag{2}$$

In equation (2), *S* is the soil property or pairwise product, *x* is the soil number (sample ID), *a* is the regression coefficient relating to that soil property and *e* is the model error. Using this approach, the relative impact of each variable (individual properties and pairwise products) on K_f could be assessed. Models using all single variable and pairwise product, just single variable, and just pairwise products were produced, and the significance (p-value) of each term compared. In order to assess the potential for nonlinear interactions a penalised spline regression as a Generalised Additive Model (GAM) was also applied via the mgcv package using the software environment R (R Core Team, 2019)[37].

The interactions chosen in the GAM analysis were based on both the outcomes of pairwise products in the exploratory MLR, and also expectations based upon physical properties (e.g. pH and clay interactions moderate the surface charge of the clay minerals, but may also impact overall charge of the glyphosate molecule to result in a non-linear relationship). Model variables were deemed significant when $p<0.05$. Models were compared through various statistical tests (R^2, AIC, and generalised cross validation (GCV) score[37]), and verified against a set of soils (7 in total) not used in the model development.

Predictions of n_f were then performed using the same models developed for K_f to determine their ability to predict the overall adsorption behaviour of glyphosate. These n_f predictions were not done during the exploratory MLR modelling as K_f was considered the most important

variable determining glyphosate adsorption levels for environmentally relevant concentrations, and the use of the same model for both variables would provide significant benefits in terms of practicality.

2.4 Results and Discussion

2.4.1 Soil Properties and Glyphosate Sorption

The experimental soils covered a wide range of soil properties, including contrasting textures, pH and OC content (Figure 4). Although the experimental soils covered a range of PBI values, 72% had PBI < 100, whilst a small cluster had high PBI values, ranging from 400-800. The measured soil properties were generally uncorrelated across the dataset, with the exception of a weak relationship between PBI and OC (Appendix Table 3). Freundlich isotherms (for e.g., Figure 5) better described the glyphosate adsorption data than did linear sorption isotherms ($R^2 > 0.91$ for all soils), with K_f values ranging between 4.61 and 186 mg kg^{-1} (L mg^{-1})$^{-1/nf}$ and n_f values between 0.94 to 1.82 (Appendix Table 1). While the Freundlich isotherms systematically over predicted sorption at high concentrations (due to a bias in power law fittings to smaller values[38]), they fit well for environmentally relevant concentrations (0-1 µg ml^{-1}), producing a closer fit to the data points than linear isotherms over this region.

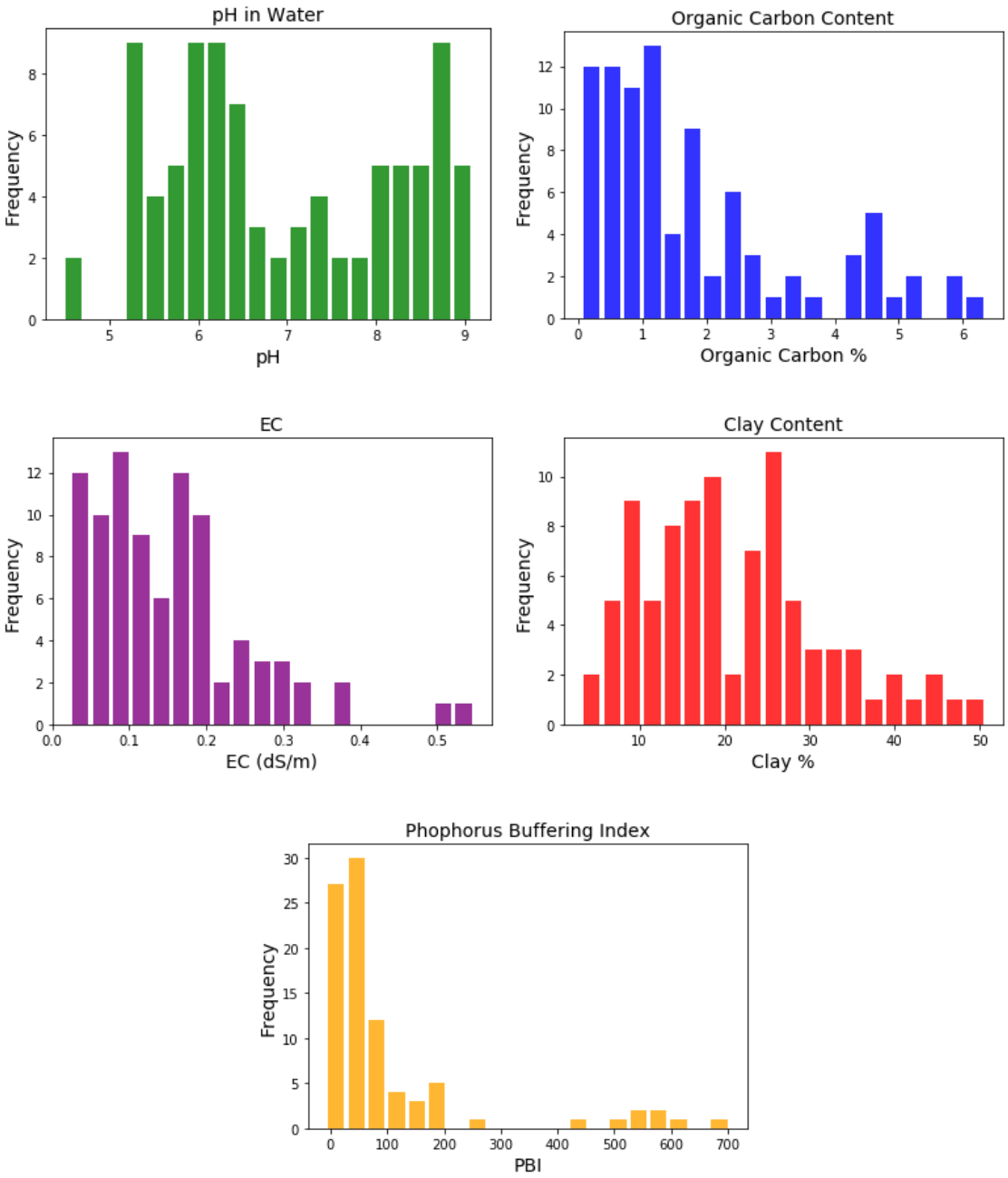

Figure 4: Histograms of Selected Soil Properties (all histograms divided into 20 bins)

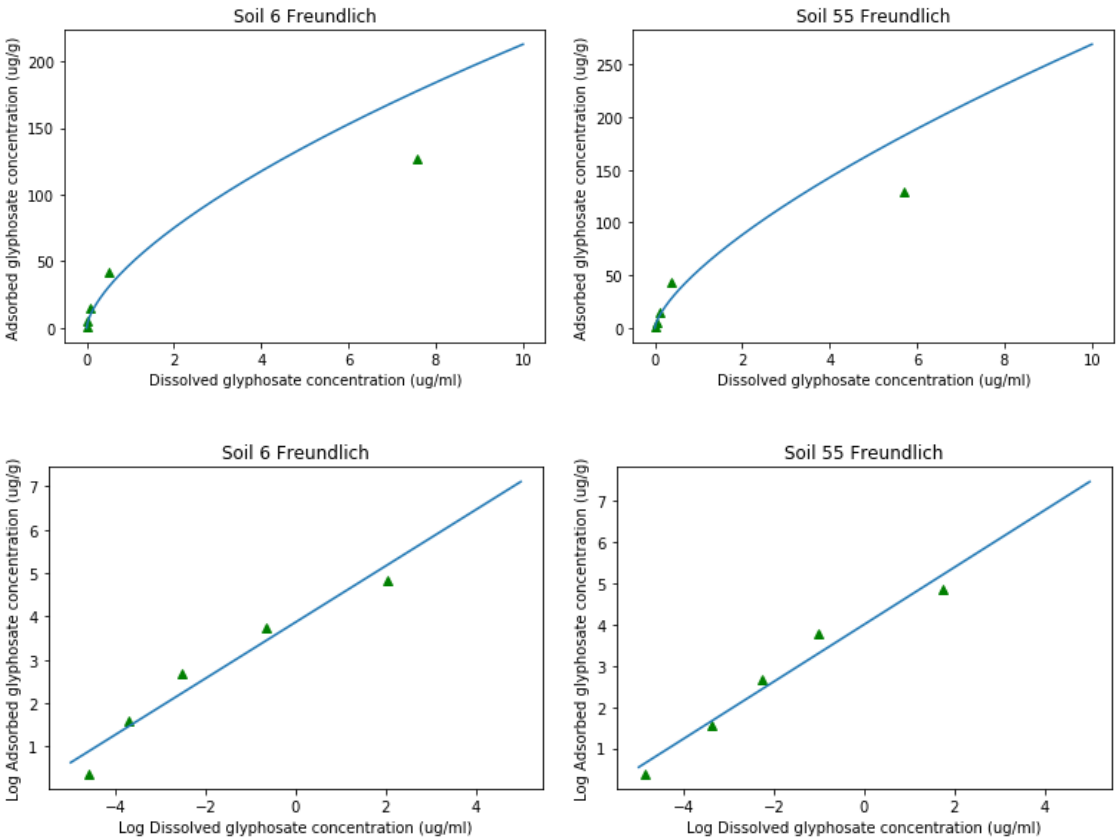

Figure 5: Glyphosate adsorption to soil 6 (left) and soil 55 (right), untransformed (top) and on a log scale (bottom). Green triangles show experimentally determined concentrations; blue lines are Freundlich isotherms fit to experimental data

Many of the soils used for this study had residual glyphosate and AMPA present prior to the adsorption studies, but at levels < 2mg kg^{-1} (data not shown). For the purpose of the predictive modelling, initial glyphosate and AMPA levels were treated as variables for prediction of K_f values, rather than being included in the calculation of isotherms, to account for any 'aging' in effects and hysteresis.

2.4.2 Linear Regression Models

A number of linear regression models (LMs) were tested to explore the potential role of different combinations of soil physicochemical properties in explaining glyphosate sorption. Of the variables tested, PBI and pH_{H_2O} were found to be the only significant ($P<0.05$) predictors of glyphosate adsorption when a single variable additive model with no pairwise interactions was considered. Inclusion of all pairwise interactions was deemed unnecessarily complex, with reduced degrees of freedom and greater potential for overfitting. Instead, addition of selected pairwise interactions on a theoretical basis was explored – this included interactions of soil textural components (clay, PBI) with pH and TOC. Amongst these predictors, clay and the interaction of PBI with pH and OC were significant ($P < 0.05$), resulting in improved fits to glyphosate sorption (Table 3, LM3) compared with the initial model (LM1). A more parsimonious model (LM2) containing only pH, PBI and their interaction was also superior to the initial model (i.e. excluding the interaction of pH and PBI), but had lower accuracy than LM3. Electrical conductivity, Colwell P, and residual glyphosate and AMPA remaining in the soil from previous applications were not significant ($P > 0.05$) in any of these models.

Table 3: Comparison of various linear models for predicting glyphosate sorption a set of calibration soils (n = 90).

Predictor Variable	LM1			LM2			LM3		
	Estimate	*Std Error*	*p*	*Estimate*	*Std Error*	*p*	*Estimate*	*Std Error*	*p*
Intercept	83.4	6.8	<0.001	52.9	10.5	<0.001	34.5	9.4	<0.001
PBI	0.25	0.01	<0.001	0.52	0.07	<0.001	0.43	0.07	<0.001
pH	-10.0	0.9	<0.001	-0.51	1.6	0.002	-3.5	1.4	0.01
Clay							0.69	0.12	<0.001
PBI:pH				-0.044	0.012	<0.001	-0.057	0.01	<0.001
PBI:TOC							0.033	0.006	<0.001
Model evaluation									
adj R^2	0.93			0.94			0.96		
RMSE	10.9			10.1			8.4		
AIC	693			682			653		
BIC	703			695			670		
ANOVA [a]				<0.001			<0.001		

[a] ANOVA for model 2 is model 1 vs model 2; ANOVA for model 3 is model 2 vs model 3

2.4.3 Non-linear Models

A wide variety of GAMs were generated based on the previous exploratory linear models. Initially (GAM-1), an interaction term for pH and PBI, along with an individual smooth term for clay was used. Individual smooth terms for both glyphosate and AMPA content were also added on a theoretical basis, in order to confirm or reject the findings of the linear modeling. A tensor interaction between pH and PBI was the most important predictor of K_f in the given soils (GAM-3, Table 4), supporting the results from the linear models, whilst clay was found to be non significant, even when allowed to interact with pH.

The only other variable found to be significant was OC, used by itself with no interactions. However, the addition of OC did little to improve the predictive capacity of the model based on tensor interaction of PBI and pH (te(PBI,pH), R^2 = 0.972), and unnecessarily increased the model complexity. A model using the pH and PBI as separate smooth terms (no interaction) was very

similar (R^2 = 0.974), however, performed worse when predicting all but one verification soil, despite the improved generalised cross validation (GCV) score. All of these models had similar Akaike information criterion (AIC), Lin's concordance correlation coefficients (R_c), and GCV scores (Table 4).

Table 4: Comparison of various generalised additive models for predicting glyphosate sorption a set of calibration soils (n = 90).

Model		**R^2**	**AIC**	**GCV**	**R_c**	**Significant Terms**
GAM-1	K_f ~ s(PBI) + s(pH)	0.974	632.3817	65.773	0.987	s(PBI), s(pH)
GAM-2	K_f ~ te(PBI, pH)	0.967	639.5185	70.802	0.985	te(PBI, pH)
GAM-3	K_f ~ te(PBI, pH) + s(OC)	0.974	630.7767	66.821	0.989	te(PBI, pH), s(OC)
GAM-4	K_f ~ te(PBI, pH) + s(clay) + s(AMPA) + s(Glyphosate)	0.967	626.0696	62.193	0.988	te(PBI, pH)

Notes: s denotes a smooth spline, te denotes a tensor product smooth; AIC = Akike Information criteria, GCV = generalized cross validation value, R_c = Lin's concordance correlation coefficient

The model using only the tensor product of pH and PBI was selected as the most appropriate model, despite the higher AIC and GCV values, as it best predicted glyphosate sorption to an external validation set of seven contrasting soils, with a minimum number of input parameters. The model displayed negligible bias within the training set (Figure 6a), accounting for non-linearity in the response of K_f to PBI and pH (Figure 6b). Four of the validation soils returned predicted K_f values within 15% of the experimentally determined K_f (**Error! Reference source not found.**5). Soil 4, which had an experimental K_f of 104.8 (a range not well represented in the dataset) gave a prediction 40% lower, at a K_f of 60.2.

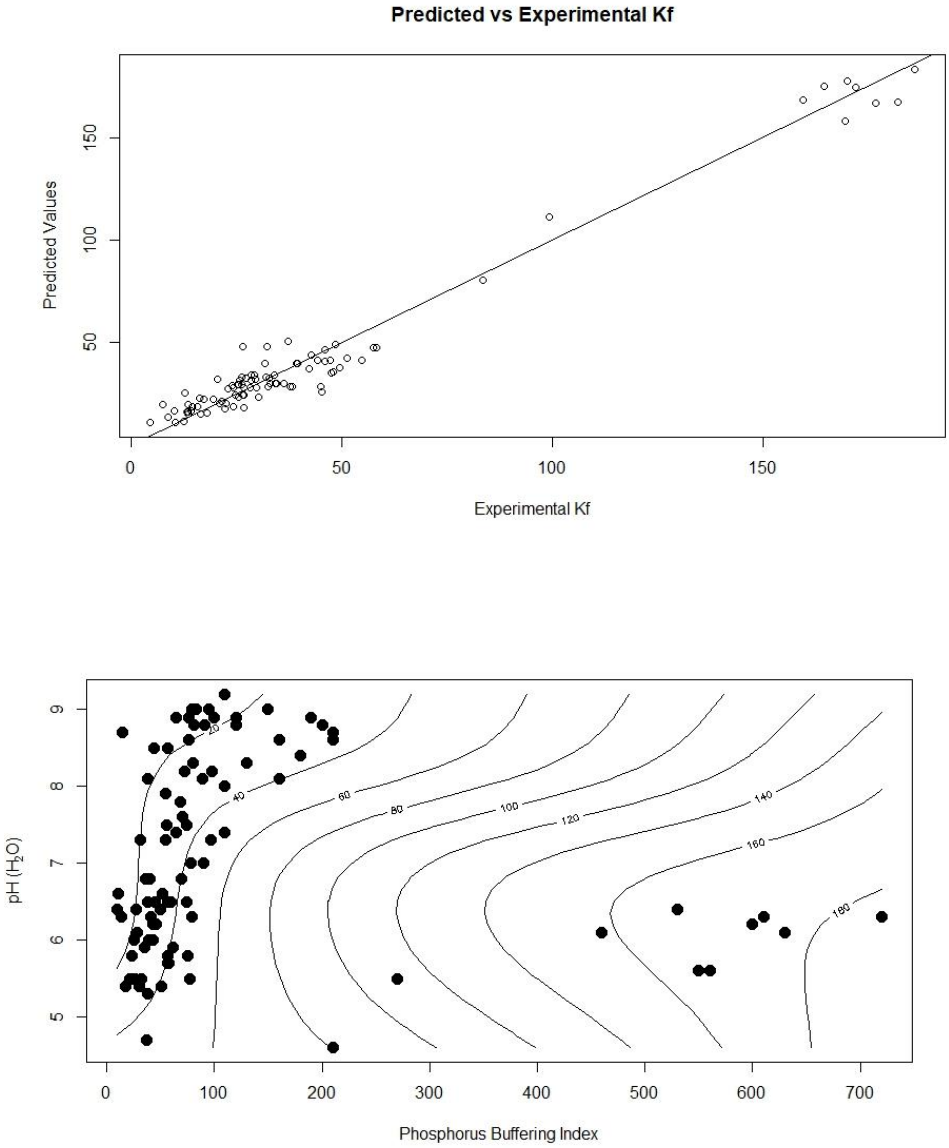

Figure 6: (a) Predicted vs Experimental K_f Values (b) Contour plot of predicted K_f values against pH and Phosphorus Buffering Index. Points represent soils in dataset

When the te(PBI, pH) model (GAM-2, Table 4) was tested for its ability to predict n_f, an R^2 of 0.73 was obtained. Despite a correlation between n_f and K_f (Figure 7), the inclusion of a K_f term as an additional predictor for n_f provided no benefit to n_f predictions. Predictions for n_f were within 32% for 6 of 7 soils in the validation set, with an error of 51% for the remaining validation soil (Soil 2, Table 5). Given the change in adsorption produced by n_f at environmentally relevant levels compared to the change produced by K_f, the PBI-pH tensor model maintained acceptable

accuracy for predicting glyphosate sorption in soil concentrations of 0-70 mg kg $^{-1}$, with the exclusion of Soil 1 (Appendix Figure 1). This range extends beyond typical concentrations found in the topsoil (0-5 or 0-10 cm), which generally fall below 10 mg kg^{-1} [4, 10, 12, 39].

Table 5: Predictions of Kf and nf for soils in the validation set using the PBI-pH tensor model

Soil ID	PBI	pH	Experimental K_f	Predicted K_f	% Error	Experimental n_f	Predicted n_f	% Error
1	11	6.9	25.5	10.8	58	1.41	1.72	22
2	15	5.8	19.4	19.6	1	1.09	1.65	51
3	60	5.2	43.9	46.9	7	1.18	1.39	18
4	110	6.7	104.8	60.2	43	1.05	1.39	32
5	120	5.5	46.7	66.3	42	1.11	1.27	14
6	130	7	56.7	65.3	15	1.12	1.39	24
7	210	8.6	31.4	34.4	10	1.13	1.43	27

**Additional soil details may be found in Appendix Table 2*

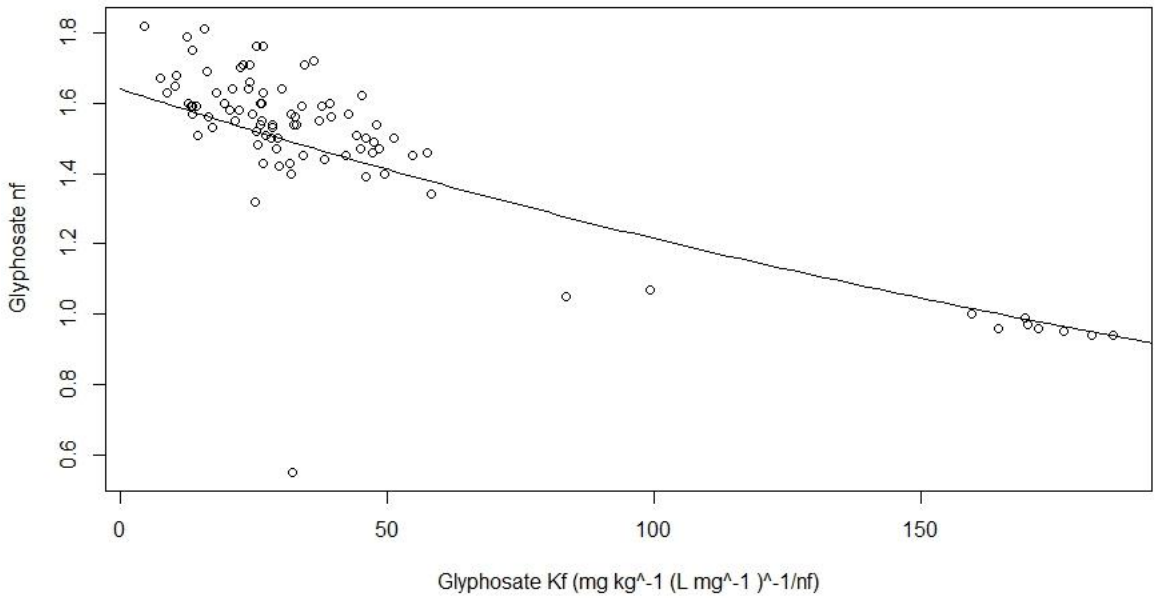

Figure 7: Plot of Kf against nf values for the calibration dataset with exponential trendline

2.4.4 Discussion and Implications

The ability to accurately predict adsorption of glyphosate is not only important for understanding glyphosate movement and bioavailability in different soils, but can also be used along with other soil properties such as organic matter to predict the half-life of the herbicide[40-41]. The models developed here, using a more comprehensive dataset compared to previous studies, show significant promise for estimating glyphosate mobility across a wide range of soil types.

A key innovation in this research was the inclusion of a measure of the phosphorus binding capacity, in this case the PBI, as a predictor for glyphosate sorption. Although there is substantial literature describing the similarities of glyphosate sorption with P sorption[7-8, 22, 24, 42], until now there has been no attempt to formalise the use of a phosphorus binding measure, such as PBI, for predicting glyphosate sorption. Linear regression modelling confirmed the utility of PBI as a predictor for glyphosate sorption compared with other variables such as clay content and pH, which have previously been shown to be important[43-45]. While our model did not explicitly determine the soil clay mineralogy, or quantify other chelating metals (e.g. Fe or Al) as per previous glyphosate sorption models[44, 46], soil PBI is inherently related[47], and appears to account for these characteristics while being more easily measured and widely available in soil quality databases (e.g. http://www.soilquality.org.au/).

As with previous efforts, pH was also found to significantly contribute to the prediction of glyphosate sorption, primarily through an interaction with PBI. We propose that the drop in K_f at higher pH is due to the change in surface charge of metal oxide minerals, and possibly due to the presence of alkali minerals such as calcite (calcium carbonate) which may bind glyphosate less strongly. As previously stated, due to glyphosate's pK_a values, protonation/deprotonation of various functional groups on the molecule are unlikely to cause the observed changes in adsorption over the higher pH range of the studied soils. The apparent reduction in adsorption

below pH = 5.8 is possibly due to the protonation of the phosphonic acid group and reduction in overall negative charge on the glyphosate molecule, but additional soils in this pH range, along with more focused protonation analysis would be required to test this hypothesis. Residual glyphosate and AMPA remaining in the soil from previous applications were found to be insignificant in determining the K_f of soils in both MLR and GAMs modelling. This is likely due to levels being significantly lower than the quantity added for adsorption trials.

Worth noting is the interaction of the K_f and n_f terms, such that two isotherms of the same K_f, may be quite different due to variance in the n_f term. Previous work by Sidoli et al.[45] addressed this by taking an average of the n_f value across all isotherms, and recalculating all K_f values such that all soils used this average n_f. This was deemed inappropriate in this case due to the large data set and much wider variation in n_f. While it would not necessarily be expected that n_f would be predicted by the same variables as K_f, this approach was investigated in order to reduce the complexity of the model, and therefore increase practicality for end users. Similarly, it would be expected that PBI, as a measure of phosphorus saturation point in a soil, would provide a good indicator for n_f.

In Australia, pH and PBI are routinely assessed by landholders through commercial laboratories for lime and P fertiliser recommendations, respectively[48-49]. While other countries tend to have their favoured P-binding indices[50-51], it is likely a similar model using these preferred indices would perform equally as well. The development of non-linear regressions using such indices offers the potential for practical management of glyphosate residues in soil, where necessary. Given that such indices incorporate many soil physical and chemical processes of relevance to glyphosate sorption there is a clear advantage to our proposed models over those requiring more complex and costly soil analysis for parameterisation. The works presented here represents a predictive model of a high goodness-of-fit (R^2 = 0.967), built from a database of a large number of samples (n = 90) with wide variability of physico-chemical properties. This

model exclusively uses pH and PBI as the required predictors for glyphosate adsorption constants (K_f and n_f). As pH and phosphorous indices are routinely measured for agronomic purposes, our work provides future opportunity for spatially-explicit glyphosate monitoring and management strategies through the use of readily available data.

2.5 Acknowledgements

The authors acknowledge the financial contributions of Monash University, The Australian Government Research Training Program and The New South Wales Department of Primary Industries to this work. The authors also acknowledge the in-kind support provided by Agriculture Victoria.

2.6 References

1. Roy, D. N.; Konar, S. K.; Banerjee, S.; Charles, D. A.; Thompson, D. G.; Prasad, R., Persistence, movement, and degradation of glyphosate in selected Canadian boreal forest soils. *Journal of Agricultural and Food Chemistry* **1989,** *37* (2), 437-440.
2. Giesy, J. P.; Dobson, S.; Solomon, K. R., Ecotoxicological risk assessment for Roundup® herbicide., *Reviews of Environmental Contamination and Toxicology: Continuation of Residue Reviews*, Ware, G. W., Ed. Springer New York: New York, NY, **2000**; pp 35-120.
3. Peterson, R. K. D.; Hulting, A. G., A comparative ecological risk assessment for herbicides used on spring wheat: the effect of glyphosate when used within a glyphosate-tolerant wheat system. *Weed Science* **2017,** *52* (5), 834-844.
4. Primost, J. E.; Marino, D. J. G.; Aparicio, V. C.; Costa, J. L.; Carriquiriborde, P., Glyphosate and AMPA, "pseudo-persistent" pollutants under real-world agricultural management practices in the Mesopotamic Pampas agroecosystem, Argentina. *Environmental Pollution* **2017,** *229*, 771-779.
5. Bott, S.; Tesfamariam, T.; Kania, A.; Eman, B.; Aslan, N.; Römheld, V.; Neumann, G., Phytotoxicity of glyphosate soil residues re-mobilised by phosphate fertilisation. *Plant and Soil* **2011,** *342* (1), 249-263.
6. Kanissery, R. G.; Welsh, A.; Sims, G. K., Effect of soil aeration and phosphate addition on the microbial bioavailability of carbon-14-glyphosate. *Journal of Environmental Quality* **2015,** *44* (1), 137-144.
7. Gimsing, A. L.; Borggaard, O. K., Effect of phosphate on the adsorption of glyphosate on soils, clay minerals and oxides. *International Journal of Environmental Analytical Chemistry* **2002,** *82* (8-9), 545-552.
8. Wang, Y. J.; Zhou, D. M.; Sun, R. J., Effects of phosphate on the adsorption of glyphosate on three different types of Chinese soils. *Journal of Environmental Science* **2005,** *17* (5), 711-5.
9. Norgaard, T.; Moldrup, P.; Ferré, T. P. A.; Olsen, P.; Rosenbom, A. E.; de Jonge, L. W., Leaching of glyphosate and aminomethylphosphonic acid from an agricultural field over a twelve-year period. *Vadose Zone Journal* **2014,** *13* (10).
10. Battaglin, W. A.; Meyer, M. T.; Kuivila, K. M.; Dietze, J. E., Glyphosate and Its degradation product AMPA occur frequently and widely in U.S. soils, surface water,

groundwater, and precipitation. *JAWRA Journal of the American Water Resources Association* **2014,** *50* (2), 275-290.
11. Saunders, E. L.; Pezeshki, R., Glyphosate in runoff waters and in the root-zone: A review. *Toxics* **2015,** *3* (4), 462-480.
12. Silva, V.; Montanarella, L.; Jones, A.; Fernández-Ugalde, O.; Mol, H. G. J.; Ritsema, C. J.; Geissen, V., Distribution of glyphosate and aminomethylphosphonic acid (AMPA) in agricultural topsoils of the European Union. *Science of The Total Environment* **2018,** *621*, 1352-1359.
13. Chang, F.; Simcik, M. F.; Capel, P. D., Occurrence and fate of the herbicide glyphosate and its degradate aminomethylphosphonic acid in the atmosphere. *Environmental Toxicology and Chemistry* **2011,** *30* (3), 548-555.
14. Rosenbom, A.; Haarder, B.; Badawi, N.; Gudmundsson, L.; Von Platten-Hallermund, F.; H Hansen, C.; B Nielsen, C.; Plauborg, F.; Olsen, P., *The Danish Pesticide Leaching Assessment Programme. Monitoring results May 1999–June 2016*. **2017**.
15. Simonsen, L.; Fomsgaard, I. S.; Svensmark, B.; Spliid, N. H., Fate and availability of glyphosate and AMPA in agricultural soil. *Journal of Environmental Science and Health, Part B* **2008,** *43* (5), 365-375.
16. McGrath, G. S.; Hinz, C.; Sivapalan, M., A preferential flow leaching index. *Water Resources Research* **2009,** *45* (11), W114505.
17. McGrath, G. S.; Hinz, C.; Sivapalan, M., Modelling the impact of within-storm variability of rainfall on the loading of solutes to preferential flow pathways. *European Journal of Soil Science* **2008,** *59* (1), 24-33.
18. Dollinger, J.; Dagès, C.; Negro, S.; Bailly, J.-S.; Voltz, M., Variability of glyphosate and diuron sorption capacities of ditch beds determined using new indicator-based methods. *Science of The Total Environment* **2016,** *573*, 716-726.
19. Al-Rajab, A. J.; Schiavon, M., Degradation of 14C-glyphosate and aminomethylphosphonic acid (AMPA) in three agricultural soils. *Journal of Environmental Sciences* **2010,** *22* (9), 1374-1380.
20. Sprankle, P.; Meggitt, W. F.; Penner, D., Adsorption, mobility, and microbial degradation of glyphosate in the soil. *Weed Science* **1975,** *23* (3), 229-234.
21. Morillo, E.; Undabeytia, T.; Maqueda, C.; Ramos, A., Glyphosate adsorption on soils of different characteristics.: Influence of copper addition. *Chemosphere* **2000,** *40* (1), 103-107.
22. Zhao, B.; Zhang, J.; Gong, J.; Zhang, H.; Zhang, C., Glyphosate mobility in soils by phosphate application: Laboratory column experiments. *Geoderma* **2009,** *149* (3), 290-297.
23. de Jonge, H.; Wollesen de Jonge, L., Influence of pH and solution composition on the sorption of glyphosate and prochloraz to a sandy loam soil. *Chemosphere* **1999,** *39* (5), 753-763.
24. Sheals, J.; Sjöberg, S.; Persson, P., Adsorption of glyphosate on goethite: Molecular characterization of surface complexes. *Environmental Science & Technology* **2002,** *36* (14), 3090-3095.
25. Laitinen, P.; Siimes, K.; Rämö, S.; Jauhiainen, L.; Eronen, L.; Oinonen, S.; Hartikainen, H., Effects of soil phosphorus status on environmental risk assessment of glyphosate and glufosinate-ammonium. *Journal of Environmental Quality* **2008,** *37* (3), 830-838.
26. Padilla, J. T.; Selim, H. M., Interactions among glyphosate and phosphate in soils: Laboratory retention and transport studies. *Journal of Environmental Quality* **2019,** *48* (1), 156-163.
27. Rose, T.; Van Zwieten, L.; Claassens, A.; Scanlan, C.; Rose, M., Phytotoxicity of soilborne glyphosate residues is influenced by the method of phosphorus fertiliser application. *Plant Soil* **2017**; *422*, 455-465.
28. Piccolo, A.; Celano, G.; Conte, P., Adsorption of glyphosate by humic substances. *Journal of Agricultural and Food Chemistry* **1996,** *44* (8), 2442-2446.

29. Albers, C. N.; Banta, G. T.; Hansen, P. E.; Jacobsen, O. S., The influence of organic matter on sorption and fate of glyphosate in soil – Comparing different soils and humic substances. *Environmental Pollution* **2009,** *157* (10), 2865-2870.
30. Vereecken, H., Mobility and leaching of glyphosate: a review. *Pest Management Science* **2005,** *61* (12), 1139-1151.
31. Rayment, G. E.; Lyons, D. J., *Soil chemical methods : Australasia*. CSIRO Publishing: Collingwood, Vic, **2010**.
32. Robinson, N. J.; Kitching, M., The 3D distribution of phyllosilicate clay minerals in western Victoria. *Geoderma* **2016,** *284*, 152-177.
33. Jones, E.; Oliphant, E.; Peterson, P. SciPy: Open source scientific tools for Python. **2001**
34. Hunter, J. D., Matplotlib: A 2D graphics environment. *Computing in Science & Engineering* **2007,** *9* (3), 90-95.
35. McKinney, W., Data structures for statistical computing in Python. *Proceedings of the 9th Python in Science Conference* **2010**, 51-56.
36. Oliphant, T. E., *A guide to NumPy*. Trelgol Publishing: **2006**.
37. Wood, S. mgcv: Mixed GAM computation vehicle with automatic smoothness estimation. **2018**
38. Dralle, D.; Karst, N.; Thompson, S. E., a, b careful: The challenge of scale invariance for comparative analyses in power law models of the streamflow recession. *Geophysical Research Letters* **2015,** *42* (21), 9285-9293.
39. Zhang, P.; Rose, M.; Van Zwieten, L., Direct determination of glyphosate and its metabolite AMPA in soil using mixed-mode solid-phase purification and LC-MS/MS determination on a hypercarb column. *Journal of AOAC International* **2019,** *102* (3), 952-965.
40. Ghafoor, A.; Jarvis, N. J.; Thierfelder, T.; Stenström, J., Measurements and modeling of pesticide persistence in soil at the catchment scale. *Science of The Total Environment* **2011,** *409* (10), 1900-1908.
41. Ghafoor, A.; Moeys, J.; Stenström, J.; Tranter, G.; Jarvis, N. J., Modeling spatial variation in microbial degradation of pesticides in soil. *Environmental Science & Technology* **2011,** *45* (15), 6411-6419.
42. Laitinen, P.; Rämö, S.; Nikunen, U.; Jauhiainen, L.; Siimes, K.; Turtola, E., Glyphosate and phosphorus leaching and residues in boreal sandy soil. *Plant and Soil* **2009,** *323* (1), 267-283.
43. Dollinger, J.; Dagès, C.; Voltz, M., Glyphosate sorption to soils and sediments predicted by pedotransfer functions. *Environmental Chemistry Letters* **2015,** *13* (3), 293-307.
44. Paradelo, M.; Norgaard, T.; Moldrup, P.; Ferré, T. P. A.; Kumari, K. G. I. D.; Arthur, E.; de Jonge, L. W., Prediction of the glyphosate sorption coefficient across two loamy agricultural fields. *Geoderma* **2015,** *259–260*, 224-232.
45. Sidoli, P.; Baran, N.; Angulo-Jaramillo, R., Glyphosate and AMPA adsorption in soils: laboratory experiments and pedotransfer rules. *Environmental Science and Pollution Research* **2016,** *23* (6), 5733-5742.
46. De Gerónimo, E.; Aparicio, V. C.; Costa, J. L., Glyphosate sorption to soils of Argentina. Estimation of affinity coefficient by pedotransfer function. *Geoderma* **2018,** *322*, 140-148.
47. Herlihy, M.; McGrath, D., Phosphorus fractions and adsorption characteristics in grassland soils of varied soil phosphorus status. *Nutrient Cycling in Agroecosystems* **2007,** *77* (1), 15-27.
48. Forrester, S. T.; Janik, L. J.; Soriano-Disla, J. M.; Mason, S.; Burkitt, L.; Moody, P.; Gourley, C. J. P.; McLaughlin, M. J., Use of handheld mid-infrared spectroscopy and partial least-squares regression for the prediction of the phosphorus buffering index in Australian soils. *Soil Research* **2015,** *53* (1), 67-80.

49. Bolland, M. D. A.; Windsor, D. P., Converting reactive iron, reactive aluminium, and phosphorus retention index (PRI) to the phosphorus buffering index (PBI) for sandy soils of south-western Australia. *Soil Research* **2007,** *45* (4), 262-265.
50. Daly, K.; Jeffrey, D.; Tunney, H., The effect of soil type on phosphorus sorption capacity and desorption dynamics in Irish grassland soils. *Soil Use and Management* **2001,** *17* (1), 12-20.
51. Buczko, U.; Kuchenbuch, R. O., Phosphorus indices as risk-assessment tools in the U.S.A. and Europe—a review. *Journal of Plant Nutrition and Soil Science* **2007,** *170* (4), 445-460.

3. Development of a Predictive Model for Glyphosate Adsorption in Soils Using MIR Spectra

Gavin Styles[a], Miguela Martin[a], Michael Rose[b], Lukas Van Zwieten[ab], Bayden Wood[a], Antonio F Patti[a]

[a]School of Chemistry, Monash University, Wellington Rd., Clayton, 3800, Victoria, Australia

[b]New South Wales Department of Primary Industries, 1243 Bruxner Highway, Wollongbar, 2477, New South Wales, Australia

Declarations of interest: none

3.1 Abstract

Adsorption of herbicides to soil can impact their mobility, persistence and efficacy. A method for predicting adsorption of herbicides that is rapid and relatively inexpensive would allow for more spatially explicit management of herbicide application and risk. In this study, MIR spectroscopy was used to develop a predictive model for glyphosate adsorption to 90 soils with a wide range of physico -chemical properties. Adsorption isotherms were built for glyphosate from 45 sites (and 2 sampling depths) across Australia, and this database used in conjunction with MIR spectra of the same soils to predict adsorption using a partial least squares methodology, with a venetian blinds cross validation. The K_f values of these soils ranged from 4.6 to 186 mg kg^{-1} (L mg^{-1})$^{-1/nf}$, with the final model resulting in a cross-validated R^2 and RMSECV of 0.839 and 17.34 mg kg^{-1} (L mg^{-1})$^{-1/nf}$ respectively. A strong correlation was observed between the MIR loadings associated with phosphorus buffer index, glyphosate adsorption and certain soil minerals.

3.2 Introduction

Glyphosate is the single most widely used herbicide both in Australia and globally. While traditionally considered to be of low ecological risk due to its high adsorption capacity to soil

and rapid breakdown[1-3], more recent findings have demonstrated that glyphosate can be "pseudo-persistent" when repeat applications occur more frequently than time required for complete breakdown, leading to periodic build up in some soils[4]. Environmental surveys have also detected glyphosate in rainwater[5], dust[6], waterways[7-8], sediment[9] and air[5].

Adsorption plays an important role in the environmental fate and effect of glyphosate. Adsorption behaviour regulates its persistence in soil[10], offsite mobility[11-12] and biological availability in soil[13]. Due to glyphosate's zwitterionic nature (pKa = 2, 2.6, 5.8 and 10.8, occurring due to protonation and deprotonation of the phosphonate, amine and carboxylic acid groups[14]) and the phosphonic acid group[15], adsorption behaviour is largely regulated by variable charge clay minerals and metal oxides[16]. Adsorption is generally greater in acid soils due to the more positively charged surface of these minerals, and thus a higher level of attraction of the negatively charged phosphonic acid group[17-18]. Adsorption via the phosphonic acid head also leads to competition for binding sites with inorganic phosphate in soil[19-20], and remobilisation of the glyphosate has been shown to occur upon addition of phosphorus fertiliser[7, 21-22].

While the factors influencing glyphosate adsorption in soil are relatively well known, there have been limited attempts to predict adsorption behaviour in a given soil. Current models have focused mostly on using physicochemical properties of the soil such as pH, soil texture, phosphorus content and mineralogy[23-26]. Mid-infrared reflectance (MIR) spectroscopy is an inexpensive, rapid, holistic technique that can bypass the need for the time consuming, sometimes expensive wet chemical techniques, provided adequate calibration is conducted. Infrared spectra provide information on a wide range of soil properties, and can accurately predict soil texture[27], mineralogy[28], speciation of organic matter[29] and pH[30]. Previous studies have also used MIR to produce robust predictive models for the adsorption to soil of other herbicides such as diuron[31-32], atrazine[33], lindane and linuron[34]. Although Paradelo et al (2016) also used this technique to predict glyphosate adsorption in soils with a relatively high level of

success[35], the calibration set only contained samples from two adjacent fields, covering a limited amount of variation in the soils tested.

To address the currently limited models for glyphosate sorption to soil, MIR spectra from approximately 90 soils were used to produce a model capable of predicting the K_f of a given soil for glyphosate, along with various physico-chemical properties. We hypothesised that the holistic nature of MIR would allow for an accurate predictive model for glyphosate adsorption to these contrasting soils, ultimately providing an inexpensive, practical tool to improve the site-specific understanding of glyphosate fate in soil.

3.3 Material and Methods

3.3.1 Soil and Mineral Samples and Characterisation

Goethite, kaolinite, hematite and rutile were purchased from Sigma Aldrich (Sydney, Australia), calcite was purchased from Pacific Water Technology (Brisbane, Australia), and Gibbsite was purchased from an independent minerals distributor, sourced originally from Copper Mountains, Box Elder, Utah, United States. Birnessite was produced according to the amended Attenborough method developed by Gritter and Wallace (1959)[36]. All structures were confirmed using powder x-ray diffraction (D8 Advance Eco, Bruker Corporation).

Agricultural soils were sampled in April-May 2015 from various locations (45 sites) in Australia (Appendix Table 1), with sites represented by grain cropping systems (predominantly wheat, barley and pulses), pasture and sugarcane systems. Samples were taken with a 25 mm diameter stainless steel open-faced push corer to a depth of 30 cm, and were divided into 0-10 cm and 10-30 cm layers. At each location, 12 subsamples were randomly taken from a 50 m by 50 m grid in each paddock, and these were composited as a single sample. Samples were air-dried, crushed and sieved to < 2 mm. Samples were stored air-dried until analysis. Soil pH (1:5 soil:water), EC, bicarbonate-extractable P (Colwell P) and total organic C content were determined using methods described in Rayment and Lyons (2010)[37]. Phosphorus buffering

index (PBI_{+ColP}) was determined according to Rayment and Lyons method 9I2B (2010). Briefly this involves dosing soil with 100 mg P L^{-1} solution at a soil:solution ratio of 1:10 and determining the amount of P sorbed after 17 h of mixing. PBI_{+ColP} was then calculated as the freshly sorbed P (mg P kg^{-1}) plus the Colwell-P (mg kg^{-1}), divided by the final solution P concentration (mg P L^{-1}).

MIR spectra were collected using powdered (<100 µm) soil and mineral samples and a Nicolet 6700 FTIR spectrometer (Thermofisher Scientific, Waltham, MA, USA) fitted with an Auto Diff II autosampler (Pike Technologies, Madison, WI, USA) and a KBr beam splitter. Absorption spectra were collected from 400-4000 cm^{-1}.

3.3.2 Glyphosate Sorption

^{14}C labelled glyphosate (1.85 GBq mol^{-1}) was purchased from American Radiolabelled Chemicals (Saint Louis, USA) and mixed with analytical grade glyphosate (Accustandard, New Haven, USA) to produce five one litre solutions with concentrations of 0.3, 1, 3, 9 and 27 mg L^{-1}, and standard radioactivity of ~10 nCi per sample.

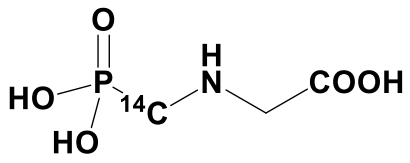

Figure 8: ^{14}C Labelled Glyphosate

Soils were irradiated under 254 nm UV light (1 hour, <1 mm thick layer, mixed and respread every 20 minutes) prior to adsorption experiments in order to inhibit microbial degradation of the glyphosate. Respiration measurements (headspace CO_2 concentration in a closed, analysed by gas chromatography) indicated a reduction in soil respiration by up to 60% due to UV exposure. Sorption trials were conducted with a 1:5 soil-to-liquid ratio at five concentrations of glyphosate (0.3, 1, 3, 9 and 27 mg L^{-1}) using 1 g aliquots of air dried soil. Soil-glyphosate mixtures were mixed on an end-over-end shaker (33 rpm) at 22 °C for 24 hours to allow equilibration, before being centrifuged at 2600 x G for 20 min (Thermo Scientific Megafuge 8). The

supernatant was then removed and filtered through a 0.2 µm polyethylene (Merck) membrane to remove any remaining clay particles. Supernatant (2 mL) was then mixed with scintillation cocktail (18 mL, Optifluor, PerkinElmer) and glyphosate concentration determined by scintillation counting (Tricarb 2810, Packard). The amount of adsorbed glyphosate was then determined indirectly by subtracting equilibrium glyphosate concentration from initial glyphosate concentration. Controls conducted in the same manner without soil material showed negligible adsorption of glyphosate to the centrifuge tubes or filters. A microbial degradation control was conducted using a 0.5 M NaOH trap for CO_2, these trials showed <1% mineralisation of glyphosate to CO_2 over 24 hours in four contrasting soils within the calibration set.

Sorption coefficients were calculated, where *C* is concentration of glyphosate in solution (µg ml^{-1}) and *x* is the concentration of glyphosate adsorbed to the soil (µg g^{-1}). The parameters K_f and *n* of the Freundlich isotherm:

$$x = K_f C^{\frac{1}{n}}$$

were calculated using the full concentration range and regression of the log-transformed concentrations.

3.3.3 Data Analysis

MIR spectra were imported, pre-processed, and analysed using MATLAB (Natick, MA, USA) and PLS_Toolbox (Eigenvector Research Inc., Manson, WA, USA)[38]. Spectra were smoothed by the Savitsky-Golay[39] method using 9 smoothing points and a polynomial order of 2 in a symmetric kernel before mean centering. Principle component analysis (PCA)[40] was conducted for the set of spectra to identify potential outliers and the overall variation in the dataset. PCA is a technique by which an *n x m* covariance matrix is built, consisting of *m* spectral absorbance values and *n* spectra. Eigen vectors, or the principle components (PCs), and their associated

eigenvalues were then calculated from this matrix to summarise the variation in the dataset. Samples were 'scored' along these PCs and plotted in 2 to 3 dimensions, in order to visualise variation among samples. The loadings, or the weights of the spectral features in each PC, were used to identify the chemical components associated with the variation in the data.

Predictive models of K_f and other soil physicochemical properties were subsequently developed via partial least squares regression (PLS-R)[41], a technique which acts similarly to principle component analysis. However, where PCA and PCR are unsupervised methods, PLS-R uses reference values to build the scores and loadings. As such, PLS-R allows for the combining and adjustment of principle components in order to reduce error and produce a more accurate prediction. As the data set was randomly ordered with respect to the reference Y responses, models were cross validated using venetian blinds, with 10 data splits and a single sample per blind. In this method, a subset containing every 10th sample of the data block was used as a validation set for a model built from the remaining dataset, and this process was repeated 10 times on a subsequent subset. This was done as no additional independent set was available for model validation, and the use of leave-one-out alone can lead to artificially positive results due to over fitting of each new validation sample[42].

3.4 Results and Discussion

Physico-chemical analysis of the soils used in this showed a wide variation in physical soil properties and glyphosate adsorption (K_f) values (Table 6, Appendix Table 1). The K_f values for glyphosate measured here encompass and extend the range of values previously reported in literature[23-25].

Table 6: Distribution of soil properties (n=90)

Property	Min	Max	Mean	SD	Median
pH_{Water}	4.6	9.2	7.1	1.3	6.7
Clay (%)	4.39	51.78	22.11	10.52	19.86
TOC (%)	0.21	6.50	1.92	1.61	1.40
EC (dS/m)	0.04	0.56	0.16	0.10	0.15
$PBI_{Colwell\ P}$	10.0	720.0	118.4	154.2	69.5
K_f	4.56	186.11	42.19	43.16	29.37

**SD = standard deviation, TOC = total organic carbon, EC = electrical conductivity, PBI = phosphorus buffering index*

Previous studies have shown that no single variable correlates with *Kf* strongly enough to suggest a single driving factor in glyphosate adsorption[23-26]. Univariate correlations of soil properties and respective adorption coefficients (K_f) for our dataset supported this notion (Appendix Table 3). However, high PBI and low pH appeared to be good predictors of an increased affinity for glyphosate adsorption.

To further understand the MIR spectra and physicochemical attributes of these soils, MIR spectra of pure minerals commonly found in soil were also collected (Figure 9).

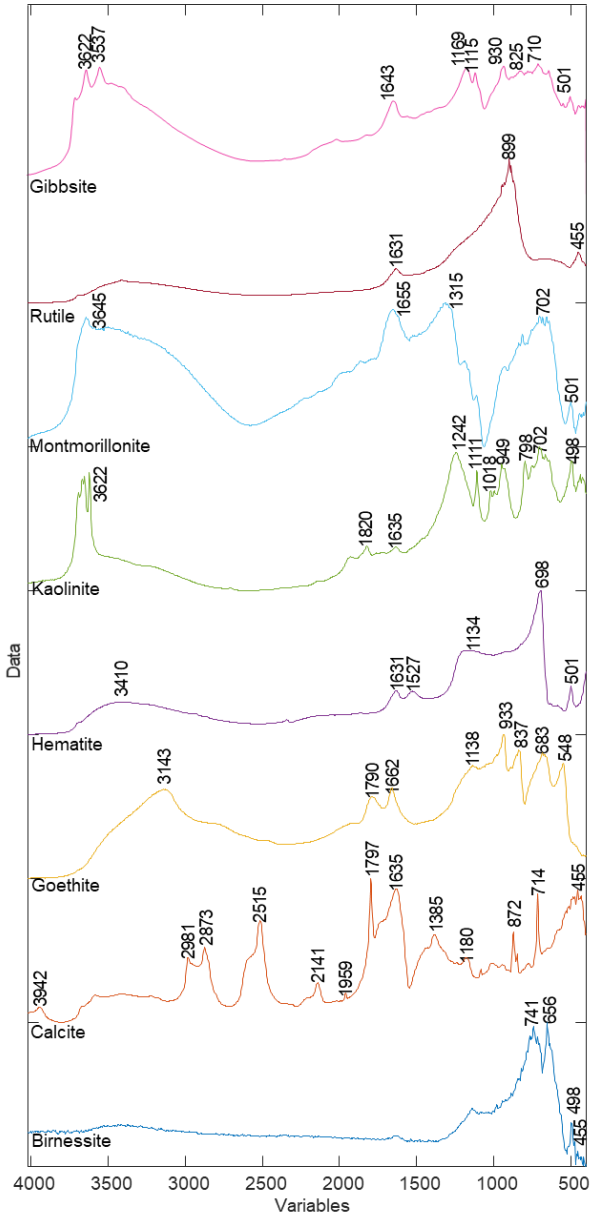

Figure 9: MIR spectra of mineral standards

The spectral data did not reveal any obvious visual trends that could be readily assigned to relevant physicochemical properties or K_f values. However, inspection of the overlapped soil spectra (Figure 10) suggested that certain mineral components were more frequent in soils from particular locations, specifically kaolinite (bands around 3600-3700cm^{-1} region) and calcite (bands around 2500 cm^{-1}) in a number of WA and SA soils, respectively.

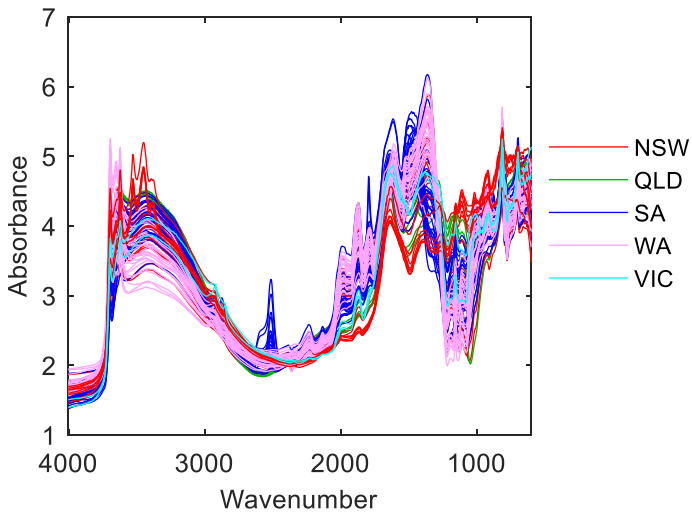

Figure 10: Spectral data, normalised using standard normal variate (SNV)

PCA models of the data revealed no spectral outliers based on a plot of Q-residuals against Hotelling's T^2, confirming that the entire database of 90 soils was suitable for the development of regression models (Figure 11). PCA also showed some clustering along PC 3 according to the State from where the sample was collected, due to spectral bands associated with the aforementioned minerals as well as bands at 1504 cm^{-1} and 1346 cm^{-1}. Although spectral bands associated with calcite peaks were present in a number of soils from SA, the even spread of SA across the PCA, implies a limited influence of calcite in describing the variation across the whole dataset, relative to the bands at 3695, 1346 and 1504 nm with higher loadings. .

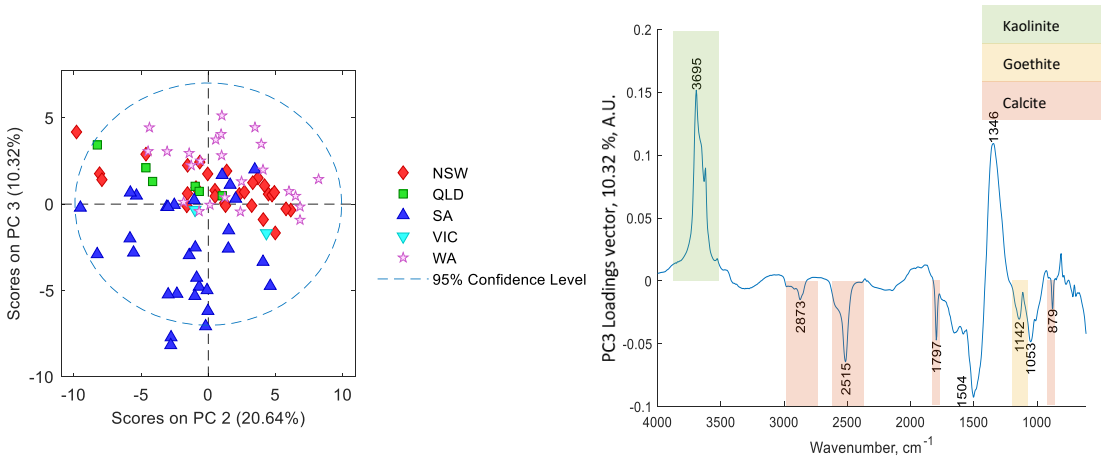

Figure 11: PCA scores plot (left) and the associated PC1 loadings (right) of the spectral database

Because glyphosate adsorption behaviour is strongly influenced by pH and soil mineralogy related to P-sorption[15-18], initial modelling revolved around predicting soil pH and phosphorus buffer index (PBI) from MIR spectra as a "proof of concept". These attributes were selected due to their role in glyphosate adsorption and previous reports demonstrating their amenability to MIR prediction[30, 43-44]. This proved successful, with pH and PBI models producing cross-validated R^2 values of 0.824 and 0.848 respectively. These models also produced a relatively low error, with cross validated real mean squared error (RMSECV) scores of 0.53 for pH and 60.08 for PBI. By visual comparison with the spectra of the pure minerals, it appears calcite is positively correlated with pH, which is a helpful check, given the alkali nature of calcium carbonate. Janik and Skjemstad (1995)[45] also reported a positive MIR loading between smectite-associate wavebands and pH, as well as negative MIR loadings between kaolin- and gibbsite- associated wavebands and pH smectite, but these relationships were not clear with our calibration set. Other authors have also shown that MIR predictions of pH are often related to other factors such as exchangeable cations, organic acids and/or carbonates (Minasny et al 2009[46]; Reeves et al 2010[47]), and these may confound any associations with standard mineral spectra.

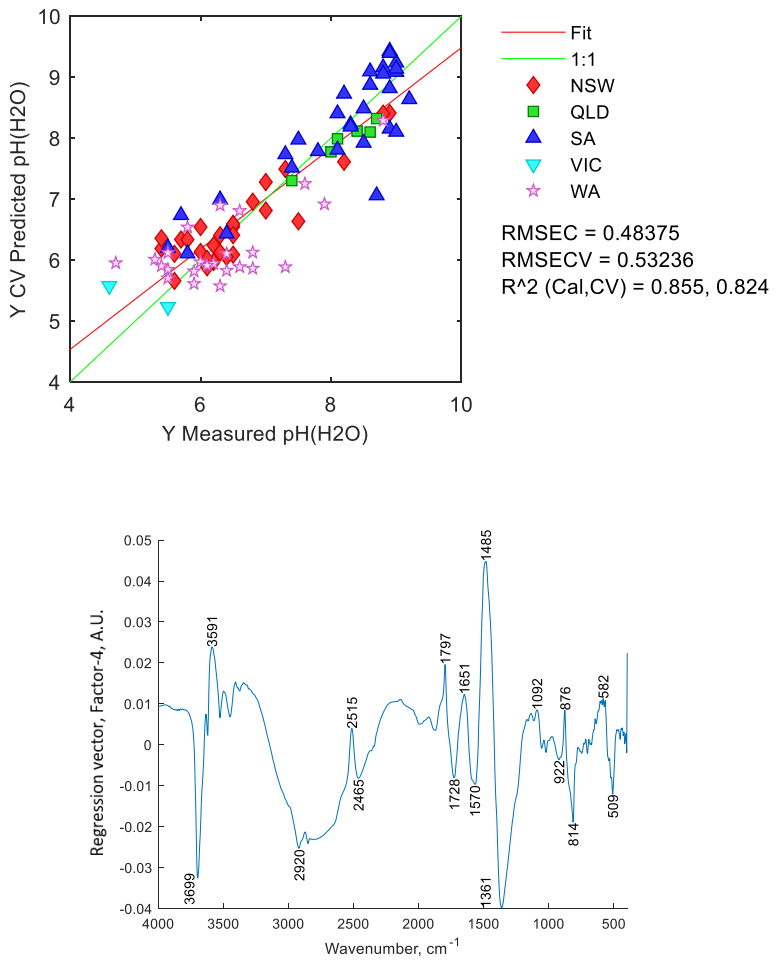

Figure 12: Experimental vs predicted values (top) and PLS-R loadings (bottom) for pH predictions

In contrast, some mineral assignments for PBI could be speculated (Figure 13) on the basis of additional information in additional latent variable loadings. Despite some overlap between mineral spectra, particularly kaolinite and gibbsite from 3500-3700 cm^{-1}, there was a clear positive association of gibbsite with PBI appearing in the 3rd factor loading, and negative association of kaolinite in the 4th factor loading. A lack of spectral data for other minerals (e.g. quartz, other alumina-silicates) and various organic matter fractions prevent a more complete interpretation of the MIR loadings, but the seven reference minerals included for reference here help to contextualise the existing knowledge of glyphosate and phosphate adsorption to soil minerals such as metal oxides[48-51].

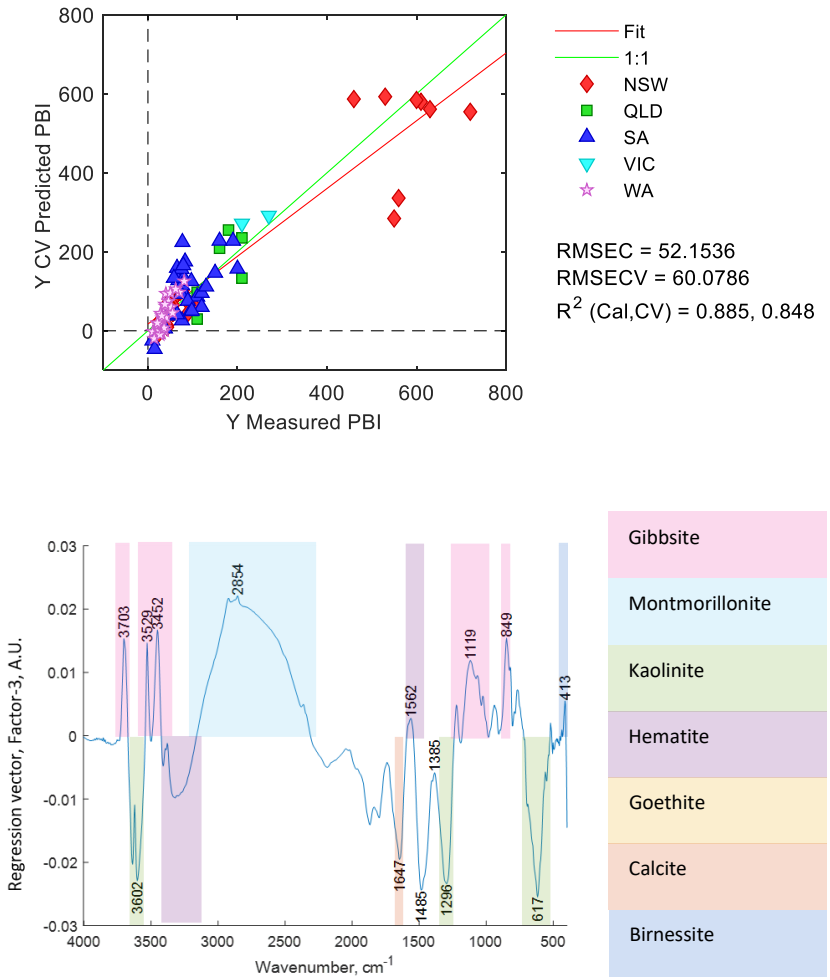

Figure 13: Experimental vs predicted values (top) and PLS-R loadings (bottom) for PBI predictions

Based on the success of these two models (a high R^2 in comparison to similar literature models[30, 43-44]), a predictive model for glyphosate adsorption (K_f) was subsequently developed. A PLS-R based model for K_f provided good results, with cross-validated R^2 and RMSECV values of 0.839 and 17.34 mg kg^{-1} (L mg^{-1})$^{-1/nf}$ respectively. These are at the higher end of previously reported values (E.g. r2 0.74-0.93) for similar MIR based models for prediction of herbicide adsorption[25, 31, 33]. A clear gap is seen in the dataset seen between K_f values of 60 and 160, which leads to less reliable predictions in this region. However, the model overall is a strong proof of concept for the prediction of glyphosate adsorption coefficients in soil, and the framework would likely provide even greater results if the dataset were to be expanded to include a larger number of soil samples.

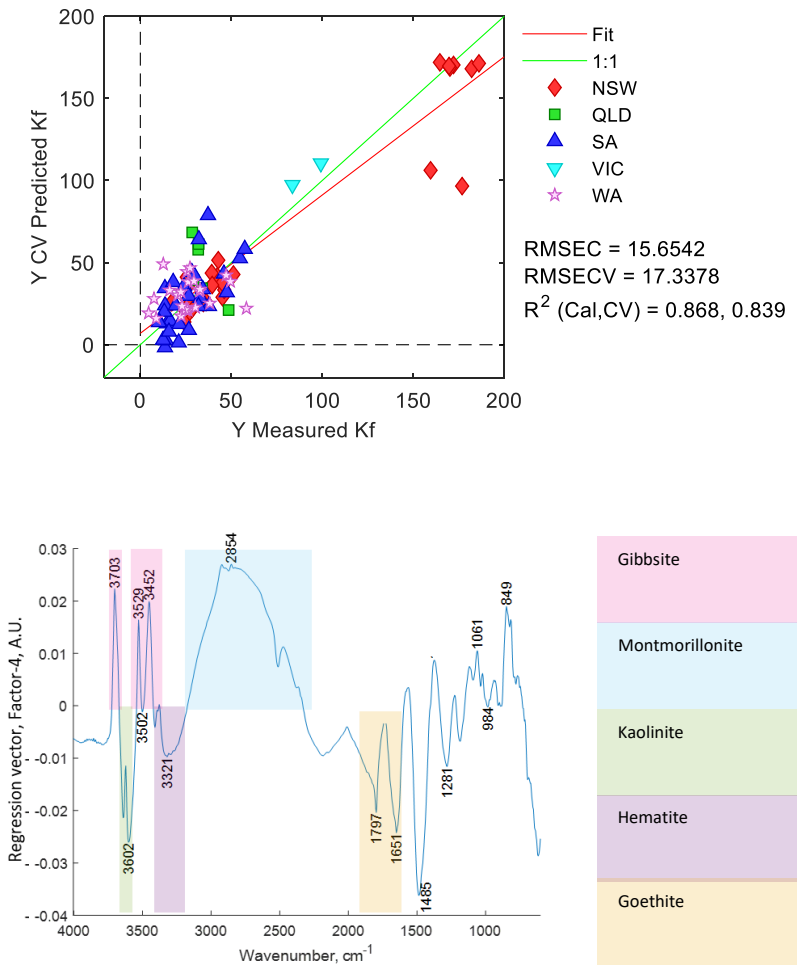

Figure 14: Predicted vs experimental values (top) and PLS-R loadings (bottom) for K_f predictions

A particularly interesting feature of this model, is how closely the predictions and loadings resemble that of the PBI model. This further supports previous findings around the inherent link between glyphosate and phosphate adsorption in soil (Chapter 2). As with PBI, MIR loadings associated with soil kaolinite content (and hematite) appear negatively correlated with glyphosate binding. While it is possible that calcite also has a negative association with K_f, as appears to be the case with PBI (Figure 14), there is uncertainty due the overlap of goethite bands around wavelengths from 1650-1800 cm^{-1}. There was a noticeable positive association of gibbsite on the loading scores of the glyphosate adsorption model, similar to the PBI models, evident in the 3700 and 1730 cm^{-1} regions. The apparent 0 loading of the peak at 1730 cm^{-1} is cause by overlap with the negatively associated goethite peak, and the overall assignment of gibbsite rather than montmorillonite was chosen due to the shape of the peaks at 3700 cm^{-1} in

combination with the presence of the peak at 1730 cm^{-1}. Because the high K_f (K_f >150) soils used in this model are known to have a high gibbsite content, the model was rerun with these samples removed to check for any unnecessary model bias towards these soils and corresponding overestimation of gibbsite influence on adsorption of glyphosate. This model produced a cross-validated R^2 of 0.567 and an RMSECV of 10.355 mg kg^{-1} (L mg^{-1})$^{-1/nf}$, and while there was a reduction in the magnitude of gibbsite related loading scores, they were by no means completely removed. This reduction in goodness-of-fit, along with apparent low level of biasing due to gibbsite, led to the original model including high K_f soils being considered the best choice.

Finally, although no distinct bands were attributable to rutile, this may be due to a lack of rutile in the soils tested and/or the relative lack of features in the rutile MIR spectra. Further analysis of the soil database would be required to confirm this. Important bands appeared at 1485 cm^{-1} in all three loadings, and 1361 cm^{-1} in pH, neither of which were assignable with any of the mineral spectra, and are likely to be due to inorganic carbonate and nitrate ions respectively[52].

The predictive model developed in this study has applications for improved management and risk assessment of soil glyphosate. The rapid and inexpensive nature of MIR spectroscopy allows for a widespread application, including immediate sampling and analysis in the field. This in turn leads to far more spatially explicit development of management strategies of glyphosate usage, in particular around risks of leaching and persistence, providing both environmental and economic benefits. The model developed in this study shows improvements over similar previously reported models in the form of a larger database of soils, and improvements in goodness-of-fit. It also confirms the importance of certain minerals such as montmorillonite and gibbsite in the adsorption affinity of glyphosate for soils.

3.5 References

1. Roy, D. N.; Konar, S. K.; Banerjee, S.; Charles, D. A.; Thompson, D. G.; Prasad, R., Persistence, movement, and degradation of glyphosate in selected Canadian boreal forest soils. *Journal of Agricultural and Food Chemistry* **1989,** *37* (2), 437-440.
2. Giesy, J. P.; Dobson, S.; Solomon, K. R., Ecotoxicological risk assessment for Roundup® herbicide. In *Reviews of Environmental Contamination and Toxicology: Continuation of Residue Reviews*, Ware, G. W., Ed. Springer New York: New York, NY, **2000**; pp 35-120.
3. Peterson, R. K. D.; Hulting, A. G., A comparative ecological risk assessment for herbicides used on spring wheat: the effect of glyphosate when used within a glyphosate-tolerant wheat system. *Weed Science* **2017,** *52* (5), 834-844.
4. Primost, J. E.; Marino, D. J. G.; Aparicio, V. C.; Costa, J. L.; Carriquiriborde, P., Glyphosate and AMPA, "pseudo-persistent" pollutants under real-world agricultural management practices in the Mesopotamic Pampas agroecosystem, Argentina. *Environmental Pollution* **2017,** *229*, 771-779.
5. Chang, F.; Simcik, M. F.; Capel, P. D., Occurrence and fate of the herbicide glyphosate and its degradate aminomethylphosphonic acid in the atmosphere. *Environmental Toxicology and Chemistry* **2011,** *30* (3), 548-555.
6. Mendez, M. J.; Aimar, S. B.; Aparicio, V. C.; Ramirez Haberkon, N. B.; Buschiazzo, D. E.; De Gerónimo, E.; Costa, J. L., Glyphosate and aminomethylphosphonic acid (AMPA) contents in the respirable dust emitted by an agricultural soil of the central semiarid region of Argentina. *Aeolian Research* **2017,** *29*, 23-29.
7. Rosenbom, A.; Haarder, B.; Badawi, N.; Gudmundsson, L.; Von Platten-Hallermund, F.; H Hansen, C.; B Nielsen, C.; Plauborg, F.; Olsen, P., *The Danish Pesticide Leaching Assessment Programme. Monitoring results May 1999–June 2016*. **2017**.
8. Saunders, E. L.; Pezeshki, R., Glyphosate in runoff waters and in the root-zone: A review. *Toxics* **2015,** *3* (4), 462-480.
9. Battaglin, W. A.; Meyer, M. T.; Kuivila, K. M.; Dietze, J. E., Glyphosate and its degradation product AMPA occur frequently and 2idely in U.S. soils, surface water, groundwater, and precipitation. *Journal of the American Water Resources Association* **2014,** *50* (2), 275-290.
10. Al-Rajab, A. J.; Schiavon, M., Degradation of ^{14}C-glyphosate and aminomethylphosphonic acid (AMPA) in three agricultural soils. *Journal of Environmental Sciences* **2010,** *22* (9), 1374-1380.
11. McGrath, G. S.; Hinz, C.; Sivapalan, M., A preferential flow leaching index. *Water Resources Research* **2009,** *45* (11), W114505.
12. McGrath, G. S.; Hinz, C.; Sivapalan, M., Modelling the impact of within-storm variability of rainfall on the loading of solutes to preferential flow pathways. *European Journal of Soil Science* **2008,** *59* (1), 24-33.
13. Simonsen, L.; Fomsgaard, I. S.; Svensmark, B.; Spliid, N. H., Fate and availability of glyphosate and AMPA in agricultural soil. *Journal of Environmental Science and Health, Part B* **2008,** *43* (5), 365-375.
14. Sprankle, P.; Meggitt, W. F.; Penner, D., Adsorption, mobility, and microbial degradation of glyphosate in the soil. *Weed Science* **1975,** *23* (3), 229-234.
15. Sheals, J.; Sjöberg, S.; Persson, P., Adsorption of glyphosate on goethite: Molecular characterization of surface complexes. *Environmental Science & Technology* **2002,** *36* (14), 3090-3095.
16. Morillo, E.; Undabeytia, T.; Maqueda, C.; Ramos, A., Glyphosate adsorption on soils of different characteristics.: Influence of copper addition. *Chemosphere* **2000,** *40* (1), 103-107.
17. Zhao, B.; Zhang, J.; Gong, J.; Zhang, H.; Zhang, C., Glyphosate mobility in soils by phosphate application: Laboratory column experiments. *Geoderma* **2009,** *149* (3), 290-297.

18. de Jonge, H.; Wollesen de Jonge, L., Influence of pH and solution composition on the sorption of glyphosate and prochloraz to a sandy loam soil. *Chemosphere* **1999,** *39* (5), 753-763.
19. Laitinen, P.; Siimes, K.; Rämö, S.; Jauhiainen, L.; Eronen, L.; Oinonen, S.; Hartikainen, H., Effects of soil phosphorus status on environmental risk assessment of glyphosate and glufosinate-ammonium. *Journal of Environmental Quality* **2008,** *37* (3), 830-838.
20. Padilla, J. T.; Selim, H. M., Interactions among glyphosate and phosphate in soils: Laboratory retention and transport studies. *Journal of Environmental Quality* **2019,** *48* (1), 156-163.
21. Rose, T.; Van Zwieten, L.; Claassens, A.; Scanlan, C.; Rose, M., Phytotoxicity of soilborne glyphosate residues is influenced by the method of phosphorus fertiliser application. *Plant Soil* **2017**; *422*, 455-465.
22. Bott, S.; Tesfamariam, T.; Kania, A.; Eman, B.; Aslan, N.; Römheld, V.; Neumann, G., Phytotoxicity of glyphosate soil residues re-mobilised by phosphate fertilisation. *Plant and Soil* **2011,** *342* (1), 249-263.
23. De Gerónimo, E.; Aparicio, V. C.; Costa, J. L., Glyphosate sorption to soils of Argentina. Estimation of affinity coefficient by pedotransfer function. *Geoderma* **2018,** *322*, 140-148.
24. Dollinger, J.; Dagès, C.; Voltz, M., Glyphosate sorption to soils and sediments predicted by pedotransfer functions. *Environmental Chemistry Letters* **2015,** *13* (3), 293-307.
25. Paradelo, M.; Norgaard, T.; Moldrup, P.; Ferré, T. P. A.; Kumari, K. G. I. D.; Arthur, E.; de Jonge, L. W., Prediction of the glyphosate sorption coefficient across two loamy agricultural fields. *Geoderma* **2015,** *259–260*, 224-232.
26. Sidoli, P.; Baran, N.; Angulo-Jaramillo, R., Glyphosate and AMPA adsorption in soils: laboratory experiments and pedotransfer rules. *Environmental Science and Pollution Research* **2016,** *23* (6), 5733-5742.
27. Hobley, E. U.; Prater, I., Estimating soil texture from vis–NIR spectra. *European Journal of Soil Science* **2019,** *70* (1), 83-95.
28. Robinson, N. J.; Kitching, M., The 3D distribution of phyllosilicate clay minerals in western Victoria. *Geoderma* **2016,** *284*, 152-177.
29. Baldock, J. A.; Hawke, B.; Sanderman, J.; Macdonald, L. M., Predicting contents of carbon and its component fractions in Australian soils from diffuse reflectance mid-infrared spectra. *Soil Research* **2013,** *51* (8), 577-595.
30. Pirie, A.; Singh, B.; Islam, K., Ultra-violet, visible, near-infrared, and mid-infrared diffuse reflectance spectroscopic techniques to predict several soil properties. *Soil Research* **2005,** *43* (6), 713-721.
31. Forouzangohar, M.; Kookana, R. S.; Forrester, S. T.; Smernik, R. J.; Chittleborough, D. J., Midinfrared spectroscopy and chemometrics to predict diuron sorption coefficients in soils. *Environmental Science & Technology* **2008,** *42* (9), 3283-3288.
32. Forouzangohar, M.; Cozzolino, D.; Kookana, R. S.; Smernik, R. J.; Forrester, S. T.; Chittleborough, D. J., Direct comparison between visible near- and mid-infrared spectroscopy for describing diuron sorption in soils. *Environmental Science & Technology* **2009,** *43* (11), 4049-4055.
33. Kookana, R. S.; Janik, L. J.; Forouzangohar, M.; Forrester, S. T., Prediction of atrazine sorption coefficients in soils using mid-infrared spectroscopy and partial least-squares analysis. *Journal of Agricultural and Food Chemistry* **2008,** *56* (9), 3208-3213.
34. Bengtsson, S.; Berglöf, T.; Sjöqvist, T., Predicting the leachability of pesticides from soils using near-infrared reflectance. *Journal of Agricultural and Food Chemistry* **1996,** *44* (8), 2260-2265.
35. Paradelo, M.; Hermansen, C.; Knadel, M.; Moldrup, P.; Greve, M. H.; de Jonge, L. W., Field-scale predictions of soil contaminant sorption using visible–near infrared spectroscopy. *Journal of Near Infrared Spectroscopy* **2016,** *24* (3), 281-291.

36. Gritter, R. J.; Wallace, T. J., The manganese dioxide oxidation of allylic alcohols. *The Journal of Organic Chemistry* **1959,** *24* (8), 1051-1056.
37. Rayment, G. E.; Lyons, D. J., *Soil chemical methods : Australasia*. CSIRO Publishing: Collingwood, Vic, **2010**.
38. Wise, B. M.; Gallagher, N.; Bro, R.; Shaver, J.; Windig, W.; Koch, R. S., PLS Toolbox 4.0. *Eigenvector Research Incorporated: Wenatchee, WA, USA* **2007**, 99-162.
39. Savitzky, A.; Golay, M. J., Smoothing and differentiation of data by simplified least squares procedures. *Analytical chemistry* **1964,** *36* (8), 1627-1639.
40. Hubert, M.; Rousseeuw, P. J.; Verboven, S., A fast method for robust principal components with applications to chemometrics. *Chemometrics and Intelligent Laboratory Systems* **2002,** *60* (1-2), 101-111.
41. Hubert, M.; Branden, K. V., Robust methods for partial least squares regression. *Journal of Chemometrics: A Journal of the Chemometrics Society* **2003,** *17* (10), 537-549.
42. Baumann, K., Cross-validation as the objective function for variable-selection techniques. *TrAC Trends in Analytical Chemistry* **2003,** *22* (6), 395-406.
43. Viscarra Rossel, R. A.; Walvoort, D. J. J.; McBratney, A. B.; Janik, L. J.; Skjemstad, J. O., Visible, near infrared, mid infrared or combined diffuse reflectance spectroscopy for simultaneous assessment of various soil properties. *Geoderma* **2006,** *131* (1), 59-75.
44. Forrester, S. T.; Janik, L. J.; Soriano-Disla, J. M.; Mason, S.; Burkitt, L.; Moody, P.; Gourley, C. J. P.; McLaughlin, M. J., Use of handheld mid-infrared spectroscopy and partial least-squares regression for the prediction of the phosphorus buffering index in Australian soils. *Soil Research* **2015,** *53* (1), 67-80.
45. Janik, L.; Skjemstad, J., Characterization and analysis of soils using mid-infrared partial least-squares .2. Correlations with some laboratory data. *Soil Research* **1995,** *33* (4), 637-650.
46. Minasny, B.; Tranter, G.; McBratney, A. B.; Brough, D. M.; Murphy, B. W., Regional transferability of mid-infrared diffuse reflectance spectroscopic prediction for soil chemical properties. *Geoderma* **2009,** *153* (1), 155-162.
47. Reeves, J. B., Near- versus mid-infrared diffuse reflectance spectroscopy for soil analysis emphasizing carbon and laboratory versus on-site analysis: Where are we and what needs to be done? *Geoderma* **2010,** *158* (1), 3-14.
48. Geelhoed, J. S.; Hiemstra, T.; Van Riemsdijk, W. H., Phosphate and sulfate adsorption on goethite: Single anion and competitive adsorption. *Geochimica et Cosmochimica Acta* **1997,** *61* (12), 2389-2396.
49. Barrow, N. J., A simple equation to describe sorption of anions by goethite. *European Journal of Soil Science* **1999,** *50* (1), 151-155.
50. Gimsing, A. L.; Borggaard, O. K., Effect of phosphate on the adsorption of glyphosate on soils, clay minerals and oxides. *International Journal of Environmental Analytical Chemistry* **2002,** *82* (8-9), 545-552.
51. Glass, R. L., Adsorption of glyphosate by soils and clay minerals. *Journal of Agricultural and Food Chemistry* **1987,** *35* (4), 497-500.
52. Miller, F. A.; Wilkins, C. H., Infrared spectra and characteristic frequencies of inorganic ions. *Analytical Chemistry* **1952,** *24* (8), 1253-1294.

4. Adsorption of Glyphosate to Model Soil Minerals

Gavin Styles[a], Antonio F Patti[a], Michael Rose[b], Lukas Van Zwieten[b], Bart Follink[a]

[a]School of Chemistry, Monash University, Wellington Rd., Clayton, 3800, Victoria, Australia

[b]New South Wales Department of Primary Industries, 1243 Bruxner Highway, Wollongbar, 2477, New South Wales, Australia

Declarations of interest: none

4.1 Abstract

Adsorption of glyphosate on a series of model soil minerals, including metal oxides and fixed charge clay minerals, was studied in order to develop a greater understanding of the mechanisms controlling glyphosate adsorption, and therefore mobility, breakdown and bioavailability, in soils. While Langmuir isotherms described the experimental results well, dependency of the Langmuir maximum adsorption capacity of glyphosate on the pH of the system suggested sorption mechanisms beyond those assumed in the Langmuir model. A Frumkin-Fowler-Guggenheim adsorption model, taking into account coverage-dependent lateral interactions in the adsorbed phase, provided more rational assumptions and improved fits. A decrease in both the energy of adsorption and apparent maximum adsorption capacity with increasing pH across all minerals investigated suggests increasing electrostatic repulsion between glyphosate adsorbate molecules with pH, along with a decreasing electrostatic attraction for the charged surface. These results are valuable in understanding glyphosate behaviour in the environment, both in terms of the development of predictive models of glyphosate behaviour, and in understanding the impacts of various changes to agronomic soil procedures, such as liming and claying.

4.2 Introduction

Glyphosate (N-(phosphonomethyl)glycine) is the most widely used herbicide worldwide, and is considered to have a low-risk ecological profile compared with other commonly used herbicides. This is in part because of its low inherent toxicity to non-target organisms including soil biota[1],

a relatively rapid breakdown rate, and a high adsorption affinity to soil[2-4]. However, glyphosate and its main breakdown product aminomethylphosphonic acid (AMPA) have recently been shown to be 'pseudo-persistent' in some soils due to the frequency of use outweighing the rate of breakdown, potentially leading to periodic accumulation in soil[5]. This pseudo-persistence may also increase the risk for off-site movement[6]. Recent surveys have frequently detected glyphosate in a wide variety of environments, including sediment[7], water[8], soil[9], dust[10] and rainwater[11].

Biological exposure to glyphosate is regulated by its persistence, mobility and bioavailability. These factors are, in turn, largely regulated by its adsorption to soil. Sorption can moderate the impacts of glyphosate by reducing its uptake by plants[12], as well as influencing pathways for mobilization through the soil[13-14], including its movement to waterways during a flooding event[15]. Sorption is also known to significantly affect the persistence of glyphosate in soil[16].

Glyphosate exists as a zwitterion in soil, with a negatively charged phosphonic acid and carboxylic acid group and a positively charged amine group, depending on the pH of the soil[17]. It primarily binds to amorphous soil minerals such as iron and aluminium oxides and hydroxides[18]. Soil pH and mineralogy therefore have a significant effect on binding, with lower adsorption generally observed at higher soil pH values[19]. This is thought to result from the change in surface charge on soil minerals, rather than the change in ionic form of glyphosate (pK_a = 2, 2.6, 5.8 and 10.8, for protonation and deprotonation of the phosphate, amine and carboxylic acid groups, respectively), as glyphosate is negatively charged at pH above 2.6[17]. Most metal oxides found in soil are positively charged at environmentally relevant pH, however, as pH increases, negatively charged sites may develop[20]. The binding of glyphosate to metal oxide surfaces has been shown to occur predominantly through the phosphonic acid functional group of the molecule[21]. As such, competition may occur between glyphosate and inorganic phosphate[22-23]. Soil-borne residues of glyphosate may be re-released by the addition of P

fertiliser, increasing the risk of herbicide injury in rotational crops in some soil types[24-26], though previous work has suggested the rate of desorption is independent of the competing entering ligand[27]. Based on this binding through the phosphate head group, it is to be expected that glyphosate shows a high affinity for metal oxides, similar to phosphate[28-29].

Adsorption of anions such as glyphosate and phosphate to metal oxides has been modelled using a variety of isotherms, such as the Freundlich[30] and Langmuir[31] isotherms. However, as stated by Barrow (1999)[32] "Neither of these is fully satisfactory because they do not apply over a wide sorption range and because they do not comply with the known characteristics of sorption". As such, Barrow derived an equation that is functionally identical to the Frumkin-Fowler-Guggenheim (FFG) isotherm[32], as this allows for lateral interactions between adsorbate molecules, and for a changing energy of adsorption relative to fractional occupancy of the surface. All of the above isotherms work on the assumptions that adsorption occurs only in a monolayer on the surface, and that the surface is energetically homogeneous[33].

Due to the general paucity of information on the mechanisms in which glyphosate adsorbs to the various soil minerals, this study aims to develop an understanding of the sorption behaviour and mechanism as it relates to individual components in the soil, such as metal oxides and fixed charge clay minerals. Previous work conducted by the authors used a general additive model to predict glyphosate adsorption in soil. However, this statistical method based on empirical data did not allow an in-depth analysis of the physico-chemical mechanism of glyphosate interaction with individual components of the soil. Mechanistic understanding of adsorption would allow for the improvement of regulatory procedures, and an understanding of the impact of agronomic soil management techniques, such as liming and "claying", may have on herbicide behaviour. This information would also be essential as inputs for mechanistic models of the behaviour and fate of organic agrochemicals, like glyphosate in soil, based on frameworks such as ORCHESTRA[34].

4.3 Materials and Methods

4.3.1 Materials

Goethite, kaolinite, hematite and rutile were purchased from Sigma Aldrich (Sydney, Australia), calcite was purchased from Pacific Water Technology (Brisbane, Australia), and Gibbsite was purchased from an independent minerals distributor, sourced originally from Copper Mountains, Box Elder, Utah, United States. All structures were confirmed using powder x-ray diffraction (D8 Advance Eco, Bruker Corporation).

^{14}C labelled glyphosate (1.85 GBq mol^{-1}) was purchased from American Radiolabelled Chemicals (Saint Louis, USA) and mixed with analytical grade unlabelled glyphosate (Accustandard, New Haven, USA) to produce seven one litre solutions of varying concentration (0.3, 1, 3, 9, 27, 100, 500 and 1000 mg L^{-1}; standard radioactivity of ~10 nCi per 5 ml for all concentrations).

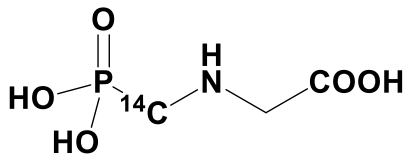

Figure 15: ^{14}C Labelled Glyphosate

4.3.2 Mineral Analysis

Powder X-ray diffraction was performed using a D8 Advance Eco (Bruker Corporation), with a scanning angle from 5° to 70°, a step size of 0.019° (3335 steps total) and CuK_{α} radiation. Spectra were compared to known database samples to confirm mineral identity. Braun-Emmett-Teller (BET) surface area was determined from N_2 gas physisorption measurements with a Micromeritics 3Flex. Mineral samples were initially degassed under vacuum with moderate heating (50 °C) for 24-48 h then N_2 gas sorption measurements conducted at 77 K at relative pressure (P/P_0 , where p is the equilibrium pressure and P_0 the saturation pressure of the dosed N_2 at 77 K) values from ~0.07 to 0.2. BET surface area values were determined as the slope of the linear region of plots of $1/[Q(P_0/P - 1)]$ vs P/P_0, where Q is the amount of adsorbed N_2 (mol

N_2 g^{-1} sample). The mass of sample used during the physisorption measurements was determined using an analytical balance as the difference between the empty sample tube and the sample tube containing degassed sample. Surface area by methylene blue adsorption was conducted using the method outlined by Kipling and Wilson[35] using methylene blue obtained from Sigma Aldrich. Scanning Electron Microscopy (SEM) was conducted using a Magellan 400 FEGSEM.

4.3.3 Glyphosate Adsorption

Adsorption experiments were conducted with a 1:5 w/w soil-to-liquid ratio at seven concentrations of glyphosate (0.3, 1, 3, 9, 27, 500 and 1000 mg L^{-1}) and at 3 pH values. One gram of mineral was placed in a 15 ml centrifuge tube, and the radiolabelled glyphosate in 0.05 M KCl solution (5 mL) was added. The solution was adjusted to pH 5, 7 or 9 with 0.5M KOH and HNO_3. A KCl solution was used in order to reduce impacts of changing salt concentration during pH adjustment. Mineral-glyphosate mixtures were rotated end-over-end (33 rpm) at 22 ^{o}C for 24 hours to allow equilibration, before being centrifuged at 2600 g for 20 min (Thermo Scientific Megafuge 8). The supernatant was removed and filtered through a 0.2 µm polyethylene (Merck) membrane to remove any remaining solid particles. The filtered supernatant (2 mL) was mixed with scintillation cocktail (18 mL, Optifluor, PerkinElmer) and the residual radioactivity determined by scintillation counting (Tricarb 2810, Packard). Previous experiments using CO_2 trapping had shown <1% mineralisation of glyphosate over 24 hours in the experimental conditions, and as such, this residual reactivity could be treated as a valid measure of glyphosate concentration in solution.

The amount of adsorbed glyphosate was determined indirectly from depletion measurements by subtracting the equilibrium glyphosate concentration from initial glyphosate concentration. Controls conducted in the same manner without mineral material showed negligible (<0.1%) adsorption of glyphosate to the centrifuge tubes or filters.

Adsorption coefficients were calculated using the Langmuir isotherm (Equation 1):

$$\frac{\theta}{1-\theta} = K_L C \tag{1}$$

where C is concentration of glyphosate in solution (µg ml^{-1}), K_L is a constant describing the energy of adsorption and θ is the fractional surface coverage, calculated as (Equation 2):

$$\theta = \frac{q}{q_{max}} \tag{2}$$

Where q is the concentration of glyphosate adsorbed to the mineral component (µg g^{-1}) and q_{max} is the maximum adsorption density.

The Frumkin-Fowler-Guggenheim (FFG) adsorption model[36-37] was also used to describe and analyse the adsorption behaviour of glyphosate (Equation 3):

$$\frac{\theta}{1-\theta} e^{b\theta} = K_{Fr} C \tag{3}$$

In this equation b is a term accounting for the lateral interaction between adsorbed species, and K_{Fr} is a constant describing the energy of adsorption. The use of a FFG adsorption model requires an initial maximum adsorption to be determined before other variables (b and K_{Fr}) can be calculated. The maximum adsorption was therefore estimated by using the maximum adsorption case observed during trials (goethite, pH 3.5), an extremely high concentration of glyphosate (5000 µg ml^{-1}) and solving for the Langmuir parameters (equivalent to FFG at b = 0). This was then determined to be reasonable based on geometric considerations shown in the results and discussion section. The full concentration range was used for all calculations.

4.4 Results and Discussion

Adsorption trials using goethite and a 5000 ug ml^{-1} glyphosate solution at pH 3.5 gave a maximum observed adsorption of ~715 µg/m^2 after normalisation based on surface area (53.1 m^2 g^{-1}), allowing usage with all tested minerals. This spatial view of adsorption maxima may be

taken due to the assumed homogeneous nature of the chemical structure of the mineral surfaces, which would lead to the number of possible "binding sites" well exceeding the spatial potential for adsorption. This is equivalent to 4.23 x 10^{-6} mol/m^2, which is equivalent to 2.55 x 10^{18} molecules/m^2. Thus the surface coverage area of a glyphosate molecule in the adsorbed state is about 40 $Å^2$, which is similar to a theoretical total possible maximum value of 175 $Å^2$ calculated via geometrical considerations of the adsorbed glyphosate molecule (Appendix Figure 2).

Allowing for the rotation of other bonds within the molecule, the deprotonation of the carboxylic acid group and the statistical likelihood of two tails being in the same place along the arc such that they intercept, 40 Å appears to be a realistic spacing.

Surface area results are shown in Table 7. The observed surface area of gibbsite based on BET seemed exceedingly high, particularly given its relatively low adsorption of glyphosate in early adsorption experiments, and its surface area was determined by methylene blue adsorption from solution. In non-porous materials, methylene blue produces surface area measurements within 40% of the BET measurement, however tends to give much lower values in porous materials[38]. Scanning electron microscopy (SEM) was used to explore the discrepancy between the two measurements, where BET provided a surface area three times greater than that derived from methylene blue adsorption. This showed the gibbsite structure to be composed of platelets and hollow needles, with an interior diameter of 6-8 nm (Figure 16). It is unlikely that the charged glyphosate molecules will enter the hollow needles of the gibbsite due to both spatial (size of the glyphosate molecule) and entropic considerations. A similar phenomenon is expected to occur for the large methylene blue molecules and, as such, for further analysis, the methylene blue value for surface area was taken as the "effective" surface area available for glyphosate adsorption.

Table 7: Surface area of minerals by BET (all excluding gibbsite) or methylene blue adsorption (gibbsite)

Mineral	Surface Area (m^2 g^{-1})
Calcite	0.33
Gibbsite	51.3
Goethite	7.0
Hematite	9.7
Kaolinite	8.3
Rutile	23.9

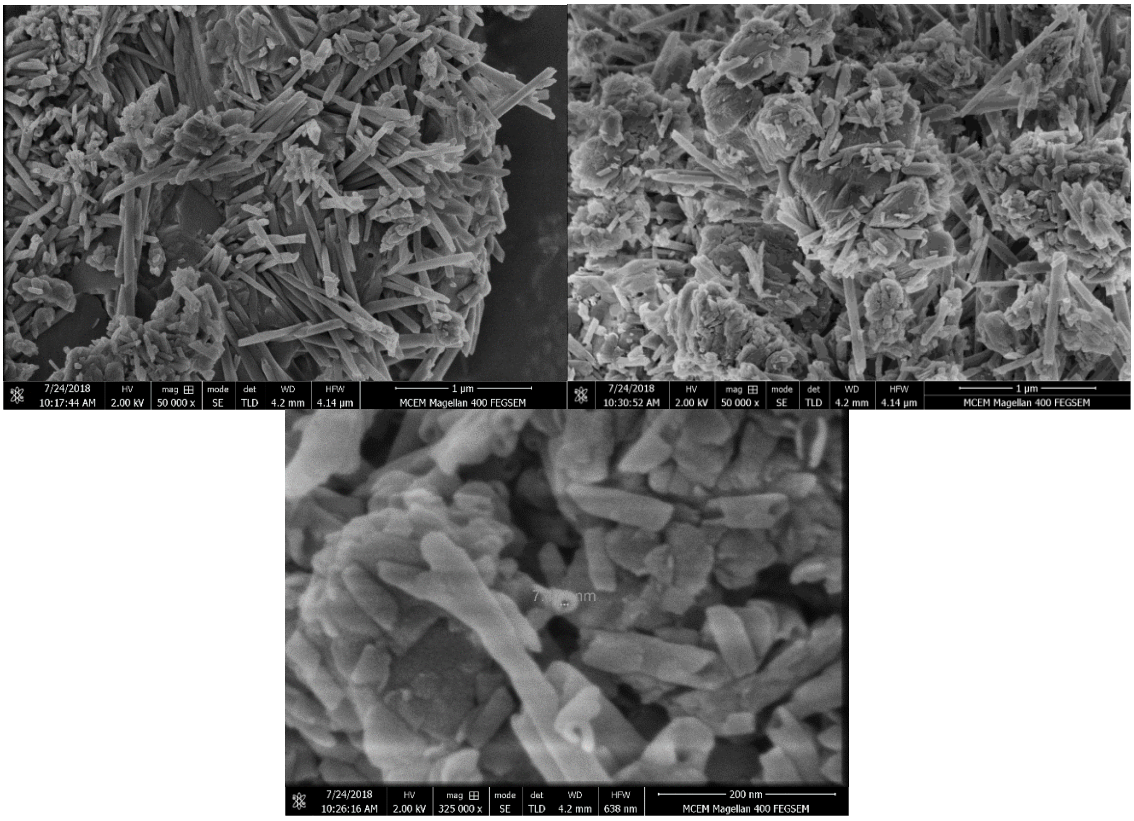

Figure 16: SEM images of gibbsite surface

Data from the adsorption experiments were fitted using the Langmuir equation, leading to close fits, shown in Appendix Table 4. However, this produces q_{max} values showing significant variation with pH. This change in apparent q_{max} is physically unrealistic, as all minerals tested (excluding calcite) are stable across the pH range used, and thus should not experience significant physical changes due to pH. This means that the geometrically determined maximum adsorption should remain steady, and only the energy of adsorption should show significant variation, due to changes in surface charge of the mineral. Thus it is expected that all isotherms at different pH

values would converge to the same plateau of maximum adsorption. This is however, not what is observed. While the Langmuir equation provides a useful tool for initial analysis of these results (R^2 > 0.9 in most cases, Appendix Table 4), it does not account adequately for all interactions occurring in the adsorption process, as it assumes a consistent energy of adsorption independent of the level of occupancy on the surface.

While both Langmuir and FFG isotherms allow for changes in attraction of the adsorbate to the adsorbent surface (in this case likely due to variations in electrostatic attraction/repulsion), the variation of apparent maximum adsorption with pH suggested there to be lateral interactions between the adsorbate molecules. This prevents a spatial saturation being reached at the solution concentrations investigated (spatial saturation would likely require an unachievable "infinite" concentration). To account for lateral interactions in the adsorbed phase, the FFG equation was applied. This leads to a lower "apparent" q_{max} with decreasing pH, while still allowing maximum adsorption to be spatially defined. When defining a system by the FFG equation, it is possible to reach a point where, due to lateral repulsion, it is increasingly unfavourable for further adsorption to occur despite an increasing concentration of adsorbate. An example of comparison of the fit of a Frumkin-Fowler-Guggenheim isotherm to the data against the Langmuir isotherm is shown in Figure 17. The use of a FFG isotherm shows a slower filling of adsorption sites, and a plateau is not reached as rapidly. It should be noted that the isotherms shown in Figure 17 are based on data that only takes into account adsorption for solution concentrations up to 1000 ug ml^{-1}, while adsorption experiments were conducted up to a 5000 ug ml^{-1} solution concentration. As such, the plateauing of the Langmuir isotherm shows that it does not fit for the true potential adsorption capacity when using data that does not reach this point, while the FFG has already accounted for this, while allowing for the possibility of other phenomena leading to a different "apparent" maximum.

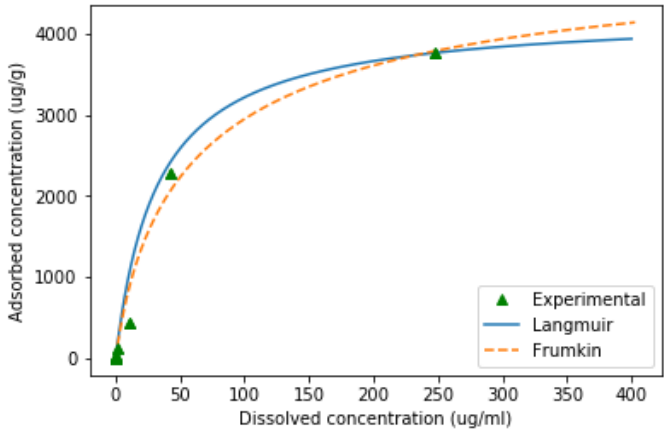

Figure 17: Langmuir and Frumkin-Fowler-Guggenheim isotherms of glyphosate adsorption on Goethite at pH 3.5

The results of FFG isotherm fitting for all minerals, using this experimentally determined q_{max}, can be seen in Table 8 and Figure 18.

Table 8: Fitted Frumkin-Fowler-Guggenheim Isotherm Values

Mineral	K_{Fr}			b			R^2		
	Acid	*Neutral*	*Basic*	*Acid*	*Neutral*	*Basic*	*Acid*	*Neutral*	*Basic*
Calcite*	N/A	0.56	0.38	N/A	7.00	3.98	N/A	0.87	0.93
Gibbsite	N/A	0.003	0.004	N/A	66.7	85.3	N/A	0.78	0.90
Goethite	0.023	0.034	0.029	0.81	3.40	32.6	0.26	0.97	0.99
Hematite	0.013	0.026	0.009	23.6	53.7	102.7	0.97	0.99	0.93
Kaolinite	0.013	0.011	0.003	25.8	31.7	38.5	0.97	0.98	0.92
Rutile	0.007	0.008	0.006	0.45	4.88	34.9	0.09	0.85	0.99

**Calcite adsorption not performed below pH 7 due to dissolution of calcite*

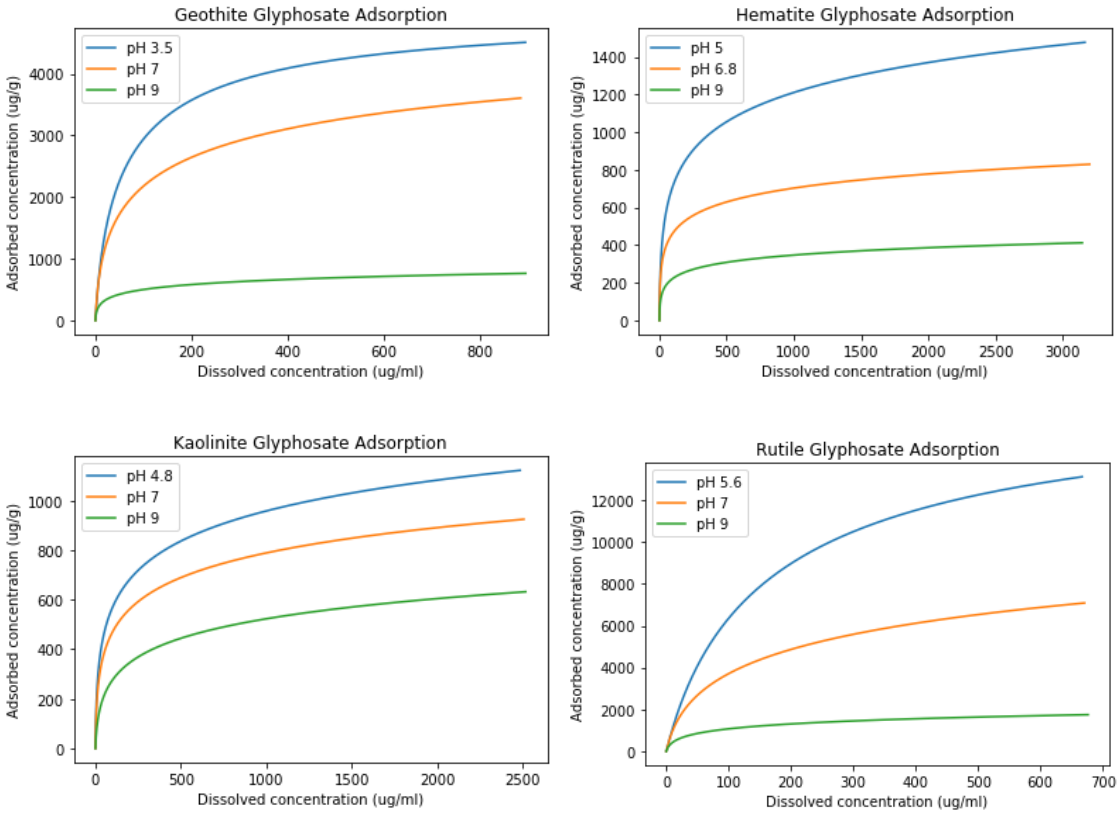

Figure 18: Fitted Frumkin-Fowler-Guggenheim isotherms of various minerals

A decrease in pH resulted in increased *b* values (Table 8) across all minerals. This is well visually represented in Figure 18, with higher "apparent" maximum adsorption at lower pH. Also worth noting is the varying scales of each set of isotherms. While the increased adsorption to rutile may be explained by a much larger surface area, the significantly lower adsorption to hematite and kaolinite when compared to goethite cannot be explained this way. Similarly, kaolinite shows a much smaller relative change in adsorption for changing pH than other minerals.

This decreasing *b* with pH can be ascribed to an increase in electrostatic repulsive forces between glyphosate molecules with increasing pH, as there is an increasing level of deprotonation of the adsorbate molecules[17, 33]. Kaolinite, being a fixed charged mineral, showed a significantly lower change in *b* across the pH range when compared to the variable charge metal oxides. This suggests that *b* is related not only to lateral interactions of the adsorbate, but also the charge and charge adaptation of the adsorbent, as was shown to be the case for the adsorption of organic cations onto charged silveriodide by de Keizer and Lyklema (1980)[33]. Thus

the electrostatic component of the energy of adsorption appears determined by a balance of repulsion between adsorbate molecules, and attraction of the adsorbate to the adsorbent surface. Rutile and goethite in particular show a significant change in the *b* term as pH shifts from 7 to 9. This is likely due to a reversal of the charge sign upon passing through the point of zero charge of the mineral, altering the attraction of the adsorbed glyphosate molecules. In order to further analyse the electrostatic component of b, detailed double layer studies would be required[39]. For the present purpose, it suffices to conclude that lateral interactions in the adsorbed phase play a crucial role in determining the adsorbed amounts of glyphosate onto oxides.

Similarly, the observed change in apparent maximum adsorption may be explained by the increasing repulsion between the adsorbent molecules (all negatively charged, in most cases 2-). As *b* approaches 0, there is a marked reduction in goodness-of-fit (R^2) for both rutile and goethite. While this is mostly an artefact due to saturation not being reached in the case of rutile (and thus an artificially low R^2, despite the good fit of the isotherm to the data), with a maximum adsorbed concentration of 4716 µg g^{-1} being reached. This is significantly less than the theoretical maximum of 8613 µg g^{-1} (based on surface area of the sample), and as seen in Figure 19, does not fall far outside of the linear range of adsorption. This low level of surface saturation is unlikely to be the reason for the poor goodness-of-fit for goethite, as the adsorbed concentrations reached are much closer to the assumed maximum adsorption capacity. This case may be ascribed to a number of factors, most likely to electronic repulsion becoming a negligible factor, other factors such as surface topology which influence adsorption behaviour, that are not accounted for by our isotherm model, become increasingly important. A second possible reason is that the chosen adsorption maximum may not in fact be the "real" adsorption maximum (and is not close to it), and glyphosate takes up less space than assumed. The most likely cause of this discrepancy is the assumption that goethite at pH 3.5 represents a $b = 0$ scenario. The other possible cause is that due to the impossibility of using an "infinite"

glyphosate concentration, a true q_{max} is never reached in adsorption experiments. Given its extremely high experimental capacity for glyphosate, in light of potential practical agricultural issues further investigation of the goethite-glyphosate system is warranted, particularly around the physical nature of the goethite sample used and its relevance for soil samples.

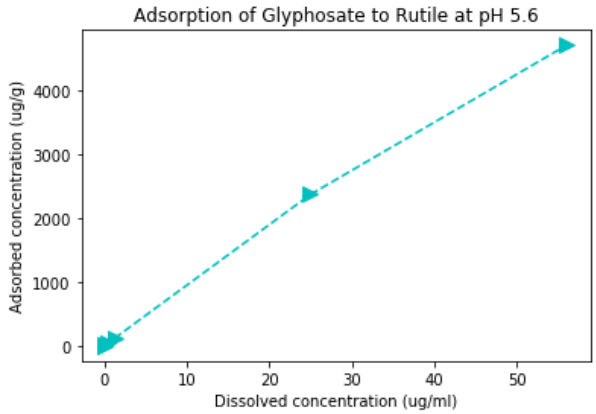

Figure 19: Adsorption of glyphosate to rutile at pH 5.6 (unfitted)

Calcite shows a decrease in *b* with decreasing pH, in contrast to the other minerals investigated. The reason for this likely lies in the increased solubility of calcite with decreasing pH, which produces a secondary effect on adsorption capacity, in the form of reduced surface area, that cannot be disentangled from the primary pH effect discussed above. It should also be noted that P-XRD experiments showed that along with (or perhaps instead of) surface adsorption, glyphosate and calcite react to form a calcium-glyphosate complex that is chemically similar to calcium phosphate. Figure 20 shows the overlap of the diffraction patterns of calcium phosphate and the resulting material from calcium glyphosate adsorption trials, both of which are distinct from the original calcite material. This suggests glyphosate-on-calcite adsorption will not follow the same spatially constrained adsorption rules that govern surface adsorption for the other minerals investigated here.

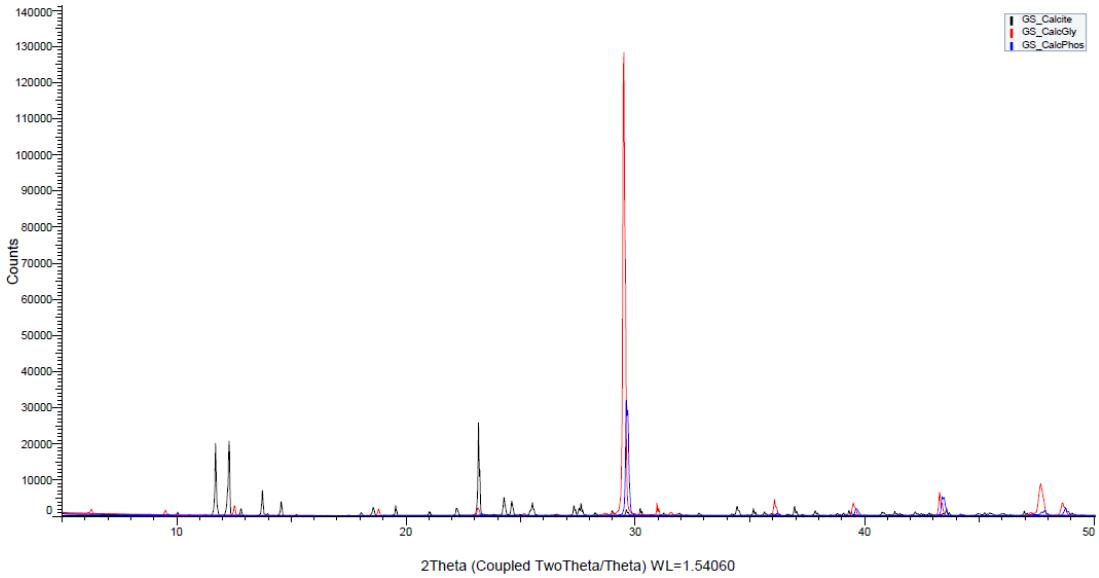

Figure 20: Powder X-Ray diffractogram of calcite (black), calcium phosphate (blue) and calcium glyphosate (red) complex

Gibbsite presents an interesting phenomenon. While adsorption was higher at pH 5 than pH 7 and 9 as with the other metal oxides, an FFG isotherm was not a good fit for this data at low pH. However, unlike rutile and goethite where this was due to saturation not being reached producing a low R^2 despite the closeness of fit of the FFG to the data, instead gibbsite presented a phenomenon where the fraction of added glyphosate adsorbed increased at high concentrations. This is illustrated in Figure 21, where the log scale isotherms of hematite and gibbsite at pH 5 are both presented. The hematite isotherm shows the "typical" FFG case, where there is a linear region, followed by a reduction in the slope of the isotherm as saturation is approached. The gibbsite isotherm however, shows a slight decrease in slope, followed by a "second stage" where the slope once again increases. This is possibly related to the porous nature of the mineral, with high concentrations of glyphosate leading to higher levels of entry into the hollow needle structure, due to a higher chemical potential (concentration) of glyphosate in solution. At higher pH it is likely that due to the more negative charge of the mineral surface (both of the exterior and interior structure surfaces) and the glyphosate molecule, adsorption inside the pores is unfavourable due to electrostatic repulsion, even at

high concentrations. Thus leading to adsorption only occurring on the exterior of the structure, following a more traditional mode of adsorption.

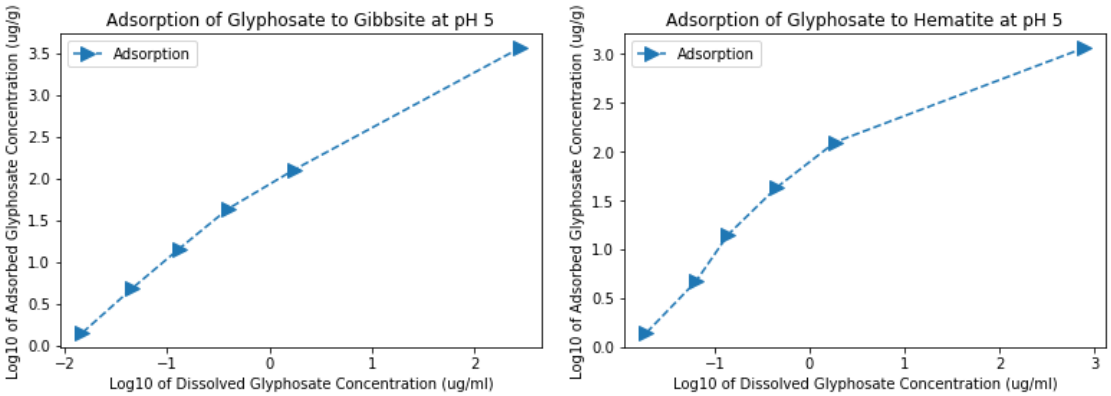

Figure 21: Adsorption of glyphosate to hematite and gibbsite at pH 5 (log_{10} scale)

This study serves as an important comparison of the Langmuir and FFG isotherms as tools for studying these model environmental systems. Langmuir and Freundlich isotherms have been ubiquitous in the study of soil systems, however this study hopes to show power and utility of the Frumkin-Fowler-Guggenheim adsorption model, and its ability to increase our understanding of adsorption processes in (variably charged) systems of practical importance in soil chemistry. It also shows the high adsorption affinity of glyphosate for these metal oxide systems, and the high capacity they have for glyphosate adsorption to the surface, and how this may be mitigated by lateral interations of the adsorbate molecules. A lack of further work into the relationship of the surface charge of these minerals to pH makes it difficult to draw conclusions on the impacts of electrostatic interactions between the adsorbate and adsorbent surface. Despite this limitation, the study remains extremely useful for use in soil science for better understanding the behaviour of glyphosate in the field, and its impacts for agricultural practice.

4.5 Acknowledgements

The SEM imagery in this paper was provided by the technicians at the Monash Center for Electron Microscopy

4.6 References

1. Rose, M. T.; Cavagnaro, T. R.; Scanlan, C. A.; Rose, T. J.; Vancov, T.; Kimber, S.; Kennedy, I. R.; Kookana, R. S.; Van Zwieten, L., Impact of herbicides on soil biology and function. In *Advances in Agronomy*, Sparks, D. L., Ed. Academic Press: **2016**; Vol. 136, pp 133-220.
2. Roy, D. N.; Konar, S. K.; Banerjee, S.; Charles, D. A.; Thompson, D. G.; Prasad, R., Persistence, movement, and degradation of glyphosate in selected Canadian boreal forest soils. *Journal of Agricultural and Food Chemistry* **1989,** *37* (2), 437-440.
3. Giesy, J. P.; Dobson, S.; Solomon, K. R., Ecotoxicological risk assessment for Roundup® herbicide. In *Reviews of Environmental Contamination and Toxicology: Continuation of Residue Reviews*, Ware, G. W., Ed. Springer New York: New York, NY, **2000**; pp 35-120.
4. Peterson, R. K. D.; Hulting, A. G., A comparative ecological risk assessment for herbicides used on spring wheat: the effect of glyphosate when used within a glyphosate-tolerant wheat system. *Weed Science* **2017,** *52* (5), 834-844.
5. Primost, J. E.; Marino, D. J. G.; Aparicio, V. C.; Costa, J. L.; Carriquiriborde, P., Glyphosate and AMPA, "pseudo-persistent" pollutants under real-world agricultural management practices in the Mesopotamic Pampas agroecosystem, Argentina. *Environmental Pollution* **2017,** *229*, 771-779.
6. Norgaard, T.; Moldrup, P.; Ferré, T. P. A.; Olsen, P.; Rosenbom, A. E.; de Jonge, L. W., Leaching of glyphosate and aminomethylphosphonic acid from an agricultural field over a twelve-year period. *Vadose Zone Journal* **2014,** *13* (10).
7. Battaglin, W. A.; Meyer, M. T.; Kuivila, K. M.; Dietze, J. E., Glyphosate and Its degradation product AMPA occur frequently and widely in U.S. soils, surface water, groundwater, and precipitation. *JAWRA Journal of the American Water Resources Association* **2014,** *50* (2), 275-290.
8. Saunders, E. L.; Pezeshki, R., Glyphosate in runoff waters and in the root-zone: A review. *Toxics* **2015,** *3* (4), 462-480.
9. Silva, V.; Montanarella, L.; Jones, A.; Fernández-Ugalde, O.; Mol, H. G. J.; Ritsema, C. J.; Geissen, V., Distribution of glyphosate and aminomethylphosphonic acid (AMPA) in agricultural topsoils of the European Union. *Science of The Total Environment* **2018,** *621*, 1352-1359.
10. Mendez, M. J.; Aimar, S. B.; Aparicio, V. C.; Ramirez Haberkon, N. B.; Buschiazzo, D. E.; De Gerónimo, E.; Costa, J. L., Glyphosate and aminomethylphosphonic acid (AMPA) contents in the respirable dust emitted by an agricultural soil of the central semiarid region of Argentina. *Aeolian Research* **2017,** *29*, 23-29.
11. Chang, F.-c.; Simcik, M. F.; Capel, P. D., Occurrence and fate of the herbicide glyphosate and its degradate aminomethylphosphonic acid in the atmosphere. *Environmental Toxicology and Chemistry* **2011,** *30* (3), 548-555.
12. Simonsen, L.; Fomsgaard, I. S.; Svensmark, B.; Spliid, N. H., Fate and availability of glyphosate and AMPA in agricultural soil. *Journal of Environmental Science and Health, Part B* **2008,** *43* (5), 365-375.
13. McGrath, G. S.; Hinz, C.; Sivapalan, M., A preferential flow leaching index. *Water Resources Research* **2009,** *45* (11), W114505.
14. McGrath, G. S.; Hinz, C.; Sivapalan, M., Modelling the impact of within-storm variability of rainfall on the loading of solutes to preferential flow pathways. *European Journal of Soil Science* **2008,** *59* (1), 24-33.
15. Dollinger, J.; Dagès, C.; Negro, S.; Bailly, J.-S.; Voltz, M., Variability of glyphosate and diuron sorption capacities of ditch beds determined using new indicator-based methods. *Science of The Total Environment* **2016,** *573*, 716-726.

16. Al-Rajab, A. J.; Schiavon, M., Degradation of 14C-glyphosate and aminomethylphosphonic acid (AMPA) in three agricultural soils. *Journal of Environmental Sciences* **2010,** *22* (9), 1374-1380.
17. Sprankle, P.; Meggitt, W. F.; Penner, D., Adsorption, mobility, and microbial degradation of glyphosate in the Soil. *Weed Science* **1975,** *23* (3), 229-234.
18. Morillo, E.; Undabeytia, T.; Maqueda, C.; Ramos, A., Glyphosate adsorption on soils of different characteristics.: Influence of copper addition. *Chemosphere* **2000,** *40* (1), 103-107.
19. Zhao, B.; Zhang, J.; Gong, J.; Zhang, H.; Zhang, C., Glyphosate mobility in soils by phosphate application: Laboratory column experiments. *Geoderma* **2009,** *149* (3), 290-297.
20. de Jonge, H.; Wollesen de Jonge, L., Influence of pH and solution composition on the sorption of glyphosate and prochloraz to a sandy loam soil. *Chemosphere* **1999,** *39* (5), 753-763.
21. Sheals, J.; Sjöberg, S.; Persson, P., Adsorption of glyphosate on goethite: molecular characterization of surface complexes. *Environmental Science & Technology* **2002,** *36* (14), 3090-3095.
22. Laitinen, P.; Siimes, K.; Rämö, S.; Jauhiainen, L.; Eronen, L.; Oinonen, S.; Hartikainen, H., Effects of soil phosphorus status on environmental risk assessment of glyphosate and glufosinate-ammonium. *Journal of Environmental Quality* **2008,** *37* (3), 830-838.
23. Padilla, J. T.; Selim, H. M., Interactions among glyphosate and phosphate in soils: Laboratory retention and transport studies. *Journal of Environmental Quality* **2019,** *48* (1), 156-163.
24. Rose, T.; Van Zwieten, L.; Claassens, A.; Scanlan, C.; Rose, M., Phytotoxicity of soilborne glyphosate residues is influenced by the method of phosphorus fertiliser application. *Plant Soil* **2017**; *422*, 455-465.
25. Rosenbom, A.; Haarder, B.; Badawi, N.; Gudmundsson, L.; Von Platten-Hallermund, F.; H Hansen, C.; B Nielsen, C.; Plauborg, F.; Olsen, P., *The Danish Pesticide Leaching Assessment Programme. Monitoring results May 1999–June 2016*. **2017**.
26. Bott, S.; Tesfamariam, T.; Kania, A.; Eman, B.; Aslan, N.; Römheld, V.; Neumann, G., Phytotoxicity of glyphosate soil residues re-mobilised by phosphate fertilisation. *Plant and Soil* **2011,** *342* (1), 249-263.
27. Arroyave, J. M.; Waiman, C. C.; Zanini, G. P.; Tan, W.; Avena, M. J., Desorption rate of glyphosate from goethite as affected by different entering ligands: hints on the desorption mechanism. *Environmental Chemistry* **2017,** *14* (5), 288-294.
28. Geelhoed, J. S.; Hiemstra, T.; Van Riemsdijk, W. H., Phosphate and sulfate adsorption on goethite: Single anion and competitive adsorption. *Geochimica et Cosmochimica Acta* **1997,** *61* (12), 2389-2396.
29. Lookman, R.; Freese, D.; Merckx, R.; Vlassak, K.; van Riemsdijk, W. H., Long-term kinetics of phosphate release from soil. *Environmental Science & Technology* **1995,** *29* (6), 1569-1575.
30. Guzman, G.; Alcantara, E.; Barron, V.; Torrent, J., Phytoavailability of phosphate adsorbed on ferrihydrite, hematite, and goethite. *Plant and Soil* **1994,** *159* (2), 219-225.
31. He, Z. L.; Yang, X.; Yuan, K. N.; Zhu, Z. X., Desorption and plant-availability of phosphate sorbed by some important minerals. *Plant and Soil* **1994,** *162* (1), 89-97.
32. Barrow, N. J., A simple equation to describe sorption of anions by goethite. *European Journal of Soil Science* **1999,** *50* (1), 151-155.
33. De Keizer, A.; Lyklema, J., Adsorption of tetraalkylammonium ions at the silver iodide—electrolyte interface. *Journal of Colloid and Interface Science* **1980,** *75* (1), 171-184.
34. Janot, N.; Pinheiro, J. P.; Botero, W. G.; Meeussen, J. C. L.; Groenenberg, J. E., PEST-ORCHESTRA, a tool for optimising advanced ion-binding model parameters: derivation of NICA-Donnan model parameters for humic substances reactivity. *Environmental Chemistry* **2017,** *14* (1), 31-38.

35. Kippling, J. J.; Wilson R. B., Adsorption of methylene blue in the determination of surface areas. *Journal of Applied Chemistry* **1960,** *10* (3), 109-113.
36. Fowler, R. H.; Guggenheim, E. A., *Statistical Thermodynamics*. Cambridge University Press: **1939**.
37. Lyklema, J., Appendix 1 - Survey of adsorption isotherms and two-dimensional equations of state for homogeneous, nonporous surfaces. Monolayer regime. In *Fundamentals of Interface and Colloid Science*, Ed. Academic Press: **1995**; Vol. 2, pp A1-1-A1-2.
38. Ferrero, F., Adsorption of methylene blue on magnesium silicate: Kinetics, equilibria and comparison with other adsorbents. *Journal of Environmental Sciences* **2010,** *22* (3), 467-473.
39. Lyklema, J., 3 - Electric double layers. In *Fundamentals of Interface and Colloid Science*, Ed. Academic Press: **1995**; Vol. 2, pp 3-1-3-232.

5. Release of Glyphosate from Soil Minerals. Effects of Salt and Phosphorus and the Implications for Fertilisation Regimes

Gavin Styles[a], Antonio F Patti[a], Michael Rose[b], Lukas Van Zwieten[a,b], Bart Follink[a]

[a]School of Chemistry, Monash University, Wellington Rd., Clayton, 3800, Victoria, Australia

[b]New South Wales Department of Primary Industries, 1243 Bruxner Highway, Wollongbar, 2477, New South Wales, Australia

Declarations of interest: none

5.1 Abstract

Glyphosate has been shown to desorb from soil upon the addition of phosphorus fertiliser, increasing its mobility and bioavailability. Little is known about the mechanisms of glyphosate desorption, particularly in the presence of competing ligands. We measured the release of glyphosate from a series of soil minerals and observed significant hysteresis, particularly for glyphosate sorption to metal oxides, over a practically relevant timescale (24 hours). Coulombic screening of charges by salts in solution lead to greater release of glyphosate from these minerals than occurs in pure water. Significant competition between glyphosate and phosphate, which binds more strongly to these minerals, was observed. The reduced level of hysteresis when phosphate was introduced suggests a dynamic adsorption/desorption equilibrium of glyphosate to the mineral surface, which leads to a displacement of glyphosate by phosphate, which has a higher binding affinity adsorbent. There is also a significantly reduced level of glyphosate adsorption to mineral surfaces previously exposed to phosphate. This has implications for the management of glyphosate and fertilisation regimes, as the altered adsorption and release levels are likely to have impacts on the bioavailability of the herbicide, and present a potential cause of injury in later crop rotations in soils which have high levels of glyphosate persistence, or in systems where high, repeated dosages of glyphosate are used.

5.2 Introduction

Glyphosate (N-(phosphonomethyl)glycine) is the most widely used herbicide both in Australia and globally[1]. It has previously been considered to have a relatively low ecological risk profile[2], owing to its low mobility[3], rapid breakdown rate, and low toxicity to non-target organisms[4]. However, recent studies have shown glyphosate to be "pseudo-persistent" due to the dose and frequency of application surpassingthe rate of breakdown, leading to periodic accumulation in the soil[5]. Glyphosate has been detected in several environmental compartments including waterways[6], soil[7], dust[8], sediment and rainwater[9]. Recent work has also demonstrated the possibility of glyphosate release upon P fertilisation[10]. Remobilisation of glyphosate can lead to increased risk of herbicide injury in later crop rotations[11] and also movement of glyphosate off-site[12].

Availability of glyphosate for plant uptake and microbial degradation is heavily regulated by its adsorption properties to soil, which in turn has impacts on the mobility of the herbicide, through altering uptake by plants[13] and pathways for mobilization through the soil[14-15]. Sorption and availability are also known to have impacts on the persistence of glyphosate[16].

Glyphosate exists as a zwitterion in soil, with a negatively charged phosphonic acid and carboxylic acid group and a positively charged amine group, depending on the pH of the soil[17]. It primarily binds to amorphous soil minerals such as iron and aluminium oxides and hydroxides[18]. Soil pH and mineralogy therefore have a significant effect on binding, with adsorption decreasing as pH increases[19]. This is mainly due to the change in surface charge on soil minerals, rather than the change in ionic form of glyphosate (pK_a = 2, 2.6, 5.8 and 10.8, occurring due to protonation and deprotonation of the phosphate, amine and carboxylic acid groups), as glyphosate is negatively charged at pH above 2.6[17]. Most metal oxides found in soil are positively charged at environmentally relevant pH, however, as pH increases, negatively charged sites may develop[20]. The binding of glyphosate to metal oxide surfaces has been shown

to occur predominantly through the phosphonic acid functional group of the molecule[21]. As such, competition may occur between glyphosate and inorganic phosphate[22-23]. Soil borne residues of glyphosate may be re-released by the addition of P fertiliser, increasing the risk of herbicide injury in rotational crops in some soil types[10-11, 24], though previous work has suggested the rate of desorption is independent of the competing entering ligand[25]. Based on this binding through the phosphate head group, it is to be expected that glyphosate shows a high affinity for metal oxides, similar to phosphate[26-27].

As such, a greater understanding of the effect of soil conditions, such as ionic strength and competition with other common soil ligands such as phosphate, is important to understanding the mobility and bioavailability of glyphosate in soil. This work systematically explored the release of glyphosate from soil minerals under various conditions. In particular, it explored the relationship between glyphosate and phosphate adsorption, with the aim to develop further understanding of the impacts of fertilisation on soils which may have high levels of glyphosate adsorption and persistence.

5.3 Materials and Methods

5.3.1 Materials

Goethite, kaolinite, hematite and rutile were purchased from Sigma Aldrich (Castle Hill, NSW, Australia), calcite was purchased from Pacific Water Technology, and gibbsite was purchased from an independent minerals distributor, sourced originally from Copper Mountains, Box Elder, Utah, United States. Powder X-ray diffraction was performed using a D8 Advance Eco (Bruker Corporation), with a scanning angle from 5° to 70°, a step size of 0.019° (3335 steps total) and a CuK_{α} radiation. Spectra of the minerals were compared to known database samples to confirm mineral identity.

^{14}C labelled glyphosate (1.85 GBq mol^{-1}) was purchased from American Radiolabelled Chemicals (Saint Louis, USA) and mixed with analytical grade unlabelled glyphosate (Accustandard, New

Haven, USA) to produce seven one litre solutions of varying concentration (0.3, 1, 3, 9, 27, 100, 500 and 1000 mg L^{-1}, standard radioactivity of ~10 nCi per 5ml for all concentrations). All other materials were purchased from Sigma Aldrich.

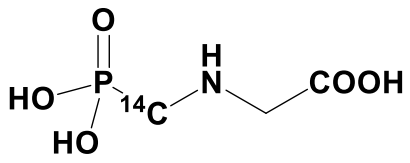

Figure 22: ^{14}C Labelled Glyphosate

5.3.2 Adsorption of Glyphosate

Adsorption experiments were conducted with a 1:5 w/w soil-to-liquid ratio at seven concentrations of glyphosate (0.3, 1, 3, 9, 27, 500 and 1000 mg L^{-1}). One gram of mineral was placed in a 15 ml centrifuge tube, and the radiolabelled glyphosate in DI water or 0.05 M KCl solution (5 g) was added and the overall mass of centrifuge tube and contents recorded. Mineral-glyphosate mixtures were rotated end-over-end (33 rpm) at 22 ^{o}C for 24 hours to allow equilibration, before being centrifuged at 2600 g for 20 min (Thermo Scientific Megafuge 8). The supernatant was removed and filtered through a 0.2 µm polyethylene (Merck) membrane to remove any remaining solid particles. An aliquot of the filtered supernatant (2 mL) was mixed with scintillation cocktail (18 mL, Optifluor, PerkinElmer) and the radioactivity determined by scintillation counting (Tricarb 2810, Packard). Previous experiments (data not shown) of trapped CO_2 had shown <1% mineralisation of glyphosate over 24 hours in the experimental conditions, and as such, this residual reactivity could be treated as a valid measure of glyphosate concentration in solution. In this experiment, pH was measured but not altered, and followed that expected from prior experiments conducted in Chapter 4.

The amount of adsorbed glyphosate was determined indirectly by subtracting the final from the initial glyphosate concentration. Controls conducted in the same manner without mineral material showed negligible (<0.1%) adsorption of glyphosate to the centrifuge tubes or filters.

Adsorption coefficients were calculated using the Langmuir isotherm, where C is concentration of glyphosate in solution (µg ml^{-1}) and q is the concentration of glyphosate adsorbed to the mineral component (µg g^{-1}),

$$\frac{\theta}{1-\theta} = K_L C \tag{1}$$

The fractional surface coverage θ is calculated as

$$\theta = \frac{q}{q_{max}} \tag{2}$$

Where q_{max} is the maximum adsorption density and K_L is a constant describing the energy of adsorption. The same experiments were also performed using soil minerals which had been pre-saturated with phosphate by undertaking the same adsorption procedure 1 g of material in 5 g of K_2HPO_4 solution (1000 mg L^{-1} P).

5.3.3 Desorption of Glyphosate

After centrifugation and removal of supernatant, fresh deionised (DI) water, 0.05M KCl solution or K_2HPO_4 (10, 100, or 1000 mg L^{-1} P), was added to return the vessel to the initial recorded mass (4.8 ml added on average). This mixture was then vortexed to disperse the mineral material in solution, and then rotated end-over-end (33 rpm) at 22 °C for 24 hours. Suspensions were centrifuged at 2600 x g for 20 min (Thermo Scientific Megafuge 8) and the supernatant removed and filtered through a 0.2 µm polyethylene (Merck) membrane to remove any remaining solid particles. Glyphosate concentrations in the supernatant were determined by the same methods as for adsorption experiments.

5.3.4 Phosphorus Analysis

Phosphate adsorption measurements were conducted in the same manner as glyphosate adsorption experiments, with K_2HPO_4 solutions (0, 10, 100, 500 and 1000 mg L^{-1} P equivalent) in place of glyphosate. Concentration of phosphate in the supernatant after equilibration was

measured using a colorimetric method based on the Colwell P method as described in Rayment and Lyons (2010)[28], with solutions being diluted in 0.5M $NaHCO_3$ to be below 1 mg L^{-1} P prior to analysis. The mixed colour reagent was produced by the following method: $(NH_4)_6Mo_7O_{24}.4H_2O$ (12 g) was dissolved in 400 mL H_2O, and added to H_2SO_4 (540 mL, 4.7 M). The resulting mixture was cooled before addition of $KSbO.C_4H_4O_6$ solution (0.267 g in 100 mL H_2O). For every 100 ml of mixed colour reagent required, L-ascorbic acid (1.067 g) was added to 100 ml of the previous solution. K_2HPO_4 standards (0, 0.2, 0.4, 0.6, 0.8 and 1 mg P L^{-1}) in 0.5M $NaHCO_3$ were produced. All samples and standards (1 mL) were neutralised with two additions of H_2SO_4 (70 µL, 2M) ten minutes apart in an Eppendorf tube, and left open overnight. Mixed colour reagent (320 µL) was added and the Eppendorf tubes shaken to mix. Aliquots (162 µL) were taken and placed in a microwell plate before being diluted with H_2O (88 µL). Readings were taken 15 minutes after dilution, to allow for colour development, using a Multiskan GO spectrophotometer (Thermo Scientific) at 650 nm.

5.4 Results and Discussion

5.4.1 Adsorption of Phosphate and Glyphosate

Adsorption of phosphate to the soil minerals was similar to glyphosate adsorption (Table 9), with goethite and rutile producing the highest levels of adsorption and calcite the lowest. P sorption onto both rutile and goethite did not reach saturation, with tested concentrations remaining in the linear region of adsorption. Calcite and gibbsite had a higher relative maximum adsorption capacity for P over glyphosate than other minerals (excluding rutile and goethite), with 7 and 5 fold higher maximum P adsorption respectively. Adsorption to calcite by both adsorbates is driven by complexation reactions, leading to the conversion of calcium carbonate to calcium phosphate[29] or calcium-glyphosate (Chapter 4). The greater adsorption of phosphate compared to glyphosate is likely due to a higher Gibbs free energy of this complexation reaction (as seen by the change in K_L, Table 9), perhaps in combination with the relatively smaller size of

the phosphate ion, allowing it access to a greater area of the calcite for reaction. This smaller cross sectional size is most likely the cause of the increased adsorption on gibbsite, as phosphate is far more likely to be able to access the hollow needles and platelets of the gibbsite structure (Chapter 4), leading to a higher effective surface area for adsorption. The relative binding of phosphate versus glyphosate onto hematite and kaolinite was more modest (2x and 3x, respectively) than other minerals, again likely due to the difference in surface area occupied by molecules of the adsorbates. This variation in adsorption capacity differences for glyphosate and phosphate is consistent with similar findings from Gimsling and Borggaard (2007)[30]. However, they also showed modest changes in the adsorption energy of the reaction, with a ~3x lower K_L indicating phosphate to be more strongly bound to the mineral surface than glyphosate. This may be due to charge differences in the phosphate and glyphosate molecules, or steric considerations. Similar differences were seen in the adsorption energy for goethite and rutile.

Table 9: Maximum adsorption of glyphosate and phosphate to soil minerals

Mineral	*Maximum adsorption (ug/g)*		*Binding affinity (K_L or K_d)*	
	Glyphosate	*Phosphate*	*Glyphosate*	*Phosphate*
Calcite	196	1458	0.285	0.0479
Gibbsite	362	1807	0.366	0.0285
Goethite	4250	N/A*	102.9^	239.4^
Hematite	696	1454	0.187	0.059
Kaolinite	952	3056	0.067	0.0193
Rutile	5556	N/A*	137.3^	191.7^

** Saturation point not reached, thus maximum adsorption could not be determined*

^ K_d values presented due to phosphorus saturation not being reached in these experiments, thus producing a poor Langmuir fit

5.4.2 Desorption in Pure Water

Stepwise desorption of glyphosate from the preloaded minerals varied considerably, with release of between 0.05 and 15% of glyphosate from the adsorbent with each addition of clean solution or "desorption step" as shown in Figure 23. While desorption from a mineral was generally within the same order of magnitude across desorption steps, there was still a large variability, such as in gibbsite where a minimum release of 0.57% and a maximum release of 8.7% of adsorbed glyphosate was observed. The most significant hysteresis was observed in goethite and rutile, and the least significant in kaolinite and hematite. While there was variability in the desorption levels, there was not a consistent decreasing trend in the level of glyphosate desorbed with each fresh addition of desorption solution. This suggests variability is not due to altering energy levels of adsorption to the surface, which is consistent with the idea that the surface is homogeneous, and that any variation in the energy of adsorption is related only to the fractional occupancy of the surface, and not the specific binding site.

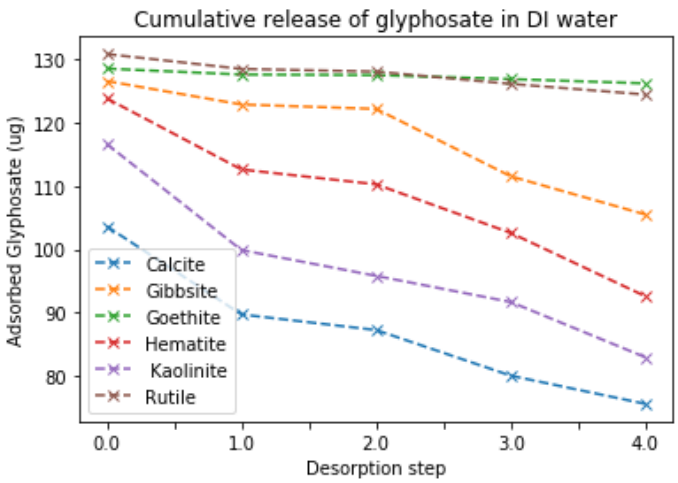

Figure 23: Cumulative desorption of glyphosate from soil minerals in DI water

5.4.3 Desorption in KCl Solution

Experiments in a 0.05M KCl solution had limited effect on the initial adsorption of glyphosate compared with water, with less than 5% difference in the initial adsorbed amounts between the two solutions for all minerals investigated. The exception was calcite, where initial adsorption

was 19% lower in KCl, likely due to the greater solubility of calcite in the KCl solution as compared to DI water. However, these experiments produced a much less variable desorption over each step, when compared to DI water which can be seen in Figure 24. Calcite showed a significantly higher glyphosate desorption in the KCl solution, possibly due to an increased solubility of the calcite-glyphosate complex (as explored earlier in this chapter) in this solution. This increase in desorption is likely due to the effect of coulombic screening by the salt ions, reducing the attraction of glyphosate to the mineral surface. Goethite, rutile and gibbsite released a greater amount of glyphosate in the KCl solution than water, with a large initial desorption step, followed by much smaller levels of desorption (e.g. Goethite releases 25% of adsorbed glyphosate on the first addition of KCl, followed by a consistent 2% release with each of the next three additions; Figure 25). This suggests that, contrary to what was suggested by the observed DI water results, there may be two distinct energy levels at which glyphosate is adsorbed to these metal oxides: one loosely bound and easily released, and the other more strongly bound and thus more likely to experience significant hysteresis. A possible reason for this may be that glyphosate does not adsorb in a single monolayer, but forms a bilayer system, or that adsorption is not constant across the surface due to non-homogeneous topology leading to edge effects. It could also be that this at least in part is a kinetic effect rather than genuine thermodynamic hysteresis, and that given a sufficient equilibration time, larger levels of glyphosate would desorb from the goethite surface. However, assuming a linear release over time, the 24 h equilibration time means that this hysteresis is occurring on a practically relevant timescale. This is an important phenomenon when considering the release of previous glyphosate applications in soils (upon fertilisation or increased rainfall). Particularly of note is the impact of the KCl solution, suggesting any fertilisation (or other increase in salt concentration in the soil) may have some effect, not just phosphorus fertilisation. While this effect is unlikely to be as significant as the addition of phosphate, which is in direct competition for the same binding sites, it may not be negligible.

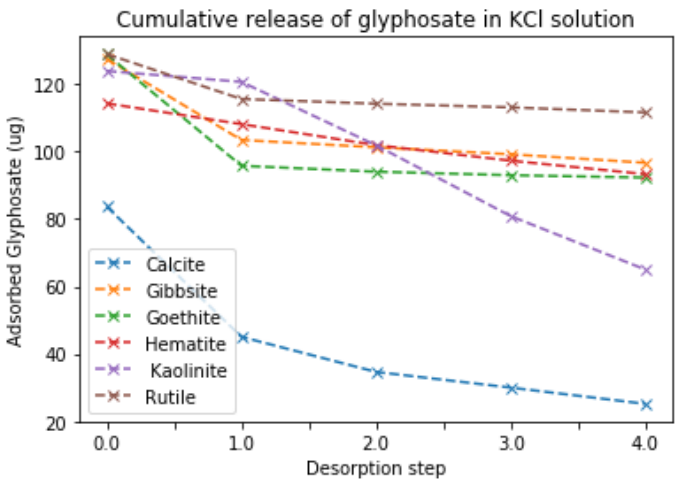

Figure 24: Cumulative desorption of glyphosate from soil minerals in KCl solution

Kaolinite also shows an increase in levels of glyphosate release, however once again the desorption was less variable, with a consistent release of 15-20% of adsorbed glyphosate with each KCl addition. The outlier in this set was hematite, which saw a decrease in variability, but also in overall desorption. This change involved going from a variable 2-10% release with each step (Figure 23), to a constant 5% release (Figure 24). This is particularly interesting given the significant differences from the other metal oxide minerals, and in particular goethite, another iron oxide.

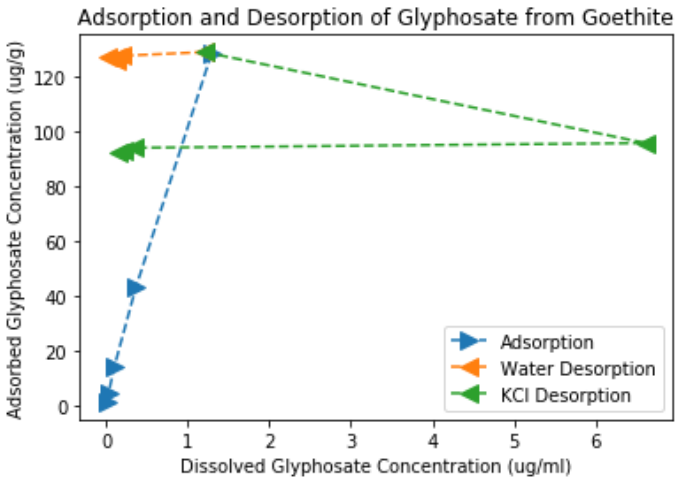

Figure 25: Comparison of desorption of glyphosate from goethite (left)) in H2O and KCl

5.4.4 Competition between Glyphosate and Phosphate

For desorption studies of glyphosate in a phosphate solution, a potassium phosphate (dibasic) solution was used with an adjusted concentration of 1000 mg/L of P. This high concentration is to mimic localised P concentrations in soil after banding with super phosphate fertiliser[31]. Under these conditions, release of glyphosate from all soil minerals increased significantly (Figure 26). In the case of hematite, the release during the initial desorption step was about 15 fold higher than the comparable KCl desorption (5.4% released in KCl, and 81.3% released in potassium phosphate solution). Given the concentration of the potassium phosphate solution is 0.032M, this cannot be explained solely by electrostatic screening effects. This suggests that phosphate ions occupy the same binding sites on these minerals as glyphosate, but with a much higher binding affinity. This addition of phosphate also leads to a much more consistent release of glyphosate, rather than the initial large release followed by much lower release steps, as previously observed for goethite, gibbsite and rutile. While this effect is still present, it is less pronounced, as illustrated by the adsorption desorption isotherm of glyphosate to goethite presented in Figure 27, with continued release of glyphosate, rather than the almost complete hysteresis seen in Figure 25.

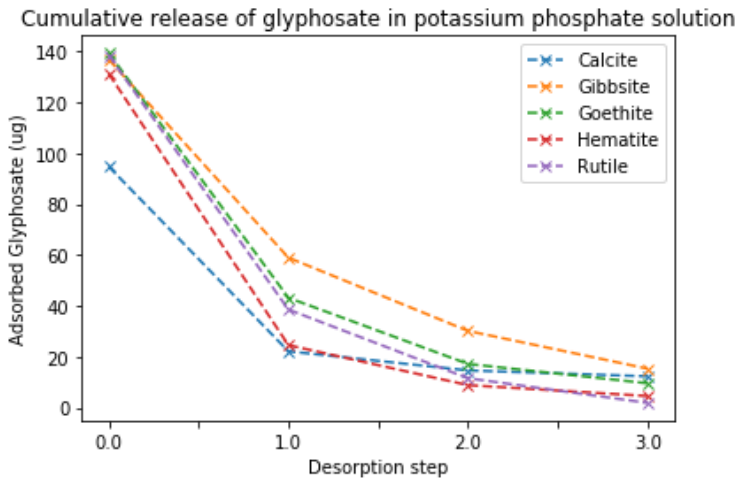

Figure 26: Cumulative desorption of glyphosate from soil minerals with potassium phosphate solution

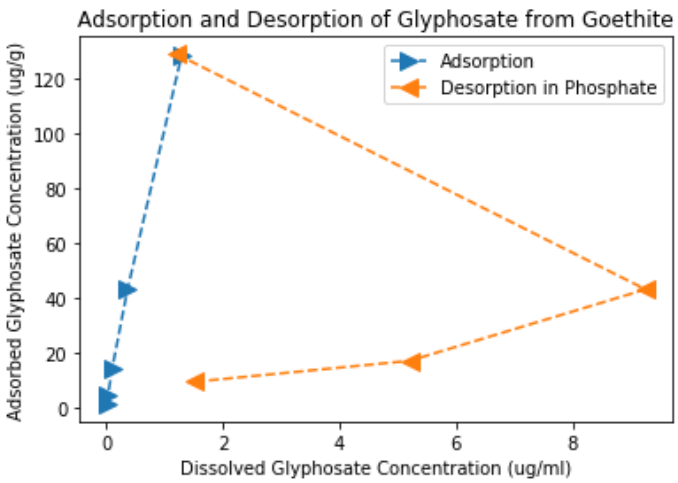

Figure 27: Desorption of glyphosate from goethite in the presence of phosphate

To demonstrate this use of the same binding sites, and probe the possibility of a "sharing" of the mineral surface, different concentrations of potassium phosphate solutions were added to minerals that had "pre-adsorbed" glyphosate, the results of which are shown in Figure 28. This proved extremely interesting, as it demonstrated that phosphate would preferentially adsorb to "open" binding sites prior to competing with glyphosate, as this is the energetically favourable scenario.

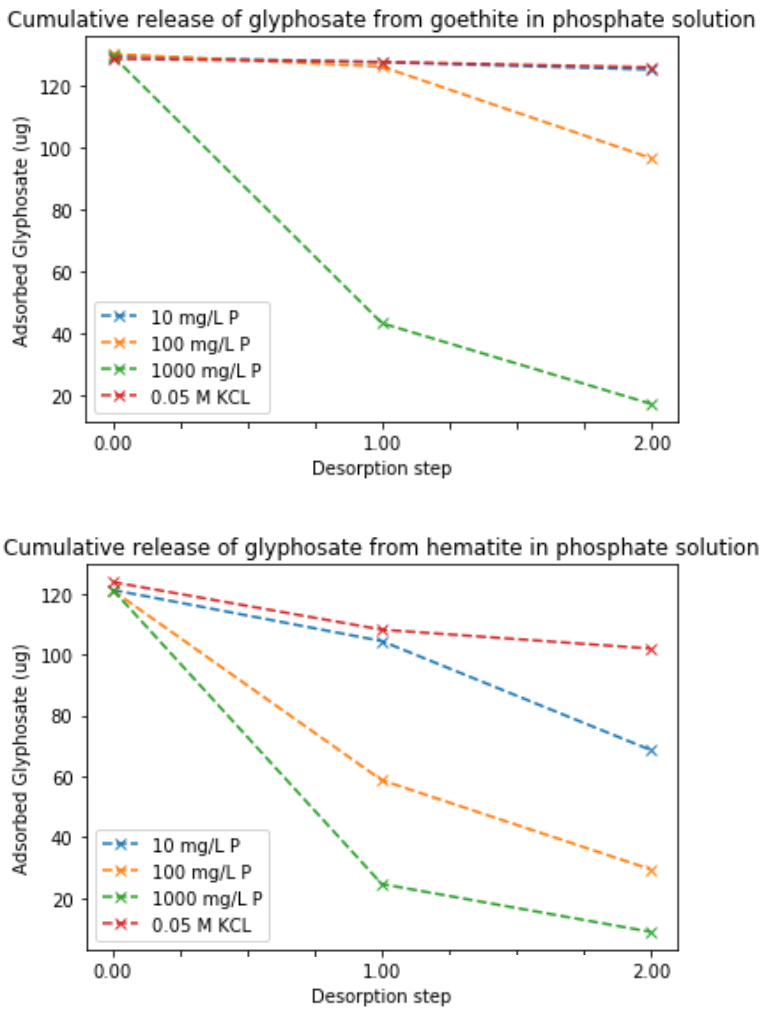

Figure 28: Desorption of glyphosate from non-saturated goethite (top) and hematite (bottom) surfaces in different concentrations of potassium phosphate

The "lag" seen in the 100 mg L^{-1} P and 10 mg L^{-1} P potassium phosphate solutions prior to glyphosate release in goethite and hematite respectively are likely caused by this phenomenon, with the surface becoming saturated with P in the initial step, followed by a desorption of glyphosate upon the addition of a phosphate beyond this level. The lower concentration of phosphate required for this to occur in hematite matches with the lower adsorption capacity of hematite for phosphate and glyphosate

This is further illustrated by Figure 29, which shows the desorption of glyphosate by entering phosphate ligands from the same goethite surface, however in this case the surface is completely saturated with glyphosate prior to the addition of phosphate. In this scenario, a

significantly lower "lag" is seen in the desorption with 100 mg L^{-1} P potassium phosphate solution, as there are almost no free adsorption sites for the phosphate to occupy prior to competition with glyphosate. It should be noted, that the extremely low levels of desorption in 10 mg L^{-1} P phosphate solution, and the apparent acceleration of glyphosate release in the second addition of 100 mg L^{-1} suggests that the surface was not completely saturated by glyphosate after the initial adsorption step.

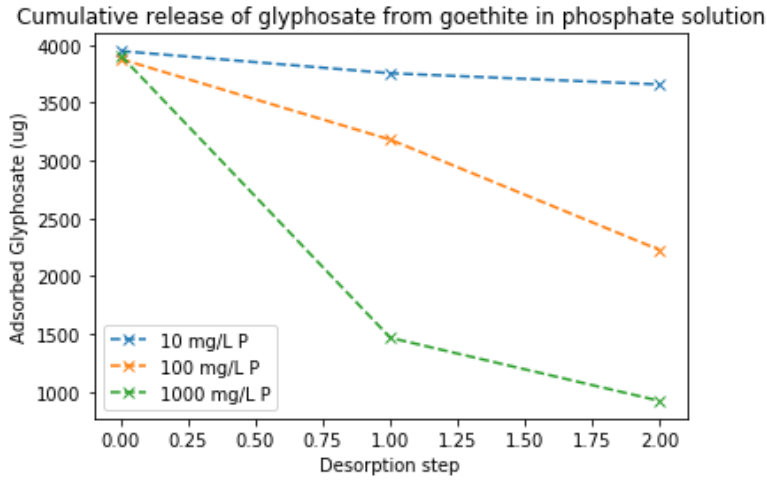

Figure 29: Desorption of glyphosate from a saturated goethite surface in different concentrations of potassium phosphate

This finding has implications for the continuous additions of phosphate fertiliser in soil, suggesting that glyphosate release may occur only after multiple rounds of fertilisation, depending on the levels of fertiliser applied, the glyphosate/phosphate adsorption capacity of the soil, and this initial rate of glyphosate application. There are also implications for the method of phosphorus fertilisation, due to the variation in localised concentration of P, particularly in practices using fertiliser "banding", where it would be feasible to give rise to a continuous release of glyphosate, as the phosphate leaches from the initial point of application to the surrounding soil.

5.5 Conclusion

The factors impacting release of glyphosate from soil minerals, including coulombic screening, and in particular the competition with phosphate ions, have significant implications for agronomic practices using banding of P fertiliser. The timing of application of both herbicide treatments and fertilisers, as well as the method by which phosphorus fertiliser is applied both have the potential to alter the rate of future release of glyphosate and the unintended consequences this may have for crop production or off site movement of glyphosate. The varied levels of hysteresis observed between the desorption in KCl solution and K_2HPO_4 solution suggest a practical risk of release of previously unavailable, bound glyphosate, and the possibility of herbicide injury in later crop rotations due to this.

5.6 References

1. Benbrook, C. M., Trends in glyphosate herbicide use in the United States and globally. *Environmental Sciences Europe* **2016,** *28* (1), 3.
2. Giesy, J. P.; Dobson, S.; Solomon, K. R., Ecotoxicological risk assessment for Roundup® herbicide. In *Reviews of Environmental Contamination and Toxicology: Continuation of Residue Reviews*, Ware, G. W., Ed. Springer New York: New York, NY, **2000**; pp 35-120.
3. Roy, D. N.; Konar, S. K.; Banerjee, S.; Charles, D. A.; Thompson, D. G.; Prasad, R., Persistence, movement, and degradation of glyphosate in selected Canadian boreal forest soils. *Journal of Agricultural and Food Chemistry* **1989,** *37* (2), 437-440.
4. Rose, M. T.; Cavagnaro, T. R.; Scanlan, C. A.; Rose, T. J.; Vancov, T.; Kimber, S.; Kennedy, I. R.; Kookana, R. S.; Van Zwieten, L., Impact of herbicides on soil biology and function. In *Advances in Agronomy*, Donald, L. S., Ed. Academic Press: **2016**; Vol. Volume 136, pp 133-220.
5. Primost, J. E.; Marino, D. J. G.; Aparicio, V. C.; Costa, J. L.; Carriquiriborde, P., Glyphosate and AMPA, "pseudo-persistent" pollutants under real-world agricultural management practices in the Mesopotamic Pampas agroecosystem, Argentina. *Environmental Pollution* **2017,** *229*, 771-779.
6. Borggaard, O. K.; Gimsing, A. L., Fate of glyphosate in soil and the possibility of leaching to ground and surface waters: a review. *Pest Management Science* **2008,** *64* (4), 441-456.
7. Silva, V.; Montanarella, L.; Jones, A.; Fernández-Ugalde, O.; Mol, H. G. J.; Ritsema, C. J.; Geissen, V., Distribution of glyphosate and aminomethylphosphonic acid (AMPA) in agricultural topsoils of the European Union. *Science of The Total Environment* **2018,** *621*, 1352-1359.
8. Mendez, M. J.; Aimar, S. B.; Aparicio, V. C.; Ramirez Haberkon, N. B.; Buschiazzo, D. E.; De Gerónimo, E.; Costa, J. L., Glyphosate and Aminomethylphosphonic acid (AMPA) contents in the respirable dust emitted by an agricultural soil of the central semiarid region of Argentina. *Aeolian Research* **2017,** *29*, 23-29.

9. Battaglin, W. A.; Meyer, M. T.; Kuivila, K. M.; Dietze, J. E., Glyphosate and Its degradation product AMPA occur frequently and widely in U.S. soils, surface water, groundwater, and precipitation. *JAWRA Journal of the American Water Resources Association* **2014,** *50* (2), 275-290.
10. Bott, S.; Tesfamariam, T.; Kania, A.; Eman, B.; Aslan, N.; Römheld, V.; Neumann, G., Phytotoxicity of glyphosate soil residues re-mobilised by phosphate fertilisation. *Plant and Soil* **2011,** *342* (1), 249-263.
11. Rose, T.; Van Zwieten, L.; Claassens, A.; Scanlan, C.; Rose, M., Phytotoxicity of soilborne glyphosate residues is influenced by the method of phosphorus fertiliser application. *Plant Soil* **2017**; *422*, 455-465.
12. Norgaard, T.; Moldrup, P.; Ferré, T. P. A.; Olsen, P.; Rosenbom, A. E.; de Jonge, L. W., Leaching of glyphosate and aminomethylphosphonic acid from an agricultural field over a twelve-year period. *Vadose Zone Journal* **2014,** *13* (10).
13. Simonsen, L.; Fomsgaard, I. S.; Svensmark, B.; Spliid, N. H., Fate and availability of glyphosate and AMPA in agricultural soil. *Journal of Environmental Science and Health, Part B* **2008,** *43* (5), 365-375.
14. McGrath, G. S.; Hinz, C.; Sivapalan, M., A preferential flow leaching index. *Water Resources Research* **2009,** *45* (11), W114505.
15. McGrath, G. S.; Hinz, C.; Sivapalan, M., Modelling the impact of within-storm variability of rainfall on the loading of solutes to preferential flow pathways. *European Journal of Soil Science* **2008,** *59* (1), 24-33.
16. Al-Rajab, A. J.; Schiavon, M., Degradation of ^{14}C-glyphosate and aminomethyl-phosphonic acid (AMPA) in three agricultural soils. *Journal of Environmental Sciences* **2010,** *22* (9), 1374-1380.
17. Sprankle, P.; Meggitt, W. F.; Penner, D., Adsorption, mobility, and microbial degradation of glyphosate in the soil. *Weed Science* **1975,** *23* (3), 229-234.
18. Morillo, E.; Undabeytia, T.; Maqueda, C.; Ramos, A., Glyphosate adsorption on soils of different characteristics.: Influence of copper addition. *Chemosphere* **2000,** *40* (1), 103-107.
19. Zhao, B.; Zhang, J.; Gong, J.; Zhang, H.; Zhang, C., Glyphosate mobility in soils by phosphate application: Laboratory column experiments. *Geoderma* **2009,** *149* (3), 290-297.
20. de Jonge, H.; Wollesen de Jonge, L., Influence of pH and solution composition on the sorption of glyphosate and prochloraz to a sandy loam soil. *Chemosphere* **1999,** *39* (5), 753-763.
21. Sheals, J.; Sjöberg, S.; Persson, P., Adsorption of glyphosate on goethite: Molecular characterization of surface complexes. *Environmental Science & Technology* **2002,** *36* (14), 3090-3095.
22. Laitinen, P.; Siimes, K.; Rämö, S.; Jauhiainen, L.; Eronen, L.; Oinonen, S.; Hartikainen, H., Effects of soil phosphorus status on environmental risk assessment of glyphosate and glufosinate-ammonium. *Journal of Environmental Quality* **2008,** *37* (3), 830-838.
23. Padilla, J. T.; Selim, H. M., Interactions among glyphosate and phosphate in soils: Laboratory retention and transport studies. *Journal of Environmental Quality* **2019,** *48* (1), 156-163.
24. Rosenbom, A.; Haarder, B.; Badawi, N.; Gudmundsson, L.; Von Platten-Hallermund, F.; H Hansen, C.; B Nielsen, C.; Plauborg, F.; Olsen, P., *The Danish Pesticide Leaching Assessment Programme. Monitoring results May 1999–June 2016*. **2017**.
25. Arroyave, J. M.; Waiman, C. C.; Zanini, G. P.; Tan, W.; Avena, M. J., Desorption rate of glyphosate from goethite as affected by different entering ligands: hints on the desorption mechanism. *Environmental Chemistry* **2017,** *14* (5), 288-294.
26. Geelhoed, J. S.; Hiemstra, T.; Van Riemsdijk, W. H., Phosphate and sulfate adsorption on goethite: Single anion and competitive adsorption. *Geochimica et Cosmochimica Acta* **1997,** *61* (12), 2389-2396.

27. Lookman, R.; Freese, D.; Merckx, R.; Vlassak, K.; van Riemsdijk, W. H., Long-Term kinetics of phosphate release from soil. *Environmental Science & Technology* **1995,** *29* (6), 1569-1575.
28. Rayment, G. E.; Lyons, D. J., *Soil chemical methods : Australasia*. CSIRO Publishing: Collingwood, Vic, **2010**.
29. Freeman, J. S.; Rowell, D. L., The adsorption and precipitation of phosphate onto calcite. *Journal of Soil Science* **1981,** *32* (1), 75-84.
30. Gimsing, A. L.; Borggaard, O. K., Phosphate and glyphosate adsorption by hematite and ferrihydrite and comparison with other variable-charge minerals. *Clays and Clay Minerals* **2007,** *55* (1), 108-114.
31. Lu, D.; Song, H.; Jiang, S.; Chen, X.; Wang, H.; Zhou, J., Integrated phosphorus placement and form for improving wheat grain yield. *Agronomy Journal* **2019,** *111* (4), 1998-2004.

6. Uptake of Imazamox by Diffusive Gradient Thin Films and a Model Plant System

Gavin Styles[a], Michael Rose[b], Lukas Van Zwieten[ab], Bart Follink[a], Mark Buecking[c], Antonio F Patti[a]

[a]School of Chemistry, Monash University, Wellington Rd., Clayton, 3800, Victoria, Australia

[b]New South Wales Department of Primary Industries, 1243 Bruxner Highway, Wollongbar, 2477, New South Wales, Australia

[c]Fraunhofer Institute of Molecular Ecology, Auf dem Aberg 1, 57392, Schmallenberg, North Rhine-Westphalia, Germany

Declarations of interest: none

6.1 Abstract

Current assessments for herbicide residues in soil rely on total extractable herbicide, and do not distinguish between "bound" and "available" herbicide. This availability for plant uptake is dependent on a wide range of factors including solubility, adsorption and soil characteristics such as water holding capacity, and as such cannot be determined by any single factor. Diffusive Gradient Thin Films (DGT) have been recently studied as a method for determining plant available herbicide in soil, due to the passive nature of their uptake, mimicking plant roots. To date, limited studies have directly compared uptake of DGTs to the uptake of plant systems. This study compares the uptake of imazamox by a DGT system to two varieties of rapeseed in four different agricultural soils. While DGTs do not provide a perfect prediction of imazamox uptake by rapeseed, they provide a more reliable estimate than adsorption capacity or water holding capacity alone, suggesting it to be a promising method for assessing plant availability of soil contaminants.

6.2 Introduction

Pesticides are integral part of modern agriculture, contributing significantly to the food production chain, improving productivity by preventing crop damage by insects, nutrient competition from weeds, and diseases caused by various bacteria and fungi[1-2]. However they also provide the potential for negative impacts on human[3], environmental[4] and animal wellbeing[5]. Herbicides can be found in soils following direct application to soil, as in the case of pre-emergence herbicides, and those that are applied to foliage post-emergence may still reach soil through rainfall washing the herbicide off the foliage, post-treatment plant matter residues or even transport and root exudates. Research has shown pesticides may have adverse effects on soil microbial community, in both diversity and activity[6-7]. Similarly herbicide persistence in the soil may lead to crop injury in later rotations[8], leading to economic drawbacks for farmers. Residual herbicides may also be taken up by non-target flora such as later crop rotations, ending up in the consumables produced, with the potential for an adverse impact on human health[9].

Routine testing for herbicide is relatively expensive and is generally based on an exhaustive extraction of the soil, giving a value of "total" herbicide present or extractable. This produces the drawback of not providing a measure of herbicide available for uptake by plants or the "bioavailable" fraction, which is often more useful for risk assessment analyses[10]. This level of bioavailability is impacted by a wide range of factors in the soil, in particular adsorption of the herbicide to the soil[11-12]. The development of a testing method which instead accounts for the bioavailable fraction would provide significant advantages in assessing the probability of crop damage and leaching at the field scale.

Imazamox (2-[(RS)-4-isopropyl-4-methyl-5-oxo-2-imidazolin2-yl]-5-methoxymethylnicotinic acid, shown in Figure 30) is a systemic herbicide that may be applied either pre- or post-emergence for the control of broad leaf weeds[13-14]. It has been shown to have a relatively long persistence in soil and is metabolised slower in acidic conditions[15], with a half-life under

laboratory conditions of 106-295 days[16]. Imazamox may also form complexes with metal ions such as Fe^{3+}[17], resulting in increased adsorption and thus persistence. These factors make imazamox a challenge with regards to herbicide carryover and crop injury in later rotations[18], and therefore an ideal candidate for evaluation of testing methods for measuring the bioavailable fraction in soil.

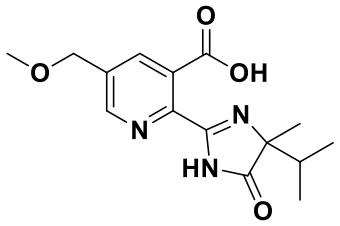

Imazamox

Figure 30: Imazamox structure

Diffusive Gradient Thin Film (DGT) sampling is an emerging technique that has been demonstrated to provide an estimate of the bioavailable fraction of nutrients (such as P fertiliser[19]) and contaminants (both organic[20] and inorganic[21]) in various environmental compartments. DGT samplers consist of a binding layer, diffusive layer, and in some cases a porous membrane filter to protect the other layers from particulate matter. The diffusive and binding layers are hydrogels, with the binding layer including an adsorbent dispersed throughout the gel. The adsorbent in the binding layer is chosen specifically to capture the analyte of interest with high affinity and capacity. The diffusive gel prevents concentration flux on the adsorbent layer, and allowing transfer from solution to the binding layer to occur solely through diffusion. Because of this, uptake of a given analyte by the DGT is dependent on the size of the exposure window, thickness of the diffusive gel, exposure time, and concentration of the analyte in the solution[22]. It is commonly assumed that lateral diffusion, and the thickness of diffusive boundary layer created at the interface of solution and sampler due to water viscosity are negligible. This situation can be described using Fick's Laws of diffusion[20], resulting in Equation (1), where *C* is the concentration of the analyte in solution, *D* is the diffusion coefficient

of the analyte, t is exposure time, A is the area of the exposure window, Δg is the thickness of the diffusive gel, and m is the mass of analyte contained in the binding layer.

$$C = \frac{m \times \Delta g}{t \times D \times A} \tag{1}$$

However, in reality, the diffusive boundary layer will not be two dimensional, and lateral diffusion can occur around the edges of the exposure window. In order to account for this, Equation (2) can be used, where k_{id} is the lateral diffusion flux increase coefficient, D_w is the diffusion coefficient of the analyte in water, and δ is the thickness of the diffusive boundary layer.

$$C = \frac{m}{k_{id} A t}\left(\frac{\Delta g}{D} + \frac{\delta}{D_w}\right) \tag{2}$$

DGTs were initially developed for assessing heavy metal contamination in waterways in 1994 by Davison and Zhang[22]. More recently, the technology has been applied in assessing the bioavailable fraction of heavy metal contamination in soil[21, 23], mineral and nutrient plant availability[19, 24], and organic contaminants in waterways[25] and soil[26]. The application of DGTs to organic contaminants in soil has been undertaken for a wide variety of pesticides in recent studies[27].

The uptake of small organic molecules by plants is complex, though generally considered to be a passive process related to the transpiration of water from the soil through the plant, due to the movement of dissolved compounds with this water into the plant mass[28-29]. However, processes such as root exudation, which may actively transport these compounds out of the plant mass[30], along with natural water filtering at the plant roots, the overall accumulation of substances from soil pore water into the plant mass may not be perfectly correlated to transpiration. As such, methods such as transpiration stream concentration factor (TCSF)[31-32], and plant uptake factor (PUF)[33] were developed to account for these phenomena. The major difference between the two measures is that TCSF treats the plant as a sink and exclusively

considers the quantity of compound transported to the shoots of the plant, by comparison for the concentration of substance in the xylem sap compared the soil pore water. In contrast, the PUF also considers compounds stored in the roots, by measuring the change in concentration of test substance in a growth media over time, making it a more appropriate method for overall plant uptake[33].

To date, limited studies have compared the uptake of DGT samplers directly to uptake by a plant species in order to determine its ability to mimic a root system, and how reliably it gives an estimation of contamination available for plant uptake. This comparison would add further credence to the use of DGTs in risk assessment scenarios, and allow a higher level of confidence in results produced through their use in a field setting. Such a comparison would require an understanding of adsorption of the contaminant to the given soils, as well as an understanding of contaminant uptake by individual plant species. This comparison would add further credence to the use of DGTs in risk assessment scenarios, and allow a higher level of confidence in results produced through their use in a field setting. With this in mind, this study aimed to evaluate DGTs for the accumulation of imazamox from four contrasting agricultural soils, comparing directly to two rapeseed varieties (one sensitive, and one resistant to imazmox), along with the adsorption of imazamox to these soils. We hypothesised that uptake by DGT systems will closely represent those of the rapeseed varieties, and that most variation in uptake will be attributable to differences in the uptake factor of the two systems.

6.3 Material and Methods

6.3.1 Materials

^{14}C labelled imazamox was provided by BASF (Ludwigshaven, Germany), and unlabelled analytical grade imazamox was purchased from Sigma Aldrich (Castle Hill, Australia). DGT housings were purchased from DGT Research (Lancaster, UK), and OASIS-HLB powder was purchased from Waters (Rydalmere, Australia). All other reagents were purchased from Sigma

Aldrich. Soils for plant growth and DGT trials, along with analysis of soil properties was provided by Fraunhofer IME (Schmallenberg, Germany). Two varieties of rapeseed where used as the test plants, one sensitive to imazamox (CWH142) and one resistant (DK Imperial CL), both provided by Dekalb DE (part of Bayer Crop Science, Germany). Soils were collected from four agricultural sites around Germany (localities listed in Table 10), to a depth of 0-20 cm and stored in open outdoor containers until required. These soils were then air dried, sieved to below 2 mm and stored in sealed containers prior to use.

6.3.2 Adsorption Experiments

Sorption of imazamox to soil was determined using a 1:5 soil-to-liquid ratio at four concentrations of imazamox (0.3, 1, 3 and 9 mg L^{-1}) and 1 g aliquots of air dried soil. Soil-imazamox mixtures were rotated on an end-over-end shaker (33 rpm) at 22 ^{o}C for 24 hours to allow equilibration, before being centrifuged at 2600 G for 20 min (Thermo Scientific Megafuge 8). The supernatant was then removed and filtered through a 0.2 µm polyethylene (Merck) membrane to remove any remaining clay particles. Supernatant (1 mL) was then mixed with scintillation cocktail (5 mL, Optifluor, PerkinElmer) and imazamox concentration determined by scintillation counting (Hidex 600 SL). The amount of adsorbed imazamox was then determined indirectly by subtracting final imazamox concentration from initial imazamox concentration. Controls conducted in the same manner without soil material showed negligible adsorption of imazamox to the centrifuge tubes or filters (<1%). Results were then fitted to produce K_d values (ml g^{-1}) using Equation (3)

$$x = K_d C \tag{3}$$

Where *x* is the concentration of adsorbed imazmox in µg of imazamox per g of soil, and *C* is the concentration of imazamox in solution (µg ml^{-1})

6.3.3 Uptake by DGT Samplers

DGT samplers were produced according to the method outlined in Challis et al. (2016)[25] with the minor modification of samplers using TiO_2 (Simga-Aldrich, Sydney, Australia) or Oasis HLB polymer resin (Waters, Rydalmere, Australia) powder as the adsorbent for the binding layer produced. The samplers were constructed from cylindrical DGT pistons (DGT Research Ltd, Lancaster, UK) with an exposure window of 2.54 cm^2, using a polysulfone filter, 0.75 mm diffusion layer of 1.5% agarose gel and a 0.75 mm binding layer of 1.5% agarose gel with an adsorbent (either TiO_2 or HLB polymer resin powder, as appropriate) dispersed throughout, as per the diagram shown in Figure 31. The uptake capacity of prepared DGT samplers was determined by suspending samplers in a solution of imazamox (20 ml, 50 µg L^{-1}) in distilled water for 48 hours. The binding layer was then removed, washed lightly in distilled water and bound imazamox extracted three times with 0.5 M KOH (3 x 2 ml). Extracts were then mixed with scintillation cocktail and radiation counted.

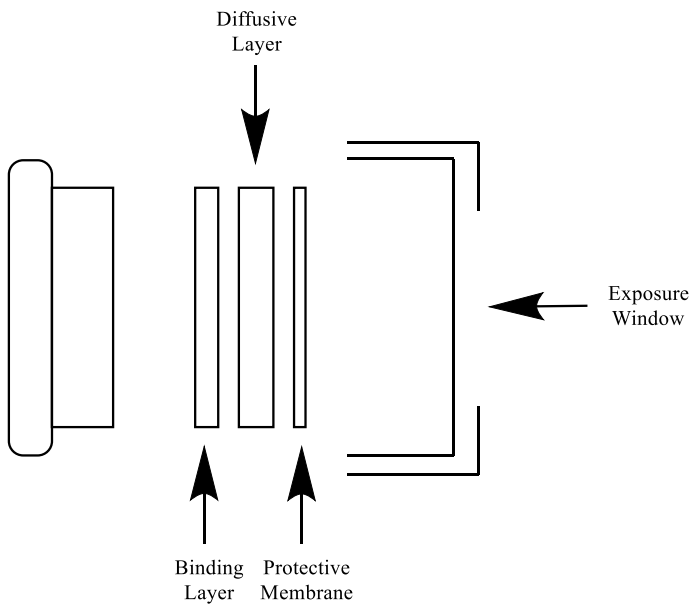

Figure 31: DGT Construction

Uptake of imazamox from soil by DGTs was conducted using a modified method of Weng et al. (2018)[26]. Here, 6 g (dry weight equivalent) of soil was placed in a polypropylene centrifuge tube

cap (diameter 4 cm, depth 1.5 cm), dosed with 420 ng of ^{14}C-labelled imazamox and water added to 80% moisture holding capacity. These soils were then allowed to equilibrate for 24 hours prior to DGT exposure. DGT samplers were pushed gently into the soil samples, and twisted lightly to ensure full contact and coverage of the exposure window. DGTs were deployed for 48 hours, before collection and analysis. After removal from soil, the binding layer was removed and washed lightly with distilled water, before being placed in 1.5ml of 0.5M KOH to extract the bound imazamox. This extraction was repeated three times, and the pooled extractant was analysed for radiation content by LSC.

6.3.4 Plant Uptake Factor

Plant uptake factor (PUF) experiments were conducted by the method reported by Lamshoeft et al. (2018)[33], with minor modifications. Germination of the two varieties of rapeseed of interest in perlite and water, before replacing the water with a 50% Hoagland nutrient solution for the early development of the seedlings. These seedlings were then transferred to vessels containing 300 ml of the same 50% Hoagland solution. The vessels were covered with foil to prevent algal growth in the nutrient solution. When the plants reach a growth stage of BBCH 13 (a growth scale used to compare phenologically similar plants[34]), the growth media was inoculated with a radiolabelled test compound (in this case imazamox). An initial period of two days was allowed for the fractionation of this compound, before initial readings of volume, and mass of test compound present. The plants are then allowed to grow for an additional 10 days, and final volume and mass measurements done. Mass is measured by taking 2 ml aliquots of the growth media for scintillation counting, and the total radiation present related to mass in the aliquot, and thus the total volume. Equation (4) is then used to determine the overall PUF

$$PUF = \frac{\ln\left(\frac{m_{final}}{m_{initial}}\right)}{\ln\left(\frac{v_{final}}{v_{initial}}\right)} \quad (4)$$

Where m is the mass of test compound, and v is the volume of solution at the initial time point (2 days post-test compound addition) and the final time point (10 days after initial sampling). A total of five replicates for each seed variety was conducted, along with two plant free controls to account for changes due to surface evaporation of the solution.

6.3.5 Plant Uptake from Soil

Uptake of imazamox by rapeseed was undertaken in 25cm diameter draining plastic pots containing 1 kg of soil held at 60% moisture capacity, with a commercially available NPK fertiliser applied prior to planting at a rate of 4 ml kg^{-1} (Fertiliser nutrient content: 8% N as urea and urea nitrate, 5% P_2O_5, 8% K_2O). Pots were maintained in individual trays to prevent loss of radiation through leaching. All soils were dosed with either 1x or 0.2x field rate (70 or 14 µg kg^{-1}, 2500 or 500 Bq) of ^{14}C labelled imazamox, excluding herbicide free controls, which were used to determine the occurrence of herbicide injury. This field rate was based on the label rate per hectare, assuming a soil bulk density of 1.5 kg m^{-3} and a herbicide penetration depth of 30 cm. This depth was chosen due to previous studies showing other imizadolinone herbicides to have the potential to leach to 40cm[35], thus 30cm was chosen as a conservative estimate of leaching potential. Initially, five seeds were planted, and this was thinned to three plants per pot post-emergence. Plants were grown for a 7 week period post sowing, in a climate controlled chamber with a 16/8 hour day night cycle, with temperature and humidity held at 22/17°C and 50/20% respectively. Plants were then destructively harvested and fresh weights measured, before drying, separating into roots and shoots, and dry masses being recorded. All plants were then ground and homogenised and radiation content determined by combustion with an Ox700 Oxidiser (Zinsser Analytic), with the emitted CO_2 captured by the Oxysolve C-400 (Zinsser Analytic) and radiation counted.

6.3.6 Data Analysis

Analysis of data from the PUF and plant growth trials was conducted in SPSS (IBM, New York, USA)[36]. Dry mass and radiation data was analysed by t-test and multi-factor ANOVA; the factors used were soil, seed variety and imazamox dosing level. Tukey's honestly significantly different (HSD, Zar 1999[37]) analysis was used for comparison of the different soil types for both root and shoot radiation at the different imazamox levels.

6.4 Results and Discussion

Initial soil characterisation was provided by Fraunhofer IME and is summarised in Table 10. The soils used covered a wide range of soil texture (clay content of 6.2-25.1%), water holding capacity (WHC, 293-697 g/kg) and carbon and nitrogen content. While the pH range covered acid and neutral soils, there were no alkaline soils in the sample set.

Table 10: Soil properties

Soil	FAO Classification	Sand	Silt	Clay	pH_{Water}	WHC	C_{org}	N_{total}	CEC
		%	%	%		g/kg	%	g/kg	mmol/kg
1	Cambisol	74.0	19.8	6.2	5.7	293	0.93	0.92	16.2
2	Luvisol	5.7	78.3	16.0	6.6	416	0.95	1.15	46.6
3	Cambisol	22.1	52.8	25.1	6.0	697	3.02	4.42	112.8
4	Fluvisol	33.0	46.7	20.3	4.8	666	1.74	2.28	44.5

6.4.1 Adsorption

All soils produced relatively low K_d values with a minimum of 0.92 and maximum of 1.73 ml g^{-1} (Table 11). There appeared to be no direct relationship between the experimentally determined K_d values and the measured soil properties, such as organic matter or clay content. This is similar to the results of Sakaliene et al. (2007)[38], who found no correlation between imazamox sorption (Kd, ranging from 0.19-0.42 ml g^{-1}) and soil organic C or pH across 7 different Baltic soils. However, it is known that imazamox may form complexes with metal ions[17] such as Fe^{3+}, as such

it may be variation in the mineralogy of the soils, which was not assessed, causing the differences in adsorption affinities for each of the four soils.

6.4.2 DGT Uptake

A comparison of DGTs constructed with either a HLB or TiO_2 adsorbent used in the binding layer showed HLB to have a significantly higher uptake of imazamox from solution. DGTs constructed with TiO_2 as the adsorbent had an average uptake of 30±5% of imazamox from solution, while those with a HLB binding layer had an uptake of 66±4% of imazamox from solution. This is at the lower end of the range previously reported in literature for other organic contaminants (18%-55% error in calculating solution concentration Challis et al. 2016[25]; 74-86% total uptake of glyphosate on TiO_2, Weng et al. 2019[26]; uptake of >80% of six out of nine polar pesticides by HLB, Chen et al. 2015[39]). However, our results for imazamox (log K_{OW} 0.73) are similar to the relatively low uptake of the herbicide chloridazon (log K_{OW} 1.14) by HLB and XAD binding layers, compared with other herbicides with greater K_{OW} partition coefficients[39]. As with chloridazon, maximum uptake required >24 h and hence HLB DGTs were deployed in soil for 48 hours, as it was expected diffusion from soil would be even slower than that in solution. The highest uptake was found to occur in soil 1, and the lowest in soil 3. The average adsorption and DGT uptake values for all soils are summarised in Table 11. Interestingly, the uptake in soils doped at 1x field rate and 0.2x field rate do not differ by a factor of 5 (excluding the case of soil 2). This is unlikely to be due to saturation effects based on the results of the DGT boundary experiments, but instead may be due to the diffusion rate of imazamox through the soil to the binding layer of the DGT. However further studies increasing exposure time would be required to confirm this.

Table 11: Adsorption K_d (ml g^{-1}) and DGT uptake values (ng)

Soil	K_d	R^2	DGT Uptake	
			1 x Field rate	*0.2 x Field rate*
1	1.07	0.99	131 ± 22	47 ± 9
2	1.73	0.99	106 ± 4	21 ± 5
3	0.92	0.99	94 ± 3	31 ± 2
4	1.51	0.98	116 ± 7	45 ± 1

6.4.3 Plant Uptake Factor

In order to produce a reference point of the uptake for imazamox from soil by the two rapeseed varieties studied, a plant uptake factor was determined. By growing plants in a hydroponic solution and allowing a pre-uptake testing window of 48 hours for partitioning of the test chemical, "availability" of imazamox for uptake by plants can be considered to be 100% of the measured initial values. The two seed varieties had similar uptake values, with both having an average PUF of less than 0.3 for imazamox. The imazamox resistant variety of rapeseed showed a slightly lower uptake of imazamox (average PUF 0.25, standard deviation 0.062) compared to the sensitive variety (average PUF 0.29, standard deviation 0.040), however a t-test (p-value of 0.281) showed this difference to be statistically non-significant. Because there was negligible change in volume of growth media or concentration of imazamox in the plant free control vessels, these results can be considered free of confounding factors such as evaporation or degradation of the test compound.

The PUFs for imazamox (molecular weight 306) into rapeseed derived here were similar to the PUF values obtained by Lamshoeft et al. (2018)[33] for compounds with molecular weight > 300, which ranged from 0.02-0.31; whereas compounds with MW<220 all had PUFs of >0.6. These values indicate that less than a third of the soil-solution phase imazamox will be absorbed by rapeseed.

6.4.4 Plant Uptake from Soil

Over the course of the seven week growth time allowed for this plant trial, significant variation in plant germination and growth was observed. Initial trial germinations using non-labelled imazamox to gauge growth conditions produced a germination index of 60-100% between pots across all soils (results not shown). However, during the main trial, the germination index varied widely from no germination to 100% germination between pots. Treatment, seed and soil type were all non-significant factors in this germination index. A removal of plants from those pots which did reach germination of more than 3/5 plants in order to prevent overcrowding and nutrient competition resulted in the removal of <2% of total radiation added in any given pot, and thus was considered to have negligible impact on the uptake of the remaining plants. No significant difference in fresh or dry weight of the final harvested plants was observed between treatments (1x field rate, 0.2x field rate or control), suggesting there was no herbicide injury occurring in either seed variety. The lack of significance of seed variety in uptake of imazamox from soil, matches up with the results of the PUF study, which showed no statistically significant difference in the uptake by either seed variety from hydroponic solution.

Radiation was measured on a normalised basis per 100 mg of dry plant matter, and was divided into above ground, and below ground radiation. There was no significant impact of plant mass on normalised radiation, suggesting imazamox uptake was a constant passive process rather than occurring during specific stages of growth. Significantly more radiation was found in the above ground portion of the plant than in the roots, suggesting translocation and storage of imazamox through the plant, rather than uptake being adsorption of the imazamox to the plant roots.

A three-way ANOVA analysis of plant uptake of imazamox showed soil type and treatment to be significant factors in both shoot and root radiation, with seed type being non-significant and no significant interactions occurring between the variables, excluding an interaction of soil and

treatment in root radiation. The significance values produced by this analysis are shown in Table 12. This analysis was conducted with the radiation uptake of each plant being kept separate, rather than averaging the total pot uptake, due to different germination levels between pots. Treatment is expected to be a significant factor in the radiation level in plants, as in a higher treatment level, the available radiation in the soil is theoretically five-fold that in the low treatment. As such this functions as a useful check for errors in experimental method or data analysis. It should also be noted the overall uptake of radiation across a single pot was well below the level of radiation initially added, thus making it unlikely there were any "starvation" effects, where plant uptake was limited due to competition with other plants in the same pot. Initial addition of imazamox was equivalent to 500 or 2500 Bq for low and high treatment rates respectively, while the total measured combined radiation in plants removed from a given pot was less than 20% of initial addition in all cases.

Table 12: Significance values from three-way ANOVA of plant uptake data

	Soil	**Seed**	**Treatment**	**Soil/Seed**	**Soil/ Treatment**	**Seed/ Treatment**	**Soil/Seed/ Treatment**
Shoot Radiation	0.000	0.166	0.000	0.353	0.158	0.168	0.860
Root Radiation	0.000	0.328	0.000	0.324	0.000	0.529	0.661
Shoot Dry Mass	0.027	0.539	0.555	0.337	0.894	0.918	0.915
Root Dry Mass	0.000	0.956	0.127	0.244	0.297	0.707	0.580

When comparing the mean uptake between soils, the highest uptake occurred in soil 1, then soil 2, soil 3 and the lowest in soil 4. There was a difference in average uptake between treatments of 40% (Field rate: 5.24 Bq/100mg, 0.2x field rate: 3.18 Bq/100mg), though this change is soil dependent, with comparison of soil and treatment uptake shown in Table 13. This variation is relatively low in comparison to the 80% decrease in added radiation between

treatments, suggesting the possibility of saturation effects reducing overall uptake in the higher treatment level.

Table 13: Mean uptake values of 14-C imazamox (Bq/100mg) by rapeseed seperated by soil and treatment rate

Soil	1x Field rate		0.2x Field Rate	
	Shoots	*Roots*	*Shoots*	*Roots*
1	7.09 ± 2.86 [a]	4.94 ± 1.15[a]	4.24 ± 2.07[a]	1.3 ± 0.37[a]
2	4.90 ± 0.76[ab]	3.60 ± 0.39[ab]	3.72 ± 1.47[ab]	0.72 ± 0.31[a]
3	2.90 ± 1.11[b]	1.51 ± 0.30[c]	2.15 ± 0.84[ab]	1.05 ± 0.70[a]
4	3.00 ± 0.92[b]	2.37 ± 2.15[bc]	1.88 ± 1.10[b]	0.68 ± 0.28[a]

[a,b,c] indicative of statistically similar subsets as determined by Tukey's HSD

6.4.5 Comparison

While DGT uptake performed better (was a closer fit to the plant uptake) than K_d, neither was a perfect predictor of imazamox availability for plant uptake, suggesting it is likely other factors such as water holding capacity (WHC) play a role. All experiments for uptake were performed at 80% water holding capacity, thus influencing the volume of pore water and thus the concentration of dissolved imazamox, as opposed to initial adsorption experiments which were conducted in a fixed water volume. A similar effect could occur in plant uptake trials with a larger volume of water available leading to higher level of transpiration through the plant (though this is unlikely to be significant, as 60% WHC is above moisture stress levels[40]), and thus higher uptake. However, soil 3 resulted in the lowest uptake of imazamox by rapeseed, and the second lowest by DGT, despite having the lowest adsorption capacity for imazamox. It is possible this is related to the fact it has the highest water holding capacity, thus leading to a lower concentration of dissolved imazamox. However, the calculated concentrations based on water holding capacity and K_d presented in Table 14 show this not to be the case, as soils 2 and 4 have a lower dissolved concentration. This suggests there are other factors impacting the availability of herbicide in soil. For example, the length of growth period may have led to the degradation of some of the imazamox in the soil, and as such, the soil with higher organic matter content

(soil 3) may have had lower imazamox concentrations over the entire growth period. This may help explain the lower plant uptake over this period, despite the higher theoretical concentration of imazamox predicted using the K_d values. Furthermore, the watering regime during this seven week growth period means that there was consistent drying and rewetting of the soils, leading to a varying amount of pore water throughout the trial, and thus a consistent cycle of adsorption and desorption of the imazamox to the soil. Previous studies have reported adsorption of an analogous herbicide, imazethapyr, to soil to increase over time[41], so higher level of imazamox adsorption to soil may have occurred during the growth trial than in initial adsorption trials, influencing the plant uptake in a soil-dependent fashion.

Table 14: Dissolved imazamox concentration in soil pore water at varying water holding capacities, with 70 ug kg^{-1} imazamox

Soil	**Imazamox pore water concentration (µg L^{-1})**	
	60% WHC	*80% WHC*
1	58.2	53.7
2	35.4	33.9
3	52.3	47.4
4	36.7	34.3

A comparison of uptake of imazamox by DGTs and rapeseed shows DGT to be a promising technology for determining plant available levels of herbicide, and a useful tool for herbicide risk assessment. Direct comparison of the two is difficult due to the various confounding factors, including the short growth period allowed for rapeseed prior to harvest, which would lead to an incomplete uptake of available imazamox in the soil. The highest total uptake from a single pot was ~680 ng of imazamox (based on converted radiation), and occurred in a high treatment soil 1 replicate. This is equivalent to 60 ng of imazamox taken up per 6 g of soil (the quantity of soil used for DGT trials), which is less than half of the amount taken up by DGTs in soil 1 at field rate applications. However, it is extremely likely that this uptake would have increased with a longer growth period, allowing the plant to reach a higher level of maturity. This can be inferred based

on the apparent relatively linear relationship between mass and radiation uptake in the trial (ie. those plants in this trial which had higher mass also had a higher total radiation content).

Along with this, different moisture levels between experiments (80% WHC for DGT and 60% WHC for plant uptake) is likely to lead to slight variations in the total available herbicide in each case, due to varying concentrations of dissolved and adsorbed herbicide, and possible minor changes in plant transpiration[40] (though these are unlikely to be significant). This variation in moisture level was due to the requirements to produce even contact across the surface of the DGT, and optimal germination and growth conditions for the rapeseed. However, despite these variations, similar trends were observed, with soil 1 producing the highest uptake at both treatment levels, and soil 3 the lowest uptake at 1x field rate in both systems, despite both having low adsorption capacity for imazamox, and relatively similar pore water concentrations of imazamox. There were discrepancies in the level of availability between the DGT and rapeseed trials across all soils, but in particular at the lower application rate, and amongst soils 2 and 4. This may be due to variations in growth conditions between soils (with soil playing a significant role in plant dry mass as seen in Table 12), and in the lower treatment, discrepancies may be caused by a higher possible degree of error in the DGT uptake due to extremely low quantities measured (nanogram scale, 0-3 Bq per extraction).

This study gives good evidence of DGT sampling being a reliable measure of available herbicide in soils, with a more accurate result than that based only adsorption capacity or other single soil properties. While some variations between DGT and plant uptake were found, and additional optimisation of the process may be required, initial results are promising. Given these results coupled with the benefits of the DGT methodology, further research into the use of DGTs for quantification of available herbicide in soils is warranted.

6.5 References

1. Cooper, J.; Dobson, H., The benefits of pesticides to mankind and the environment. *Crop Protection* **2007,** *26* (9), 1337-1348.
2. Wasim, A.; Dwaipayan, S.; Ashim, C., Impact of pesticides use in agriculture: their benefits and hazards. *Interdisciplinary Toxicology* **2009,** *2* (1), 1-12.
3. Alavanja, M. C. R.; Samanic, C.; Dosemeci, M.; Lubin, J.; Tarone, R.; Lynch, C. F.; Knott, C.; Thomas, K.; Hoppin, J. A.; Barker, J.; Coble, J.; Sandler, D. P.; Blair, A., Use of agricultural pesticides and prostate cancer risk in the agricultural health study cohort. *American Journal of Epidemiology* **2003,** *157* (9), 800-814.
4. Giesy, J. P.; Dobson, S.; Solomon, K. R., Ecotoxicological risk assessment for Roundup® herbicide. In *Reviews of Environmental Contamination and Toxicology: Continuation of Residue Reviews*, Ware, G. W., Ed. Springer New York: New York, NY, **2000**; pp 35-120.
5. Druart, C.; Millet, M.; Scheifler, R.; Delhomme, O.; de Vaufleury, A., Glyphosate and glufosinate-based herbicides: fate in soil, transfer to, and effects on land snails. *Journal of Soils and Sediments* **2011,** *11* (8), 1373-1384.
6. Rose, M. T.; Ng, E. L.; Weng, Z.; Wood, R.; Rose, T. J.; Van Zwieten, L., Minor effects of herbicides on microbial activity in agricultural soils are detected by N-transformation but not enzyme activity assays. *European Journal of Soil Biology* **2018,** *87*, 72-79.
7. Dennis, P. G.; Kukulies, T.; Forstner, C.; Orton, T. G.; Pattison, A. B., The effects of glyphosate, glufosinate, paraquat and paraquat-diquat on soil microbial activity and bacterial, archaeal and nematode diversity. *Scientific Reports* **2018,** *8* (1), 2119.
8. Blackshaw, R. E.; Harker, K. N., Wheat, field pea, and canola response to glyphosate and AMPA soil residues. *Weed Technology* **2017,** *30* (4), 985-991.
9. Fantke, P.; Charles, R.; Alencastro, L. F. d.; Friedrich, R.; Jolliet, O., Plant uptake of pesticides and human health: Dynamic modeling of residues in wheat and ingestion intake. *Chemosphere* **2011,** *85* (10), 1639-1647.
10. Ortega-Calvo, J.-J.; Harmsen, J.; Parsons, J. R.; Semple, K. T.; Aitken, M. D.; Ajao, C.; Eadsforth, C.; Galay-Burgos, M.; Naidu, R.; Oliver, R.; Peijnenburg, W. J. G. M.; Römbke, J.; Streck, G.; Versonnen, B., From bioavailability science to regulation of organic chemicals. *Environmental Science & Technology* **2015,** *49* (17), 10255-10264.
11. Kookana, R. S., The role of biochar in modifying the environmental fate, bioavailability, and efficacy of pesticides in soils: a review. *Soil Research* **2010,** *48* (7), 627-637.
12. Daly, K.; Styles, D.; Lalor, S.; Wall, D. P., Phosphorus sorption, supply potential and availability in soils with contrasting parent material and soil chemical properties. *European Journal of Soil Science* **2015,** *66* (4), 792-801.
13. Walker, G. W.; Kookana, R. S.; Smith, N. E.; Kah, M.; Doolette, C. L.; Reeves, P. T.; Lovell, W.; Anderson, D. J.; Turney, T. W.; Navarro, D. A., Ecological risk assessment of nano-enabled pesticides: A perspective on problem formulation. *Journal of Agricultural and Food Chemistry* **2018,** *66* (26), 6480-6486.
14. Eizenberg, H.; Hershenhorn, J.; Ephrath, J. E., Factors affecting the efficacy of Orobanche cumana chemical control in sunflower. *Weed Research* **2009,** *49* (3), 308-315.
15. Aichele, T. M.; Penner, D., Adsorption, Desorption, and Degradation of Imidazolinones in Soil. *Weed Technology* **2017,** *19* (1), 154-159.
16. Lewis, K. A.; Tzilivakis, J.; Warner, D. J.; Green, A., An international database for pesticide risk assessments and management. *Human and Ecological Risk Assessment: An International Journal* **2016,** *22* (4), 1050-1064.

17. Cabrera, A.; Celis, R.; Hermosín, M. C., Imazamox–clay complexes with chitosan- and iron(III)-modified smectites and their use in nanoformulations. *Pest Management Science* **2016,** *72* (7), 1285-1294.
18. Ball, D. A.; Yenish, J. P.; Alby, T., Effect of imazamox soil persistence on dryland rotational crops. *Weed Technology* **2017,** *17* (1), 161-165.
19. Davison, W.; Zhang, H., In situ speciation measurements of trace components in natural waters using thin-film gels. *Nature* **1994,** *367* (6463), 546-548.
20. Guibal, R.; Buzier, R.; Lissalde, S.; Guibaud, G., Adaptation of diffusive gradients in thin films technique to sample organic pollutants in the environment: An overview of o-DGT passive samplers. *Science of The Total Environment* **2019,** *693*, 133537.
21. Dai, Y.; Nasir, M.; Zhang, Y.; Wu, H.; Guo, H.; Lv, J., Comparison of DGT with traditional methods for assessing cadmium bioavailability to Brassica chinensis in different soils. *Scientific Reports* **2017,** *7* (1), 14206.
22. Bade, R.; Oh, S.; Shin, W. S., Diffusive gradients in thin films (DGT) for the prediction of bioavailability of heavy metals in contaminated soils to earthworm (Eisenia foetida) and oral bioavailable concentrations. *Science of The Total Environment* **2012,** *416*, 127-136.
23. Degryse, F.; Smolders, E.; Zhang, H.; Davison, W., Predicting availability of mineral elements to plants with the DGT technique: a review of experimental data and interpretation by modelling. *Environmental Chemistry* **2009,** *6* (3), 198-218.
24. Tandy, S.; Mundus, S.; Yngvesson, J.; de Bang, T. C.; Lombi, E.; Schjoerring, J. K.; Husted, S., The use of DGT for prediction of plant available copper, zinc and phosphorus in agricultural soils. *Plant and Soil* **2011,** *346* (1), 167-180.
25. Challis, J. K.; Hanson, M. L.; Wong, C. S., Development and calibration of an organic-diffusive gradients in thin films aquatic passive sampler for a diverse suite of polar organic contaminants. *Analytical Chemistry* **2016,** *88* (21), 10583-10591.
26. Weng, Z.; Rose, M. T.; Tavakkoli, E.; Van Zwieten, L.; Styles, G.; Bennett, W.; Lombi, E., Assessing plant-available glyphosate in contrasting soils by diffusive gradient in thin-films technique (DGT). *Science of The Total Environment* **2019,** *646*, 735-744.
27. Li, Y.; Chen, C.-E. L.; Chen, W.; Chen, J.; Cai, X.; Jones, K. C.; Zhang, H., Development of a passive sampling technique for measuring pesticides in waters and soils. *Journal of Agricultural and Food Chemistry* **2019,** *67* (22), 6397-6406.
28. Sheets, T. J., Uptake and distribution of simazine by oat and cotton seedlings. *Weeds* **1961,** *9* (1), 1-13.
29. Chen, W.; Li, L.; Chang, A. C.; Wu, L.; Chaney, R. L.; Smith, R.; Ajwa, H., Characterizing the solid–solution partitioning coefficient and plant uptake factor of As, Cd, and Pb in California croplands. *Agriculture, Ecosystems & Environment* **2009,** *129* (1), 212-220.
30. Viti, M. L.; Alves, P. A. T.; Mendes, K. F.; Pimpinato, R. F.; Guimaraes, A. C. D.; Torniselo, V. L., Translocation and root exudation of glyphosate by urochloa brizantha and its transport on sugarcane and citrus seedlings. *Planta Daninha* **2019,** *37*.
31. Shone, M. G. T.; Bartlett, B. O.; Wood, A. V., A comparison of the uptake and translocation of some organic herbicides and a systemic fungicide by barley: II. relationship between uptake by roots and translocation to shoots. *Journal of Experimental Botany* **1974,** *25* (85), 401-409.
32. Briggs, G. G.; Bromilow, R. H.; Evans, A. A.; Williams, M., Relationships between lipophilicity and the distribution of non-ionised chemicals in barley shoots following uptake by the roots. *Pesticide Science* **1983,** *14* (5), 492-500.
33. Lamshoeft, M.; Gao, Z.; Resseler, H.; Schriever, C.; Sur, R.; Sweeney, P.; Webb, S.; Zillgens, B.; Reitz, M. U., Evaluation of a novel test design to determine uptake of chemicals by plant roots. *Science of The Total Environment* **2018,** *613-614*, 10-19.

34. Hess, M.; Barralis, G.; Bleiholder, H.; Buhr, L.; Eggers, T.; Hack, H.; Stauss, R., Use of the extended BBCH scale—general for the descriptions of the growth stages of mono; and dicotyledonous weed species. *Weed Research* **1997,** *37* (6), 433-441.
35. Hollaway, K. L.; Kookana, R. S.; Noy, D. M.; Smith, J. G.; Wilhelm, N., Persistence and leaching of imazethapyr and flumetsulam herbicides over a 4-year period in the highly alkaline soils of south-eastern Australia. *Australian Journal of Experimental Agriculture* **2006,** *46* (5), 669-674.
36. Corp, I. *IBM SPSS Statistics for Windows, Version 25.0*, Armonk, NY, **2017**.
37. Zar, J., *Biostatistical Analysis, 4th edn.* Prentice Hall, Upper Saddle River, **1999**.
38. Sakaliene, O.; Papiernik, S. K.; Koskinen, W. C.; Spokas, K. A., Sorption and predicted mobility of herbicides in Baltic soils. *Journal of Environmental Science and Health, Part B* **2007,** *42* (6), 641-647.
39. Chen, C.-E.; Chen, W.; Ying, G.-G.; Jones, K. C.; Zhang, H., In situ measurement of solution concentrations and fluxes of sulfonamides and trimethoprim antibiotics in soils using o-DGT. *Talanta* **2015,** *132*, 902-908.
40. Verhoef, A.; Egea, G., Modeling plant transpiration under limited soil water: Comparison of different plant and soil hydraulic parameterizations and preliminary implications for their use in land surface models. *Agricultural and Forest Meteorology* **2014,** *191*, 22-32.
41. Johnson, D. H.; Shaner, D. L.; Deane, J.; Mackersie, L. A.; Tuxhorn, G., Time-dependent adsorption of imazethapyr to soil. *Weed Science* **2017,** *48* (6), 769-775.

-

7. Conclusions and Future Work

The overarching aims of this study were to increase understanding of the behaviour of glyphosate in soils, develop predictive models of its adsorption, and develop a method for measuring "available" rather than total herbicide in soils. A number of different techniques and studies were undertaken to address these aims. The possible environmental and economic impacts of herbicide usage due to persistence and leaching are at the forefront of the public conscious. These issues are directly linked to herbicide adsorption and availability in the soil. Within this thesis, a cross-disciplinary study to better understand, quantify and predict these phenomena was undertaken. This was not without its challenges due to the inherently variable nature of soil and biological systems, particularly within the plant trials conducted in Chapter 6.

Much of the available data on glyphosate adsorption is from studies conducted in Europe and the Americas, which does not account for the significantly different soils found in Australia. Similarly, the wide variation found in Australia soils is well suited to the development of pedotransfer rules for glyphosate adsorption in soil. In order to address these knowledge gaps and opportunities, a large database of soil properties and glyphosate adsorption capacity for a variety of sampling sites around Australia was developed, and this database used to produce predictive models of glyphosate adsorption based on physico-chemical properties (Chapter 2) and mid-infrared (MIR) spectra (Chapter 3). While these models are not perfectly accurate, they are relatively robust, and perform as well, if not better, than those previously reported in the literature[1-8] for glyphosate or other herbicides, and serve as a strong proof of concept. These models were based on a dataset comprising 50 soil sites around Australia, most sampled at two different depths to total 90-97 unique soils. Within this dataset, only a limited number of soils with a glyphosate K_f in the range of 100-400 were represented, and the inclusion of additional soils in this range may have served to improve the predictive capabilities of the model.

The predictive models produced in Chapters 2 and 3 of this thesis provide useful tools for the development of more spatially explicit management strategies for glyphosate usage. In particular this work shows a strong link between glyphosate and phosphorus adsorption to soil, with phosphorus buffering index (PBI) an accurate predictor of glyphosate adsorption, and the MIR loading for prediction of glyphosate K_f and PBI being extremely similar. However, additional work to expand the database on which these models are built would provide a far more robust and reliable output. Along with this, the measure of PBI, which is used in the physico-chemical model is used most commonly in Australia. As such, additional models using comparative measures of phosphorus adsorption affinity in soil more broadly used in other regions of the world would prove invaluable for the translation of this tool to those regions.

Limited prior studies have systematically investigated the adsorption/desorption of glyphosate on soil components, to fundamentally understand the impacts of pH, salt and phosphate concentrations. This information would prove invaluable in unravelling the mechanisms of glyphosate adsorption and glyphosate release upon phosphorus fertiliser addition, which has been observed in several previous studies[9-13]. Chapters 4 and 5 sought to address this, firstly through a systematic development of adsorption isotherms of glyphosate to model soil minerals at various pH levels (Chapter 4). This showed the impact of electrostatic interactions between glyphosate and the mineral surface in all cases, with the charge of the mineral surface and lateral (charge) interactions between glyphosate molecules making significant contributions to the adsorption energy and practical saturation capacity. These results lend credence to the impacts of pH seen in the models produced in Chapter 2 of this thesis. Chapter 4 also examined the current ubiquitous nature of Langmuir isotherms and shows that a Frumkin Fowler Guggenheim approach, by explicitly taking into account the aforementioned lateral interactions in the adsorbed phase, is more realistic for these systems. This study was not exhaustive, and did not account for all possible soil components. In particular it did not include studies of silicates or organic matter components such as humic substances.

The release of previously adsorbed glyphosate upon addition of phosphorus fertiliser poses a significant risk, both economically due to the possibility of herbicide injury in later crop rotation post fertilisation, but also environmentally due to the increased risk of glyphosate movement offsite. Previous studies have generally suggested this release is due to competition between glyphosate and phosphate[13], however, it has also been suggested that glyphosate desorption rates are independent of the entering ligand[14]. Further evidence of possible competition between glyphosate and phosphate ions is reflected in the importance of PBI in the models produced in both Chapters 2 and 3 of this thesis.

In order to further understand and clarify the mechanisms involved in glyphosate release, Chapter 5 involved the study of glyphosate release through desorption under different salt and phosphate concentrations. Coulombic screening of the surface charge of the mineral upon the addition of salt does have the ability to marginally increase glyphosate release from a mineral surface when compared to desorption in pure water. However, this increased release was relatively small, while the addition of phosphate (as would occur in a localised area around super phosphate banding) produced far more significant increases in glyphosate desorption. One of the most interesting findings of this work was the preference of phosphate ions to fill available binding sites on an unsaturated surface prior to competing for binding sites with glyphosate. This work has important implications for fertilisation regimes post-glyphosate application, however, no “whole” soil systems were studied in this thesis.

The adsorption/desorption work conducted in Chapters 4 and 5 makes significant strides in elucidating the root mechanisms of glyphosate sorption behaviour in soil, particularly with relation to pH and phosphate competition. The implications of this work for phosphorus fertilisation regimes are significant, and additional work which compares the release of glyphosate from “whole” soil systems under different fertilisation regimes would be a logical next step. Similarly, a study of the response of “whole” soil systems to processes such as claying

and liming in terms of glyphosate adsorption to further these results to a real-world scenarios could provide important information which could be used by agronomists and agronomic land holders in soil management.

As the need for measures of “available” herbicide in soil becomes more recognised, diffusive gradient thin-films (DGT) technology has emerged as a preferred option due to its passive nature, thus mimicking plant root systems. However, very few previous studies have directly compared the uptake of herbicides from soil by DGT and a model plant system. The final study in this thesis (Chapter 6) compared the uptake of imazamox from four different agricultural soils by DGTs and two varieties of rapeseed (one imazamox-sensitive, and the other imazamox-resistant). This showed the levels to be similar after accounting for the uptake factors of DGT and the rapeseed varieties, with soil type being the main factor impacting uptake of imazamox by both DGT and rapeseed. However, due to the variable nature of biological systems such as plants, a larger sample set would have allowed for a more robust statistical analysis. This study would have also benefited from the use of a plant system with a higher plant uptake factor (PUF) for imazamox, as this likely would have reduced variation between individual plants in the same soil.

While the study performed in Chapter 6 provides a good foundation towards verifying DGTs as a valid method for determining the available fraction of herbicide in a soil, it covers only one plant type and one herbicide. Additional trials on a similar scale using herbicides with a stronger adsorption affinity for soil or other more complex behaviours which would reduce their availability in soil would serve to further solidify these results. The uptake of imazamox by this particular DGT system was also slightly below the ideal range (>70%) and further optimisation prior to use in the field would be required.

In conclusion, the work presented in this thesis makes significant contributions to the knowledge base surrounding herbicide adsorption and availability in soils. While it is by no means comprehensive, and there remains much more work to be done, the findings provide a

solid basis for ongoing research. They build on concepts previously only lightly explored in the literature and they help further areas of knowledge that have previously been lacking. This present work has the potential to help improve agronomic practices, recommendations and management strategies surrounding herbicide usage.

7.1 References

1. De Gerónimo, E.; Aparicio, V. C.; Costa, J. L., Glyphosate sorption to soils of Argentina. Estimation of affinity coefficient by pedotransfer function. *Geoderma* **2018,** *322*, 140-148.
2. Dollinger, J.; Dagès, C.; Voltz, M., Glyphosate sorption to soils and sediments predicted by pedotransfer functions. *Environmental Chemistry Letters* **2015,** *13* (3), 293-307.
3. Paradelo, M.; Hermansen, C.; Knadel, M.; Moldrup, P.; Greve, M. H.; de Jonge, L. W., Field-scale predictions of soil contaminant sorption using visible–near infrared spectroscopy. *Journal of Near Infrared Spectroscopy* **2016,** *24* (3), 281-291.
4. Paradelo, M.; Norgaard, T.; Moldrup, P.; Ferré, T. P. A.; Kumari, K. G. I. D.; Arthur, E.; de Jonge, L. W., Prediction of the glyphosate sorption coefficient across two loamy agricultural fields. *Geoderma* **2015,** *259–260*, 224-232.
5. Sidoli, P.; Baran, N.; Angulo-Jaramillo, R., Glyphosate and AMPA adsorption in soils: laboratory experiments and pedotransfer rules. *Environmental Science and Pollution Research* **2016,** *23* (6), 5733-5742.
6. Forouzangohar, M.; Cozzolino, D.; Kookana, R. S.; Smernik, R. J.; Forrester, S. T.; Chittleborough, D. J., Direct comparison between visible near- and mid-infrared spectroscopy for describing diuron sorption in soils. *Environmental Science & Technology* **2009,** *43* (11), 4049-4055.
7. Forouzangohar, M.; Kookana, R. S.; Forrester, S. T.; Smernik, R. J.; Chittleborough, D. J., Midinfrared spectroscopy and chemometrics to predict diuron sorption coefficients in soils. *Environmental Science & Technology* **2008,** *42* (9), 3283-3288.
8. Kookana, R. S.; Janik, L. J.; Forouzangohar, M.; Forrester, S. T., Prediction of atrazine sorption coefficients in soils using mid-infrared spectroscopy and partial least-squares analysis. *Journal of Agricultural and Food Chemistry* **2008,** *56* (9), 3208-3213.
9. Gimsing, A. L.; Borggaard, O. K., Effect of phosphate on the adsorption of glyphosate on soils, clay minerals and oxides. *International Journal of Environmental Analytical Chemistry* **2002,** *82* (8-9), 545-552.
10. Kanissery, R. G.; Welsh, A.; Sims, G. K., Effect of soil aeration and phosphate addition on the microbial bioavailability of carbon-14-glyphosate. *Journal of Environmental Quality* **2015,** *44* (1), 137-44.
11. Wang, Y. J.; Zhou, D. M.; Sun, R. J., Effects of phosphate on the adsorption of glyphosate on three different types of Chinese soils. *Journal of Environmental Science* **2005,** *17* (5), 711-5.
12. Zhao, B.; Zhang, J.; Gong, J.; Zhang, H.; Zhang, C., Glyphosate mobility in soils by phosphate application: Laboratory column experiments. *Geoderma* **2009,** *149* (3), 290-297.
13. Rose, T.; Van Zwieten, L.; Claassens, A.; Scanlan, C.; Rose, M., Phytotoxicity of soilborne glyphosate residues is influenced by the method of phosphorus fertiliser application. *Plant Soil* **2017**; *422*, 455-465.
14. Arroyave, J. M.; Waiman, C. C.; Zanini, G. P.; Tan, W.; Avena, M. J., Desorption rate of glyphosate from goethite as affected by different entering ligands: hints on the desorption mechanism. *Environmental Chemistry* **2017,** *14* (5), 288-294.

Appendix

Appendix Table 1: Dataset Soil Properties

ID	Lat	Long	State	Depth	EC	pH (H_20)	Colwell Phosphorus	Phosphorus Buffer Index$_{(Colwell\ P)}$	Total Organic Carbon	Sand	Silt	Clay	Glyphosate K_f	n_f	K_d (1.5-15mg/kg)
				cm	dS/m		mg/kg		%	%	%	%			
1	-31.039	148.609	NSW	0-10	0.095	8.2	35	72	0.76	49.23	15.25	30.38	26.85	1.76	121.69
2			NSW	10-30	0.21	8.9	16	100	1.1	46.21	14.83	30.36	26.85	1.63	79.40
3	-30.693	148.481	NSW	0-10	0.13	7.3	49	55	0.77	53.06	16.21	26.56	36.14	1.72	174.04
4			NSW	10-30	0.26	8.8	16	91	0.84	44.55	15.42	35.03	24.37	1.66	64.59
5	-34.248	147.200	NSW	0-10	0.25	5.4	55	51	2	54.18	21.02	19.81	44.34	1.51	145.36
6			NSW	10-30	0.087	6.5	18	57	1.1	53.45	16.29	27.62	47.91	1.54	186.64
7	-34.289	146.950	NSW	0-10	0.11	6.2	60	43	0.95	56.43	22.30	18.61	34.62	1.71	161.19
8			NSW	10-30	0.058	6.5	15	38	0.34	54.51	18.76	24.33	45.16	1.62	114.25
9	-34.366	147.177	NSW	0-10	0.16	5.7	60	57	1.5	55.12	22.21	18.95	46.09	1.39	91.07
10			NSW	10-30	0.063	6.0	18	43	0.69	52.41	24.35	21.20	28.53	1.53	40.58
11	-34.419	147.532	NSW	0-10	0.11	6.5	50	60	1.4	52.98	17.13	26.09	42.35	1.45	81.60
12			NSW	10-30	0.094	6.8	16	69	0.57	45.86	13.67	37.04	39.25	1.60	179.14
13	-34.013	148.255	NSW	0-10	0.071	6.0	56	25	1.1	60.43	23.64	10.55	17.28	1.53	29.22
14			NSW	10-30	0.047	5.4	16	18	0.21	63.18	21.60	9.58	24.22	1.71	46.99
15	-34.613	147.763	NSW	0-10	0.24	6.5	57	74	1.4	52.04	17.18	29.14	42.85	1.57	106.37
16			NSW	10-30	0.19	7.0	13	78	0.38	55.71	13.46	30.58	51.17	1.50	156.65
17	-35.104	146.874	NSW	0-10	0.17	7.5	60	56	1.2	53.56	16.51	24.31	45.06	1.47	150.40
18			NSW	10-30	0.30	7.0	17	90	0.54	37.90	11.32	46.12	26.43	1.55	45.16
19	-34.891	147.191	NSW	0-10	0.068	6.5	59	45	1.1	56.23	19.42	21.11	25.52	1.52	44.40
20			NSW	10-30	0.054	5.8	24	57	0.67	53.11	18.87	25.64	39.51	1.56	79.56
21	-26.986	151.055	QLD	0-10	0.11	7.4	25	110	1.1	31.95	22.48	47.78	48.53	1.47	131.21
22			QLD	10-30	0.12	8.0	18	110	1.1	28.38	22.77	51.78	34.01	1.59	86.22

23	-27.096	151.218	QLD	0-10	0.21	8.1	49	160	1.8	36.11	15.51	41.94	31.82	1.43	46.80
24			QLD	10-30	0.27	8.6	20	210	1.8	36.57	18.08	40.17	29.29	1.47	51.83
25	-27.097	151.218	QLD	0-10	0.17	8.4	42	180	1.8	33.02	18.30	45.21	28.53	1.54	42.47
26			QLD	10-30	0.25	8.7	15	210	1.4	34.01	17.06	42.81	32.04	1.40	50.58
27	-34.619	140.675	SA	0-10	0.21	8.9	28	76	2.7	61.62	17.33	11.14	13.55	1.75	15.04
28			SA	10-30	0.23	9.0	20	95	2.9	56.09	16.69	14.13	14.22	1.59	20.79
29	-32.991	138.203	SA	0-10	0.22	7.8	28	68	2.5	47.01	29.36	16.94	24.03	1.64	42.80
30			SA	10-30	0.16	8.3	20	80	3	49.88	29.84	13.70	26.59	1.60	53.75
31	-32.891	136.196	SA	0-10	0.22	8.5	38	57	1.4	63.04	10.90	18.49	14.61	1.51	13.54
32			SA	10-30	0.34	9.0	21	79	2.6	56.98	7.01	24.43	16.42	1.56	20.12
33	-33.240	135.543	SA	0-10	0.33	8.6	21	76	2.6	69.45	4.78	13.35	13.61	1.57	22.52
34			SA	10-30	0.40	9.2	29	110	3	67.46	7.32	15.96	13.17	1.59	20.13
35	-33.469	136.799	SA	0-10	0.14	8.9	22	65	3.8	65.09	7.05	5.87	13.52	1.59	27.67
36			SA	10-30	0.12	9.0	15	83	3.5	61.75	4.43	6.93	18.06	1.63	35.88
37	-33.089	134.754	SA	0-10	0.14	8.8	33	120	4.5	53.02	16.27	18.80	21.51	1.55	42.07
38			SA	10-30	0.14	8.8	24	200	6.1	48.00	15.43	14.61	32.99	1.54	62.95
39	-34.470	135.427	SA	0-10	0.11	5.8	57	75	1.8	54.08	15.00	26.29	32.16	1.55	67.20
40			SA	10-30	0.060	5.5	30	77	1.2	54.40	11.97	28.50	37.19	1.55	92.16
41	-35.165	140.623	SA	0-10	0.092	6.4	24	10	0.71	87.28	6.20	4.39	10.42	1.68	14.31
42			SA	10-30	0.12	8.7	14	15	0.22	74.95	10.75	11.00	12.52	1.79	23.89
43	-35.340	140.365	SA	0-10	0.18	8.1	57	38	1.7	68.28	16.71	10.56	15.71	1.81	32.57
44			SA	10-30	0.22	8.9	34	120	3.5	55.10	16.49	18.25	21.08	1.64	48.54
45	-36.294	140.841	SA	0-10	0.32	7.5	50	74	2	49.28	13.03	30.05	47.52	1.49	120.04
46			SA	10-30	0.29	8.1	24	89	1.2	44.87	11.53	36.39	37.71	1.59	84.54
47	-35.280	139.052	SA	0-10	0.18	8.5	42	44	2.7	71.28	12.87	8.41	10.23	1.65	12.35
48			SA	10-30	0.21	9.0	25	150	4.9	57.13	11.07	13.63	19.47	1.60	38.99
49	-34.388	138.587	SA	0-10	0.16	7.4	63	65	1.4	58.11	16.07	19.60	31.98	1.57	75.93
50			SA	10-30	0.19	8.2	31	98	2.1	60.23	17.69	16.98	26.65	1.43	52.85
51	-34.427	137.831	SA	0-10	0.22	8.6	45	160	6.1	53.01	9.36	20.28	28.32	1.50	48.45
52			SA	10-30	0.19	8.9	19	190	5.2	49.52	7.14	20.34	29.78	1.42	50.32
53	-34.217	138.640	SA	0-10	0.16	7.3	64	97	2	48.73	12.72	31.11	45.93	1.50	103.68
54			SA	10-30	0.28	8.3	25	130	1.9	42.19	9.80	34.77	34.35	1.45	64.61

55	-33.299	138.598	SA	0-10	0.18	5.7	42	58	1.6	48.29	19.62	27.62	54.73	1.45	137.46
56			SA	10-30	0.089	6.3	23	79	1.2	42.73	14.55	38.55	57.40	1.46	147.59
57	-32.471	117.579	WA	0-10	0.13	6.6	19	11	0.94	76.68	14.15	7.16	4.56	1.82	3.20
58			WA	10-30	0.070	6.3	18	14	0.5	76.42	14.02	7.55	8.73	1.63	12.53
59	-32.592	117.672	WA	0-10	0.18	6.8	60	40	2.1	66.32	11.11	16.38	12.63	1.60	15.72
60			WA	10-30	0.083	6.2	33	46	1.3	64.80	9.97	18.64	25.64	1.48	49.58
61	-32.785	117.525	WA	0-10	0.52	6.0	82	39	2.6	66.99	13.54	9.88	26.36	1.54	51.59
62			WA	10-30	0.11	5.9	57	35	1.5	60.68	23.35	10.02	32.56	1.54	81.57
63	-32.670	117.291	WA	0-10	0.17	6.1	33	28	1.8	68.36	14.45	10.57	16.13	1.69	24.77
64			WA	10-30	0.049	5.5	25	32	1	74.52	11.92	10.29	20.51	1.58	31.07
65	-30.357	116.725	WA	0-10	0.093	6.6	36	52	0.82	58.23	10.00	23.72	32.80	1.56	74.90
66			WA	10-30	0.19	7.6	24	70	0.68	51.78	7.89	31.67	29.45	1.50	77.77
67	-30.286	116.620	WA	0-10	0.095	6.4	58	50	0.98	60.10	11.48	27.42	27.29	1.51	63.59
68			WA	10-30	0.091	5.9	15	62	0.39	61.50	12.12	26.57	47.17	1.46	156.07
69	-30.386	116.650	WA	0-10	0.17	5.4	49	30	0.7	64.81	14.87	19.32	26.18	1.60	68.68
70			WA	10-30	0.087	5.3	21	38	0.29	60.65	11.59	26.87	49.49	1.40	131.32
71	-30.353	117.071	WA	0-10	0.20	5.5	24	26	0.74	70.94	12.06	15.12	25.31	1.32	26.29
72			WA	10-30	0.15	4.7	7.2	37	0.25	67.25	12.62	19.91	58.29	1.34	115.67
73	-29.863	116.673	WA	0-10	0.058	6.4	36	27	0.49	66.89	15.59	16.78	22.44	1.70	43.84
74			WA	10-30	0.037	6.8	11	36	0.21	61.65	17.85	23.46	30.25	1.64	88.20
75	-29.895	116.006	WA	0-10	0.075	6.3	55	41	1.2	67.91	11.07	12.27	38.22	1.44	112.70
76			WA	10-30	0.30	8.8	16	81	1.2	53.45	9.18	26.44	22.27	1.58	44.75
77	-29.867	116.689	WA	0-10	0.079	5.8	31	23	0.46	71.40	9.86	17.33	25.61	1.76	57.87
78			WA	10-30	0.22	7.9	11	55	0.3	62.94	10.34	26.61	24.74	1.57	60.00
79	-29.798	116.112	WA	0-10	0.15	7.3	47	31	1.2	64.72	17.49	13.80	7.51	1.67	7.38
80			WA	10-30	0.56	5.5	27	21	0.57	73.53	15.80	7.93	22.92	1.71	41.23
81	-28.887	153.506	NSW	0-10	0.13	6.4	33	530	5.5	61.54	13.76	16.58	182.1	0.94	136.34
82			NSW	10-30	0.068	6.3	13	610	4.9	66.61	10.14	14.96	164.65	0.96	152.89
83	-28.819	153.391	NSW	0-10	0.09	6.2	19	600	5.5	64.52	12.88631	14.99874	172.14	0.96	195.57
84			NSW	10-30	0.062	6.1	11	630	4.5	60.99	12.82063	16.81284	170.16	0.97	206.88
85	-28.819	153.391	NSW	0-10	0.09	6.1	13	460	6.5	63.89	12.95	15.52	169.67	0.99	138.39
86			NSW	10-30	0.045	6.3	42	720	4.7	63.84	14.02	15.53	186.11	0.94	164.88

87	-28.819	153.391	NSW	0-10	0.039	5.6	32	550	4.3	33.07	21.83	34.47	176.86	0.95	158.02
88			NSW	10-30	0.052	5.6	18	560	3.2	35.48	19.91	37.04	159.53	1	138.88
89	-38.247	145.931	VIC	0-20	0.275	5.5	25	270	4.8	54.36	9.47	23.82	99.22	1.07	117.98
90	-38.042	145.792	VIC	0-20	0.389	4.6	160	210	4.9	36.66	25.14	27.50	83.6	1.05	94.44

Additional note on Table 1: K_d is the slope of a linear fit of adsorption data, K_f and n_f are fitting variables of adsorption derived from the Freundlich equation

Appendix Table 2: Reference Soil Characterisation

ID	Lat	Long	State	Depth	pH	Phosphorus Buffer Index$_{(Colwell\ P)}$	Sand	Silt	Clay	Glyphosate K_f	n_f
				cm			%	%	%		
1	-35.088	142.277	VIC	0-20	6.9	11	105.7	0.2	3.7	25.5	1.41
2	-30.803	116.671	WA	0-20	5.8	15	85.1	2.7	12.5	19.4	1.09
3	-34.485	147.468	NSW	0-20	5.2	60	45.3	26.3	24.1	43.9	1.18
4	-28.213	152.098	QLD	0-20	6.7	110	38.8	13.8	40	104.8	1.05
5	-37.791	145.457	VIC	0-20	5.5	120	56.4	23.5	8.4	46.7	1.11
6	-36.188	144.683	VIC	0-20	7	130	31.6	12.7	50.6	56.7	1.12
7	-33.165	134.685	SA	0-20	8.6	210	44.9	7.8	15.4	31.4	1.13

**Particle size predicted by IR, leading to some error (totals ≠ 100%), particularly in Soil 7 due to carbonate interference*

Appendix Figure 1: Predicted Isotherms

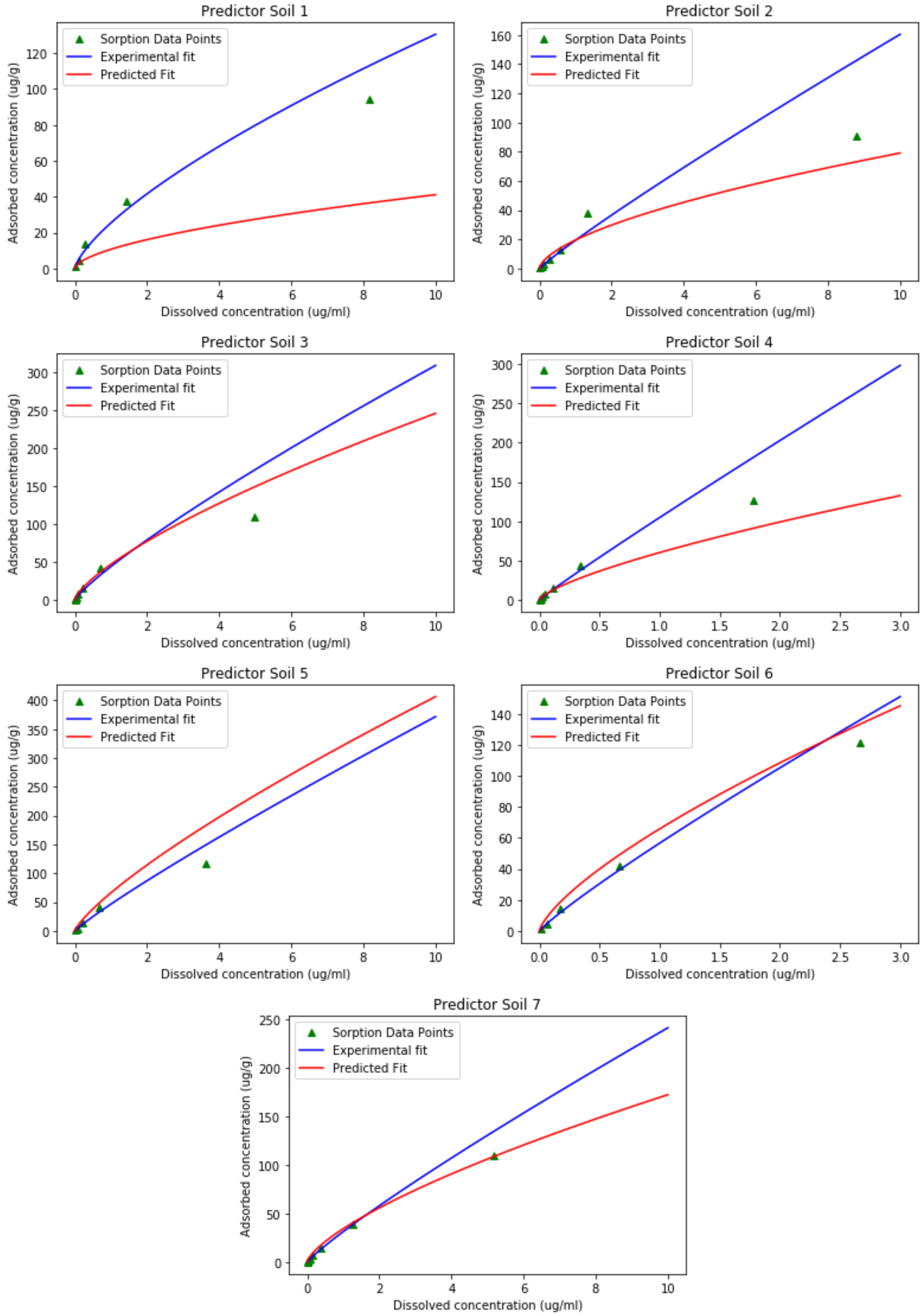

Appendix Table 3: Co-linearity of predictor variables

	EC	pH H_20	Colwell P	PBI	OC
EC	-	-	-	-	-
pH H_20	0.0936	-	-	-	-
Colwell P	0.0544	0.0631	-	-	-
PBI	0.0291	0.0092	0.0143	-	-
OC	0.0108	0.0415	0.0082	0.4795	-
Clay	0.0022	0.0077	0.0028	0.0096	0.0433

Appendix Table 4: Langmuir Fitting constants of glyphosate to mineral surfaces

Mineral	K_L			Q_{max} *(ug/g)*			R^2		
	Acid	*Neutral*	*Basic*	*Acid*	*Neutral*	*Basic*	*Acid*	*Neutral*	*Basic*
Calcite*	N/A	0.379	0.285	N/A	160.5	196.1	N/A	0.99	0.99
Gibbsite	0.024	0.032	0.058	4158.6	2632.5	1790.7	0.99	0.99	0.99
Goethite	0.032	0.031	0.016	4249.9	3242.1	761.2	0.99	0.99	0.99
Hematite	0.071	0.187	0.091	1175.5	695.5	350.4	0.99	0.99	0.99
Kaolinite	0.038	0.063	0.026	908.0	784.6	553.3	0.97	0.99	0.99
Rutile	0.010	0.024	0.056	12715.5	5557.8	1794.4	0.65	0.98	0.99

**Not performed due to high solubility at pH 5*

Appendix Figure 2: Assumed spatial arrangement of an adsorbed glyphosate molecule

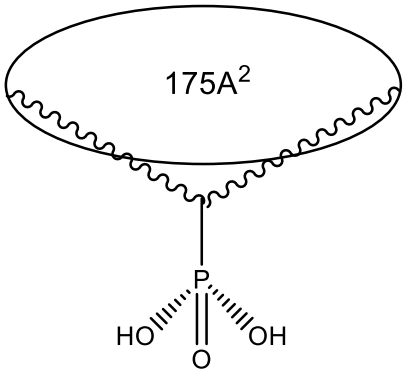

Previous work has shown glyphosate to bind through the phosphate head of the molecule[1]. Taking the phosphorus-oxygen bond length to be 1.67 angstroms[2] and the bond angle to be 110°, we can determine the area required for a phosphorus head to be 3.09 square angstroms. It needs to be considered that the phosphorus head is attached to a flexible tail. Working from the concept that the phosphorus, and thus the attached carbon, are fixed in place (excluding rotation about the P-C bond), the remaining tail that is free to move can be determined to be ~8 Å in length when fully extended (using appropriate bond angles and bond lengths). Allowing full rotation about the P-C bond, we form a cone with a side length of 8 Å, and an interior angle of 140°, producing a circular area of ~175 $Å^2$, as per Appendix Figure 2.

This is 3.5x larger than the experimentally derived 50 $Å^2$, however, allowing for the rotation of other bonds within the molecule, the deprotonation of the carboxylic acid group and the statistical likelihood of two tails being in the same place along the arc such that they intercept, 40 Å appears a feasible spacing.

1. Sheals, J.; Sjöberg, S.; Persson, P., Adsorption of Glyphosate on Goethite: Molecular Characterization of Surface Complexes. *Environmental Science & Technology* **2002,** *36* (14), 3090-3095.
2. Bartell, L. S.; Su, L.-S.; Yow, H., Lengths of phosphorus-oxygen and sulfur-oxygen bonds. Extended Hueckel molecular orbital examination of Cruickshank's d.pi.-p.pi. picture. Inorganic Chemistry 1970, 9 (8), 1903-1912.